The 30th Jerusalem Winter School in Theoretical Physics

Lecture 3
Structure of Dark Matter Halos

Frank van den Bosch
Yale University, Jan 2013

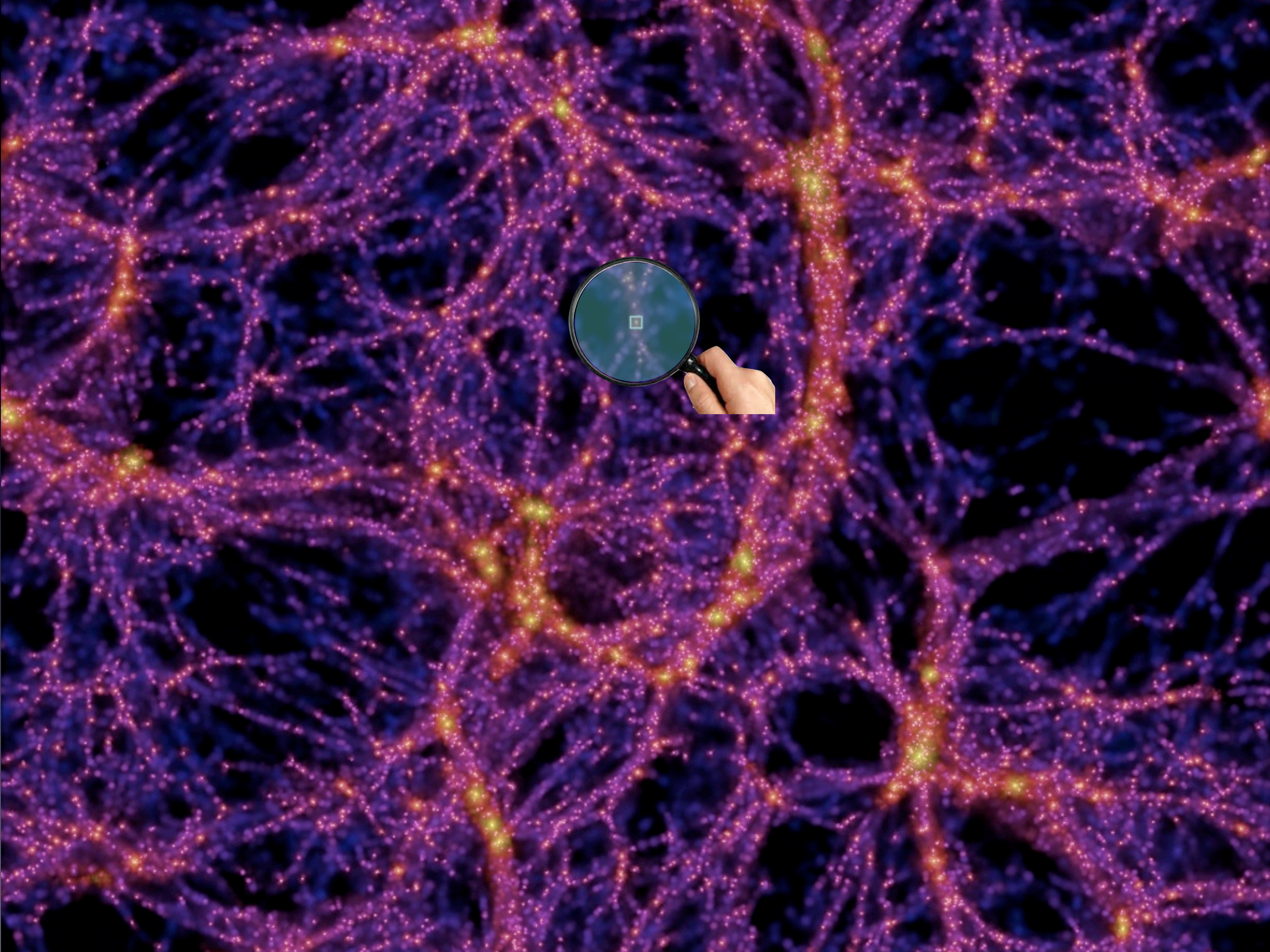

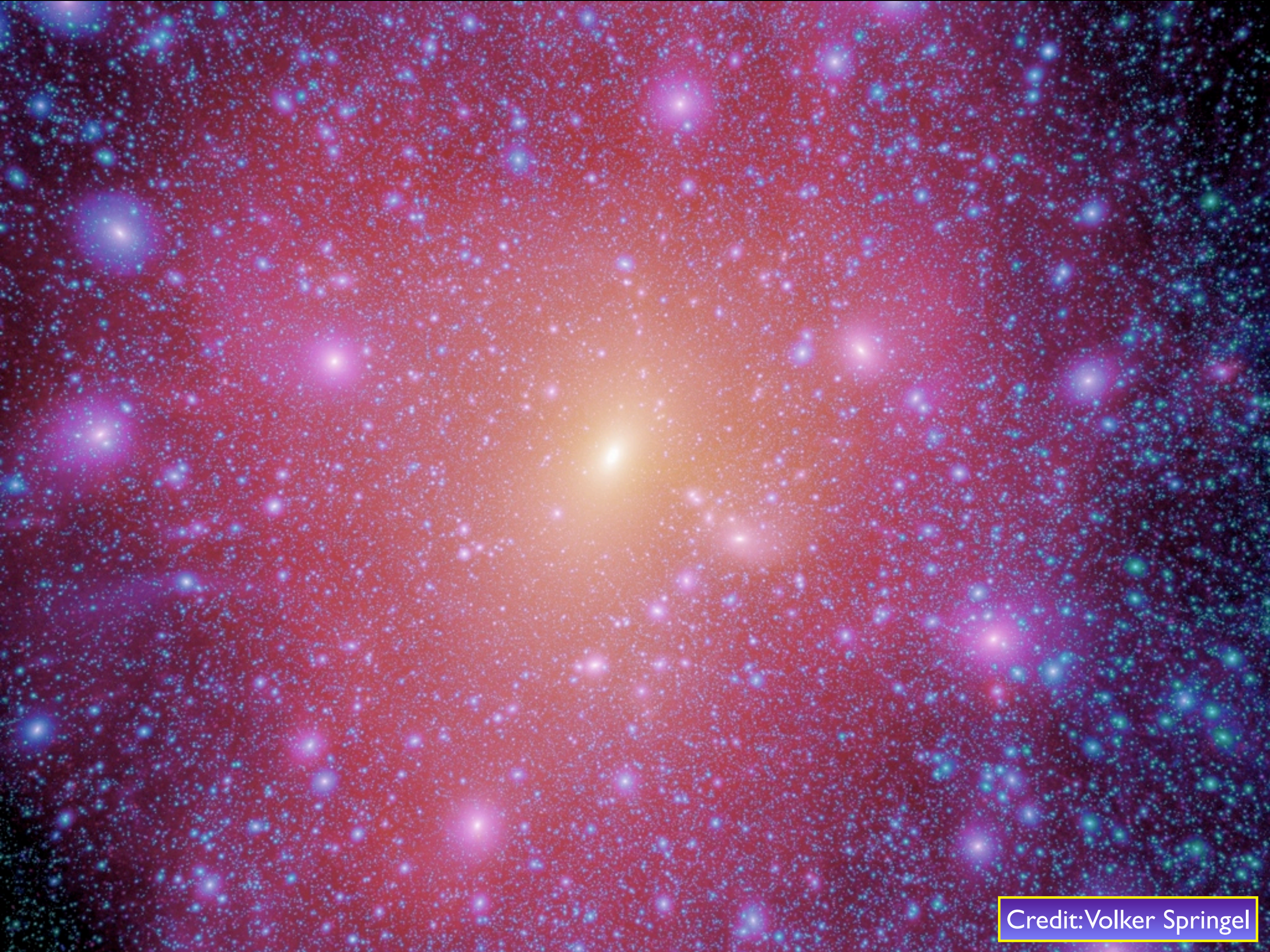
Credit: Volker Springel

Virial Relations

Before we focus on the results of numerical simulations, it is useful to derive some very general scaling relations for dark matter haloes.

According to SC model, dark matter haloes have an average overdensity well fitted by

$$\Delta_{\rm vir} \simeq \frac{18\pi^2 + 82\,x - 39\,x^2}{x+1} \qquad \text{where} \qquad x = \Omega_{\rm m}(z) - 1$$

(ΛCDM only)

It is common practice to refer to the mass, radius and circular velocity of the halo thus defined as the virial mass, $M_{\rm vir}$, virial radius, $r_{\rm vir}$, and virial velocity, $V_{\rm vir}$.

$$\bar{\rho}_{\rm h} = \frac{3M_{\rm vir}}{4\pi r_{\rm vir}^3} = \Delta_{\rm vir}(z)\,\Omega_{\rm m}(z)\,\frac{3H^2(z)}{8\pi G}$$

Using that $V_{\rm vir} \equiv \sqrt{G\,M_{\rm vir}/r_{\rm vir}}$ we then have that

$$r_{\rm vir} \simeq 163\,h^{-1}{\rm kpc}\left[\frac{M_{\rm vir}}{10^{12}h^{-1}M_\odot}\right]^{1/3}\left[\frac{\Delta_{\rm vir}}{200}\right]^{-1/3}\Omega_{\rm m,0}^{-1/3}\,(1+z)^{-1}$$

$$V_{\rm vir} \simeq 163\,{\rm km/s}\left[\frac{M_{\rm vir}}{10^{12}h^{-1}M_\odot}\right]^{1/3}\left[\frac{\Delta_{\rm vir}}{200}\right]^{1/6}\Omega_{\rm m,0}^{1/6}\,(1+z)^{1/2}$$

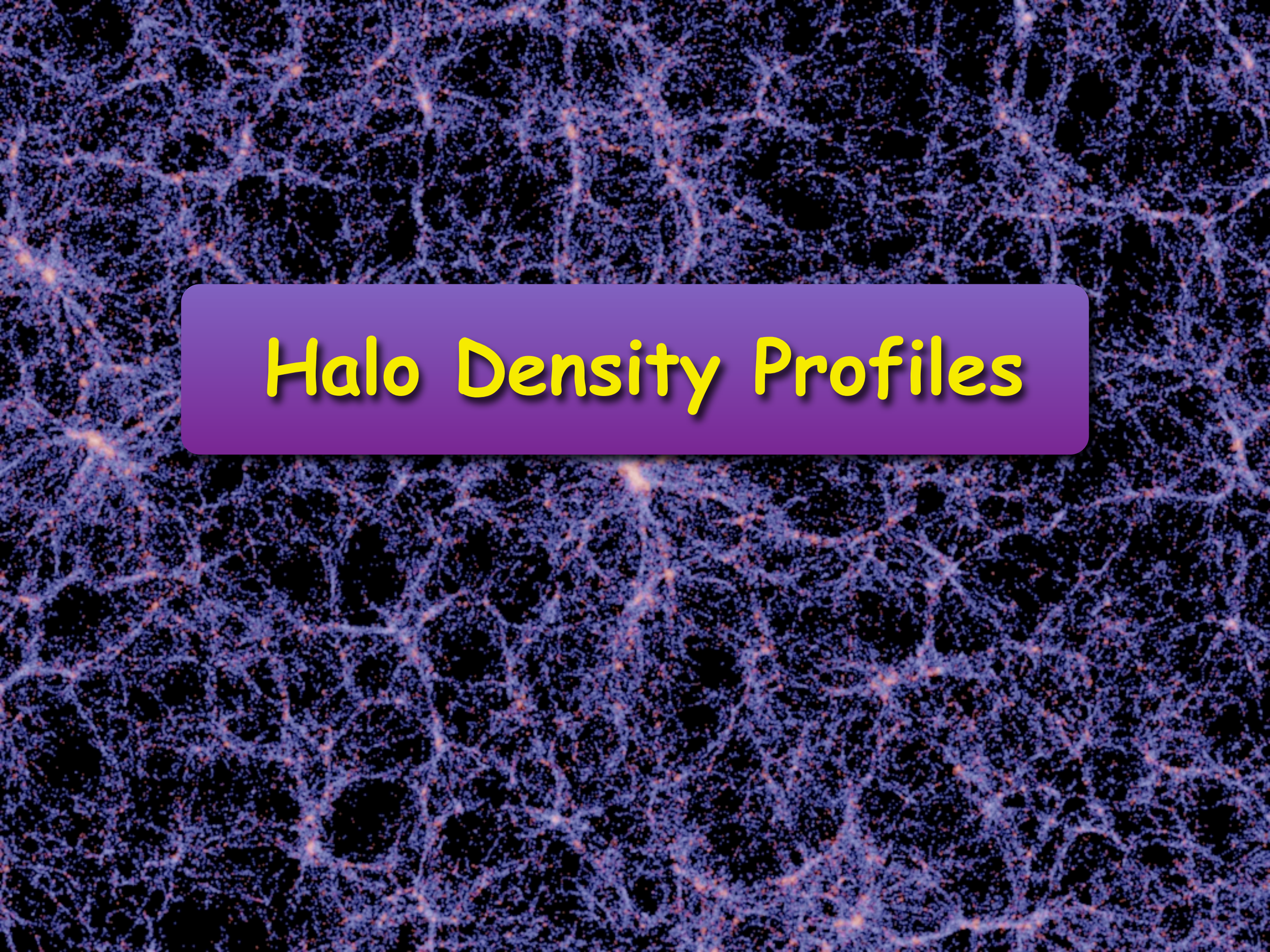

Halo Density Profiles

The NFW Profile

In 1997, Navarro, Frenk & White wrote a seminal paper in which they showed that CDM haloes in N-body simulations have a universal density profile, well fit by a double power-law...

A UNIVERSAL DENSITY PROFILE FROM HIERARCHICAL CLUSTERING

JULIO F. NAVARRO[1]
Steward Observatory, 933 North Cherry Avenue, University of Arizona, Tucson, AZ 85721-0065; jnavarro@as.arizona.edu.
CARLOS S. FRENK
Department of Physics, University of Durham, South Road, Durham DH1 3LE, England; c.s.frenk@uk.ac.durham
AND
SIMON D. M. WHITE
Max-Planck-Institut für Astrophysik, Karl-Schwarzschild-Strasse 1, 85740, Garching bei München, Germany; swhite@mpa-garching.mpg.de

Received 1996 November 13; accepted 1997 July 15

ABSTRACT

We use high-resolution N-body simulations to study the equilibrium density profiles of dark matter halos in hierarchically clustering universes. We find that all such profiles have the same shape, independent of the halo mass, the initial density fluctuation spectrum, and the values of the cosmological parameters. Spherically averaged equilibrium profiles are well fitted over two decades in radius by a simple formula originally proposed to describe the structure of galaxy clusters in a cold dark matter universe. In any particular cosmology, the two scale parameters of the fit, the halo mass and its characteristic density, are strongly correlated. Low-mass halos are significantly denser than more massive systems, a correlation that reflects the higher collapse redshift of small halos. The characteristic density of an equilibrium halo is proportional to the density of the universe at the time it was assembled. A suitable definition of this assembly time allows the same proportionality constant to be used for all the cosmologies that we have tested. We compare our results with previous work on halo density profiles and show that there is good agreement. We also provide a step-by-step analytic procedure, based on the Press-Schechter formalism, that allows accurate equilibrium profiles to be calculated as a function of mass in any hierarchical model.

Subject headings: cosmology: theory — dark matter — galaxies: halos — methods: numerical

The NFW Profile

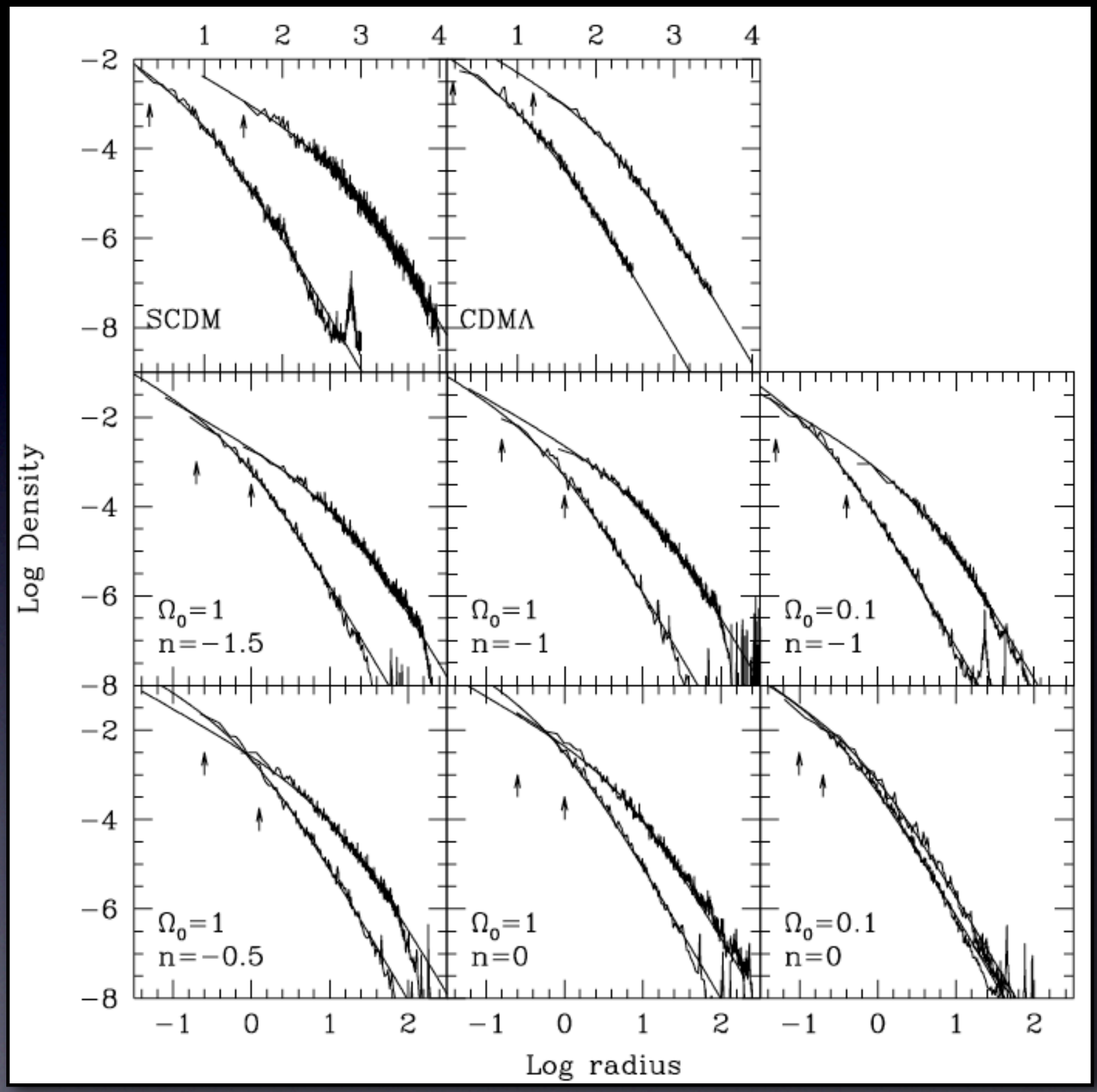

Using a suite of simulations, of different cosmologies, they showed that the density profiles of the dark matter haloes can always be fit by a universal fitting function: the NFW profile

$$\rho(r) = \rho_{\rm crit} \frac{\delta_{\rm char}}{(r/r_{\rm s})\,(1+r/r_{\rm s})^2}$$

The NFW Profile

The NFW profile is given by $\rho(r) = \rho_{\rm crit} \frac{\delta_{\rm char}}{(r/r_{\rm s})\,(1+r/r_{\rm s})^2}$

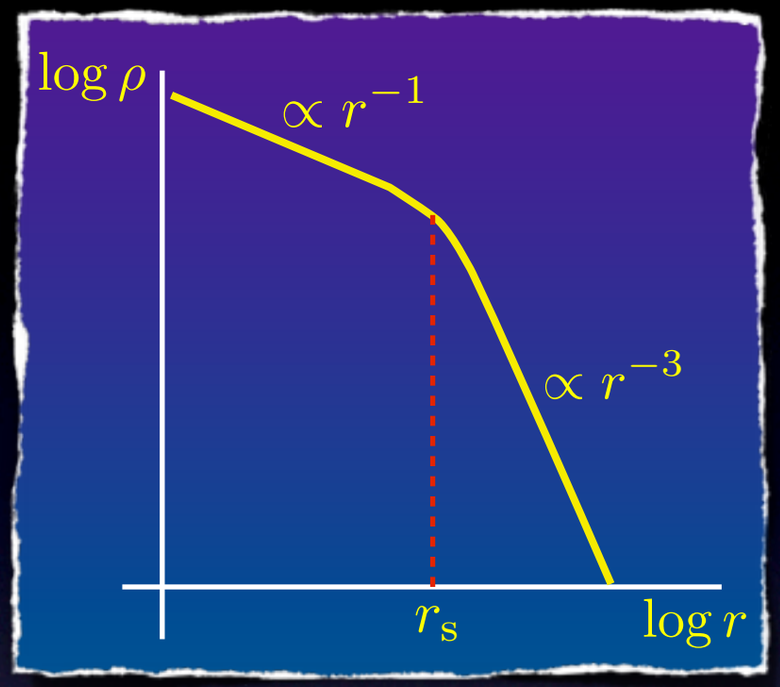

It is completely characterized by the mass $M_{\rm vir}$ and the concentration parameter $c = r_{\rm vir}/r_{\rm s}$, which is related to the characteristic overdensity according to:

$$\delta_{\rm char} = \frac{\Delta_{\rm vir}\,\Omega_{\rm m}}{3}\,\frac{c^3}{f(c)}$$

where $f(x) = \ln(1+x) + x/(1+x)$

The corresponding mass profile is $M(r) = 4\pi\rho_{\rm crit}\delta_{\rm char} r_{\rm s}^3\, f(c) = M_{\rm vir}\frac{f(cx)}{f(c)}$, where $x = r/r_{\rm vir}$

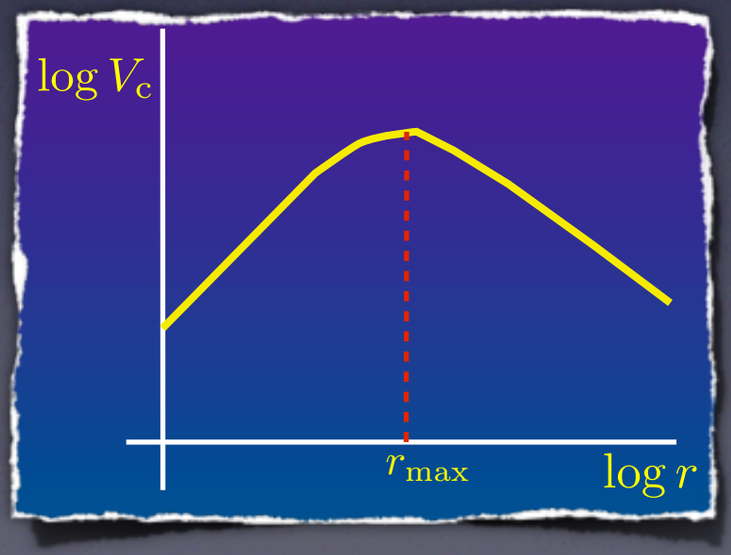

The circular velocity of an NFW profile is $V_{\rm c}(r) = V_{\rm vir}\sqrt{\frac{f(cx)}{x\,f(c)}}$

which has a maximum $V_{\rm max} \simeq 0.465 V_{\rm vir}\sqrt{c/f(c)}$ at $r_{\rm max} \simeq 2.163 r_{\rm s}$

For example, for $c = 10$ one has that $V_{\rm max} \sim 1.2 V_{\rm vir}$.

For $r \ll r_{\rm max}$ the NFW profile has $V_{\rm c} \propto r^{1/2}$.

The Concentration-Mass Relation

NFW97 showed that the characteristic overdensity, $\delta_{\rm char}$, is closely related to the halo's formation time: haloes that form (assemble) earlier are more concentrated....

Since more massive haloes assemble later (on average) they are expected to be less concentrated, giving rise to an inverted concentration-mass relation. Furthermore, because of large scatter in MAHs one expects significant scatter in this relation.

Simulations have shown that halo concentrations follow a log-normal distribution:

$$\mathcal{P}(c|M)\,{\rm d}c = \frac{1}{\sqrt{2\pi}\,\sigma_{\rm lnc}}\,\exp\left[-\frac{(\ln c - \ln \bar{c})^2}{2\sigma_{\rm lnc}^2}\right]\,\frac{{\rm d}c}{c}$$

with $\bar{c} = \bar{c}(M)$ and $\sigma_{\rm lnc} \simeq 0.25$.

Simulations have also shown that even at fixed mass, halo concentration is correlated with assembly time.
(e.g., Wechsler et al. 2002; Zhao et al. 2003)

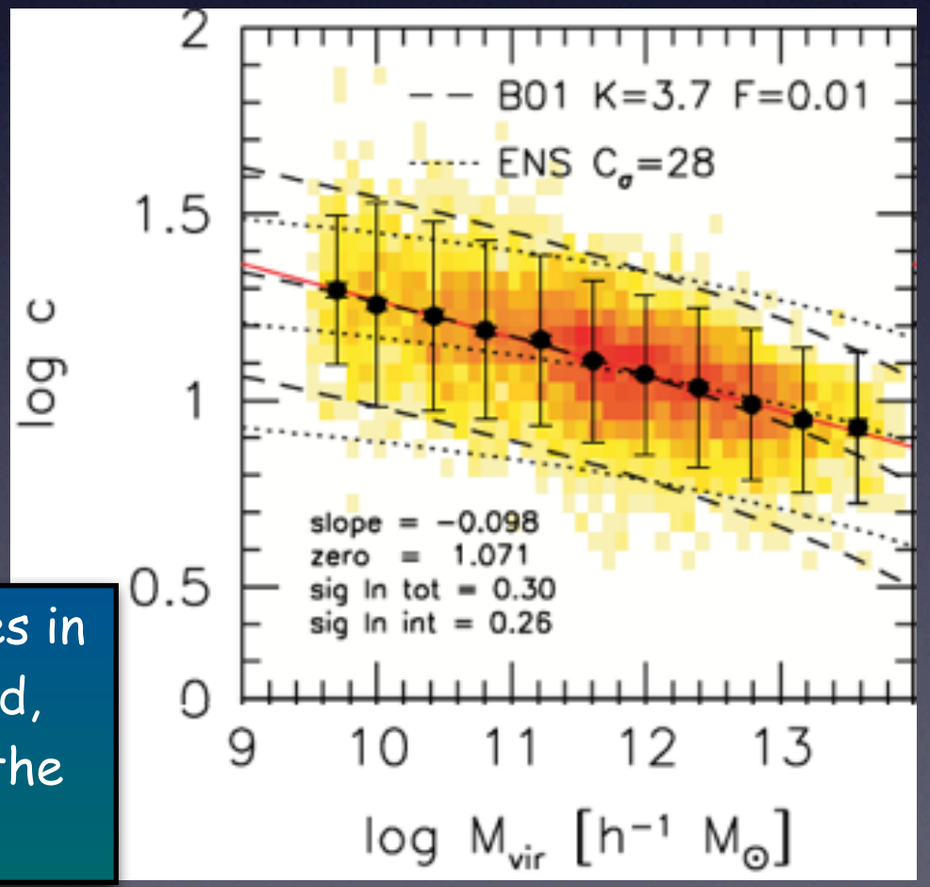

Source: Maccio et al. 2007, MNRAS, 378, 55

The concentration-mass relation of dark matter haloes in a series of N-body simulations. Note that, as expected, more massive haloes are less concentrated, and that the relation has an appreciable amount of scatter...

The Concentration-Mass Relation

Several models have been developed to compute the mean concentration as function of halo mass and cosmology. All these models assume that a halo's characteristic density is related to the mean cosmic density at some characteristic epoch in the halo's history.

(e.g., Bullock et al. 2001; Eke Navarro & Steinmetz 2001; Maccio et al. 2008; Zhao et al. 2009)

At the present, the most accurate of these models is that of Zhao et al. (2009), according to which the average concentration is

$$\bar{c}(M,t) = 4 \times \left\{ 1 + \left[\frac{t}{3.75\, t_{0.04}(M,t)} \right]^{8.4} \right\}^{1/8}$$

Here $t_{0.04}(M,t)$ is the time at which the main progenitor had acquired 4% of its final mass M.

This model is based on the following empirical fact (observed in simulations):

- central structure of halo is established through violent relaxation at early phase of rapid major mergers, leading to NFW profile with c~4.
- subsequent accretion increases mass & size of halo without adding much matter to center, causing concentration to increase with time...

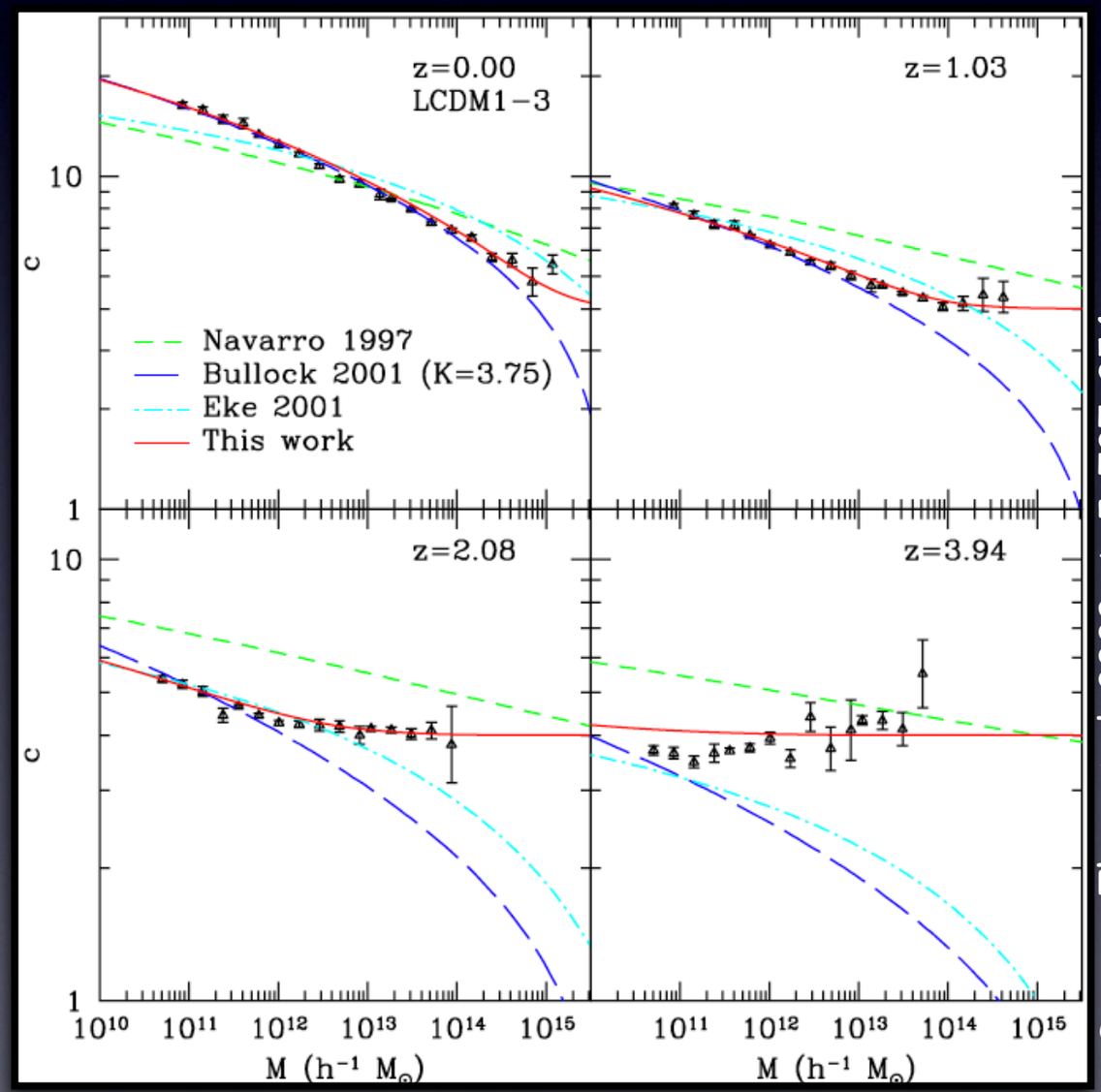

Source: Zhao et al. 2009, ApJ, 707, 354

The Cusp-Core Controversy

Around the turn of the millenium, a lively debate broke out among simulators and observers regarding the actual inner density slopes of dark matter haloes:

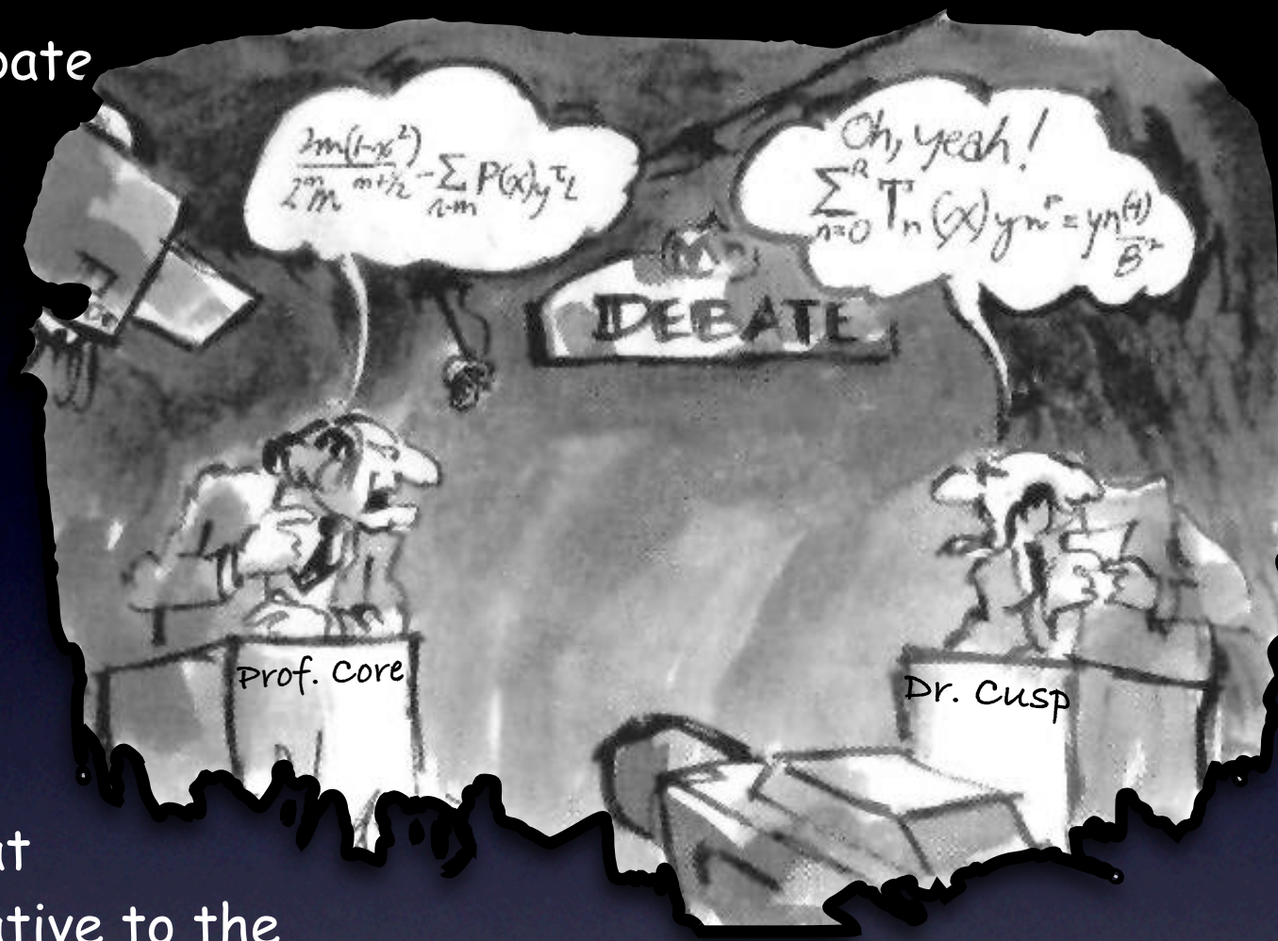

According to the NFW profile, dark matter haloes have central cusps with $\rho \propto r^{-1}$

However, several studies claimed that simulated dark matter haloes have cusps that are significantly steeper. A `popular' alternative to the NFW profile was the Moore profile, which has $\gamma = 1.5$

(e.g., Moore et al. 1998, ApJ, 499, L5; Fukushige & Makino, 2001, ApJ, 557, 533)

At around the same time, however, numerous studies claimed that the observed rotation curves of dwarf galaxies and low-surface brightness (LSB) disk galaxies indicate dark matter haloes with central cores; i.e., $\gamma = 0$

(e.g., Moore 1994; Flores & Primack 1994; McGaugh & de Blok 1998)

The Cusp-Core Controversy

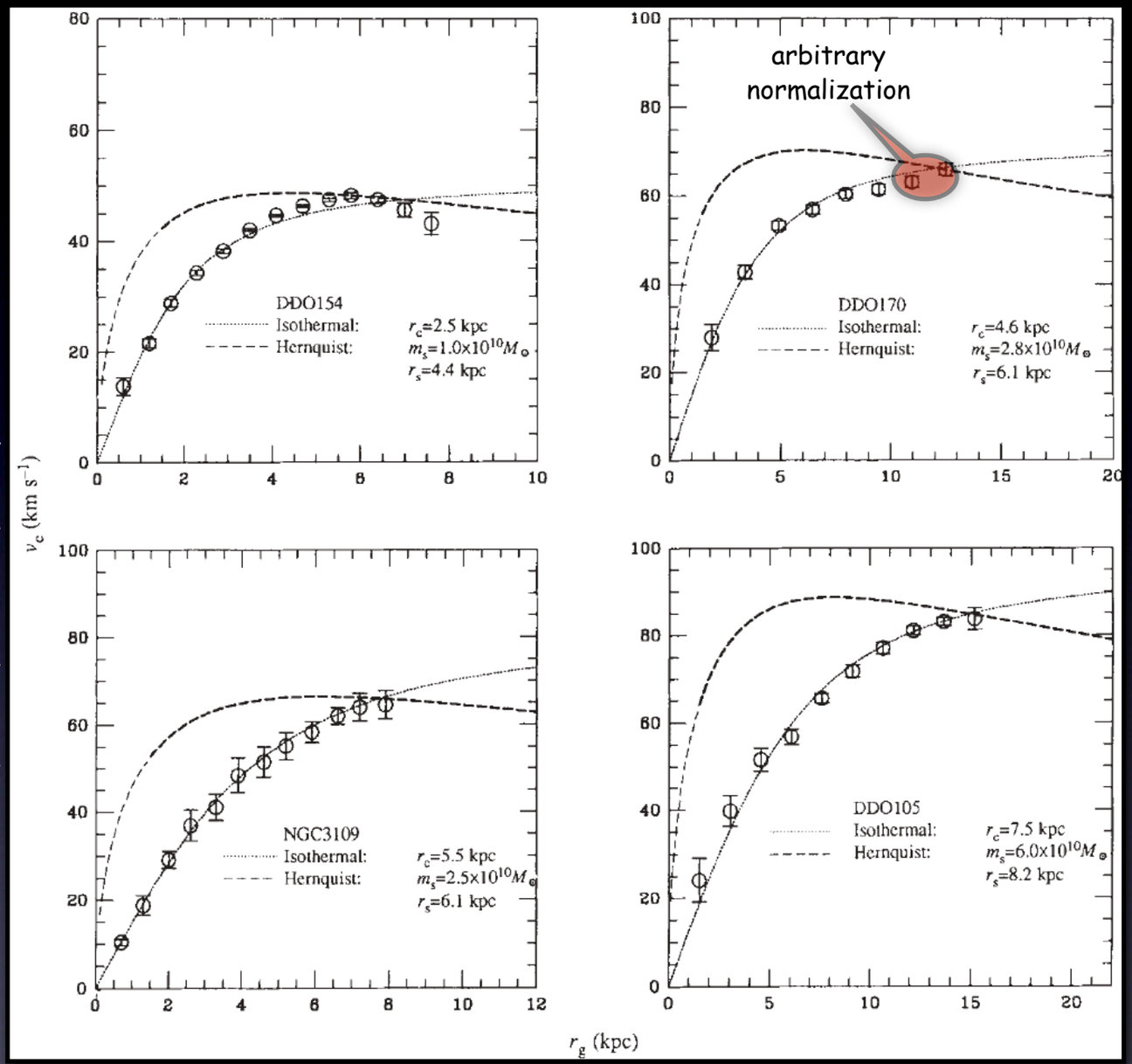

Source: Moore, 1994, Nature, 370, 629

Direct comparison of observed rotation curves with circular velocity curves of dark matter haloes reveals inconsistency....

Evidence against dissipationless dark matter from observations of galaxy haloes

Ben Moore*

Department of Astronomy, University of California, Berkeley, California 94720, USA

THERE are two different types of missing (dark) matter: the unseen matter needed to explain the high rotation velocities of atomic hydrogen in the outer parts of spiral galaxies[1,2], and the much larger amount of (non-baryonic) matter needed to prevent the universe from expanding forever[1] (producing either a 'flat' or a 'closed' Universe)[3]. Several models have been proposed to provide the dark matter required within galaxy haloes for a flat universe, of which cold dark matter (CDM) has proved the most successful at reproducing the observed large-scale structure of the Universe[4–6]. CDM belongs to a class of non-relativistic particles that interact primarily through gravity, and are named dissipationless because they cannot dissipate energy (baryonic particles can lose energy by emitting electromagnetic radiation). Here I show that the modelled small-scale properties of CDM[7–9] are fundamentally incompatible with recent observations[10–13] of dwarf galaxies, which are thought to be completely dominated by dark matter on scales larger than a kiloparsec. Thus, the hypothesis that dark matter is predominantly cold seems hard to sustain.

The Cusp-Core Controversy

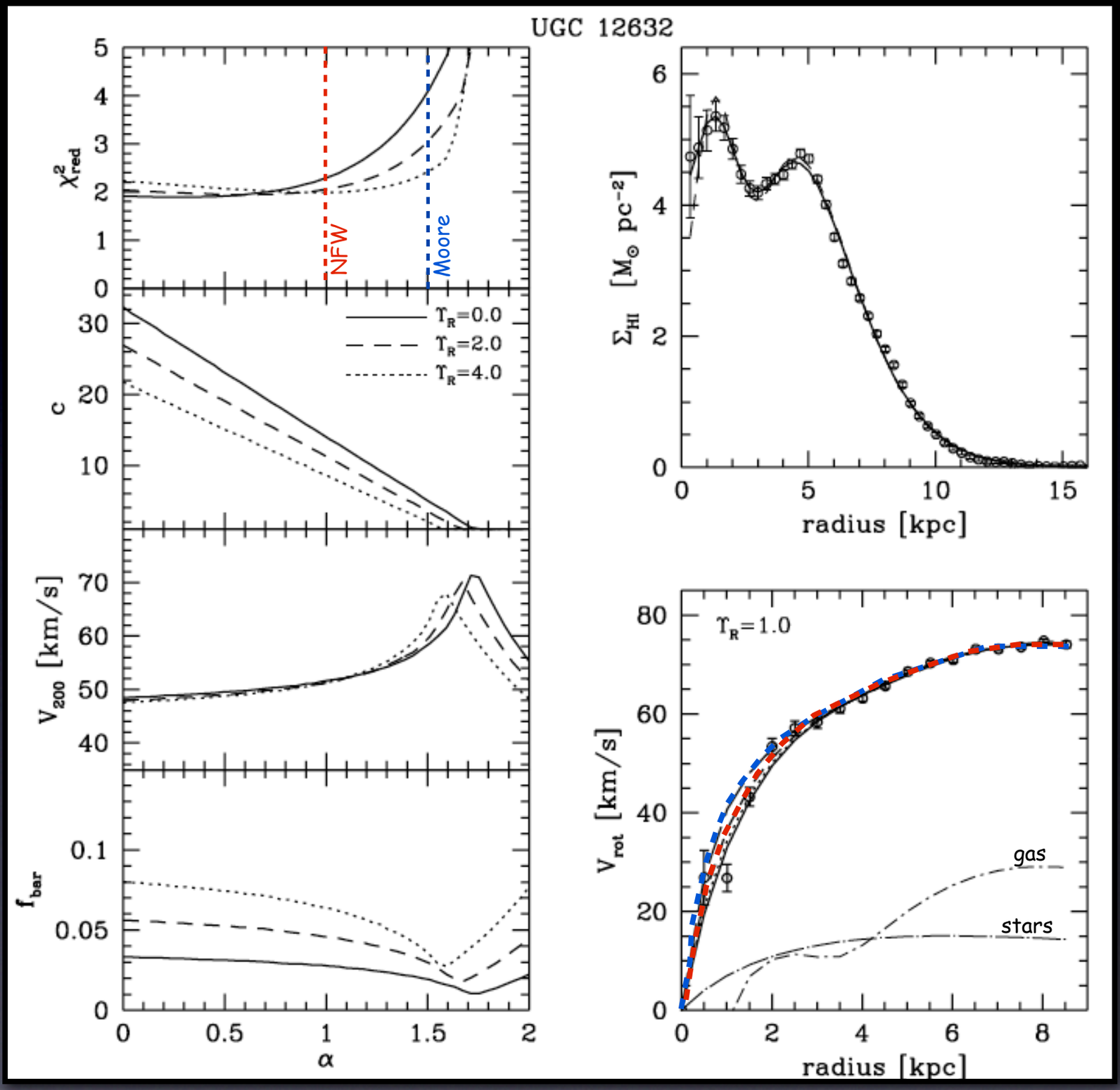

Source: van den Bosch & Swaters, 2001, MNRAS, 325, 1017

It soon became clear, though, that the existing data could not really discriminate between core and cusp, or between NFW and Moore profiles....

Beam smearing and uncertainties in the stellar mass-to-light ratios hamper unique mass decompositions.

Issues with non-circular motions due to bars, triaxiality, asymmetric drift etc. are a concern..

Better data, of higher spatial resolution was required...

van den Bosch et al., 2000
van den Bosch & Swaters, 2001
Swaters et al., 2003
Dutton et al., 2005

The Cusp-Core Controversy

One decade later:

* Spatial resolution of data has improved
* Data has consequently become more complicated
* Conclusions remain equally outlandish....

TO BE CONTINUED...

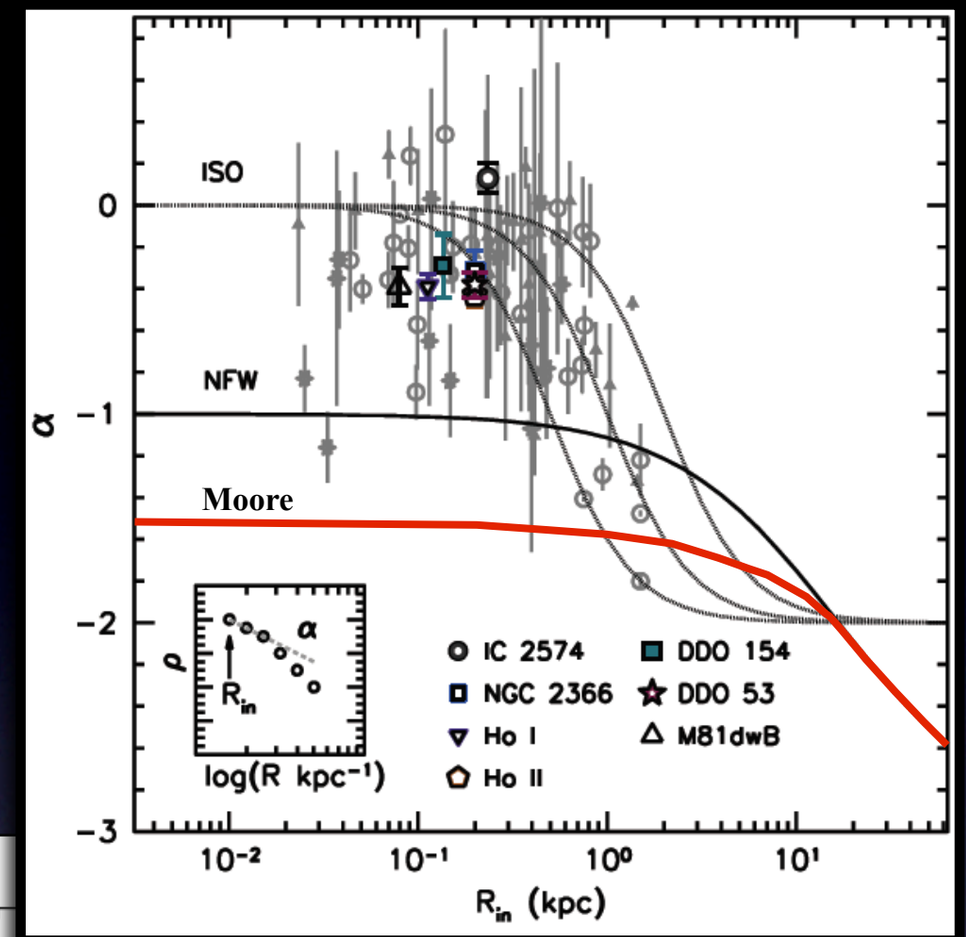

Source: Oh et al. 2011, AJ, 141, 193

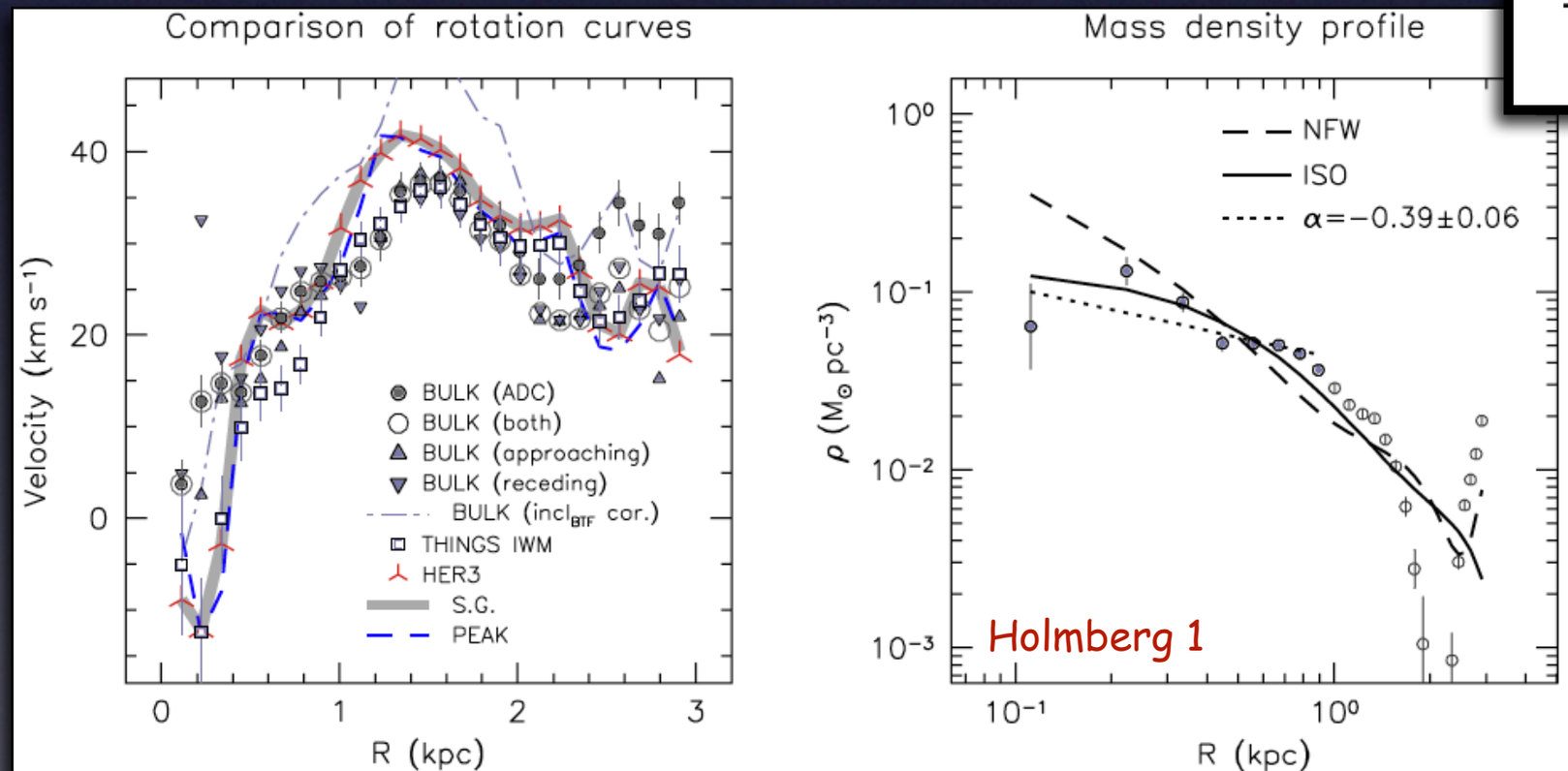

The Cusp-Core Controversy

credit: A. Pontzen & F. Governato

Even *if* observed dark matter haloes have cusps, this does not necessarily rule out CDM: Baryons to the rescue!!

Baryons may have several effects:

- they can steepen the central profile via adiabatic contraction
- they can create cores via dynamical friction
- they can create cores via three-body interactions (i.e., massive binary BHs)
- they can create cores via supernova feedback

The Cusp-Core Controversy

Of the various effects mentioned on the previous slide, only the supernova (SN) feedback one is likely to play a role in dwarf and LSB galaxies....

As shown by Pontzen & Governato (2012) SN feedback can result in impulsive heating of central region; since expansion speeds of winds are much faster than local circular speed, winds can cause changes in the potential that are virtually instantaneous (impulsive).

Repeated SN-driven outflows out of the central regions of (dwarf) galaxies may therefore create cores in their dark matter haloes.

Source: Pontzen & Governato, 2012, MNRAS, 412, 3464

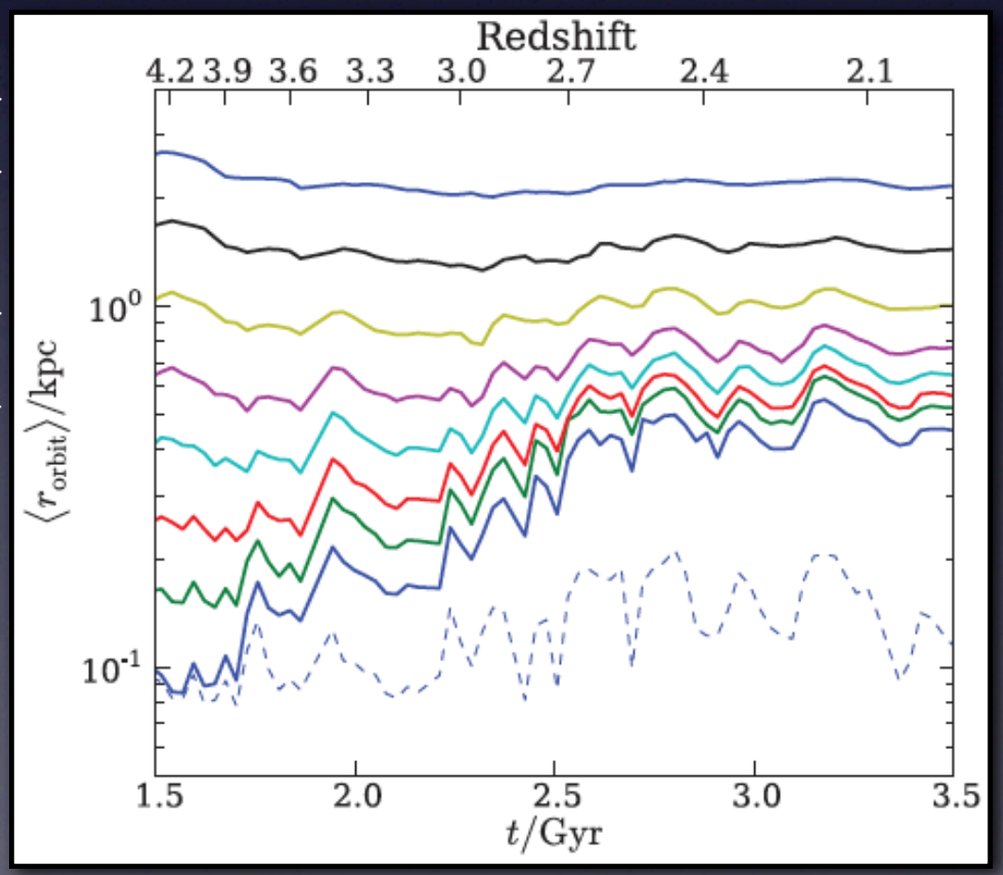

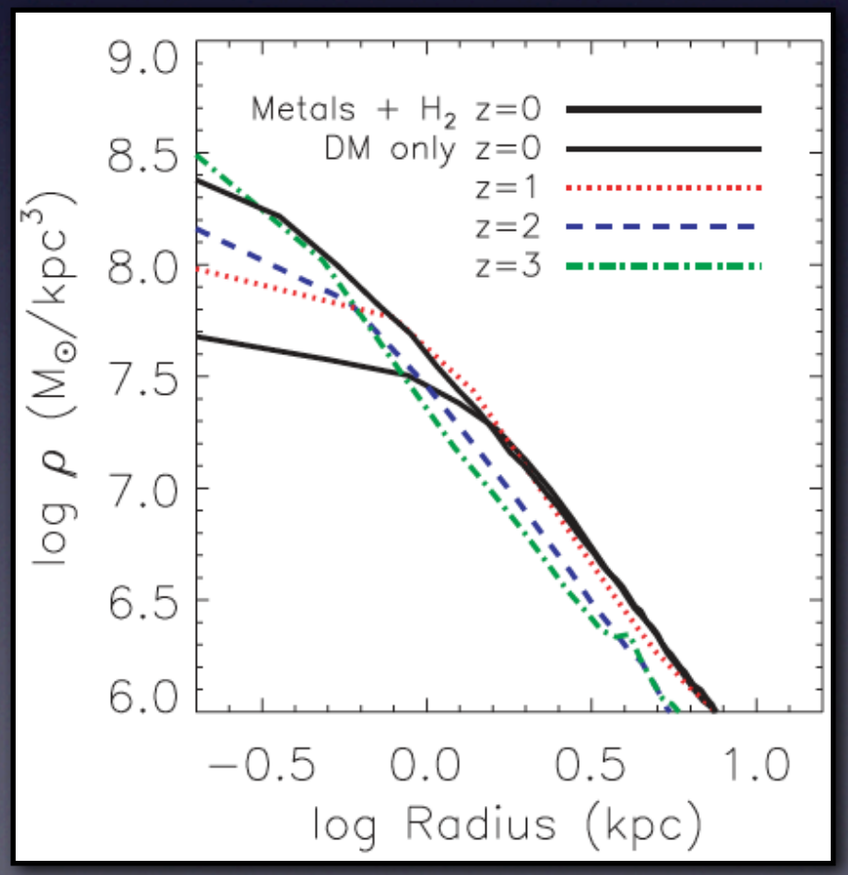

Source: Governato et al., 2012, MNRAS, 422, 1231

Halo Density Profiles in the New Millenium

While the cusp-core controversy continues, the dispute among simulators as to the exact cusp-slope of dark matter haloes has largely been resolved...

Part of the discrepancy was related to resolution issues in the simulations.

But the main solution seems to be that dark matter haloes do not have double power-law density profiles....Neither NFW- nor Moore-profile are perfect fits...

Source: Navarro et al. 2004, MNRAS, 349, 1039

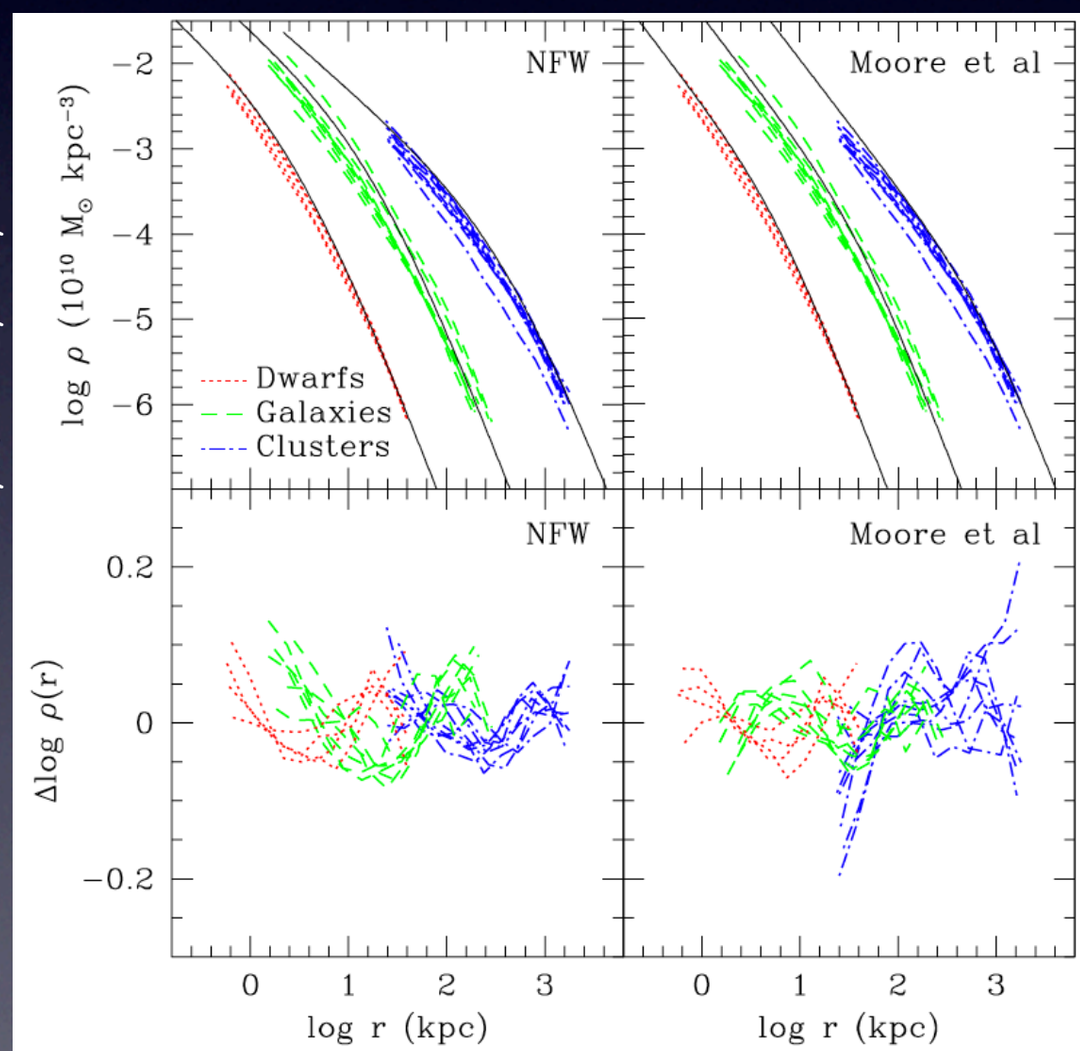

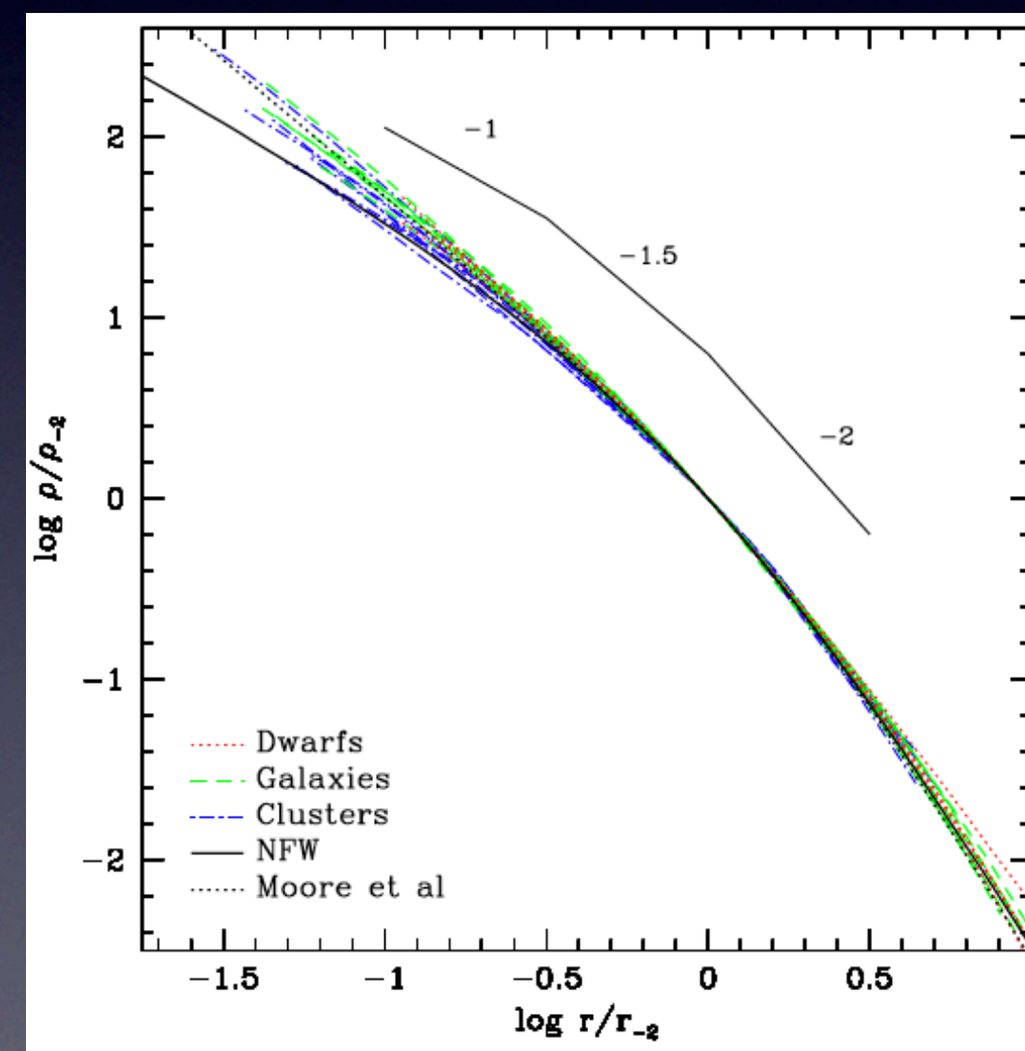

The Einasto Profile

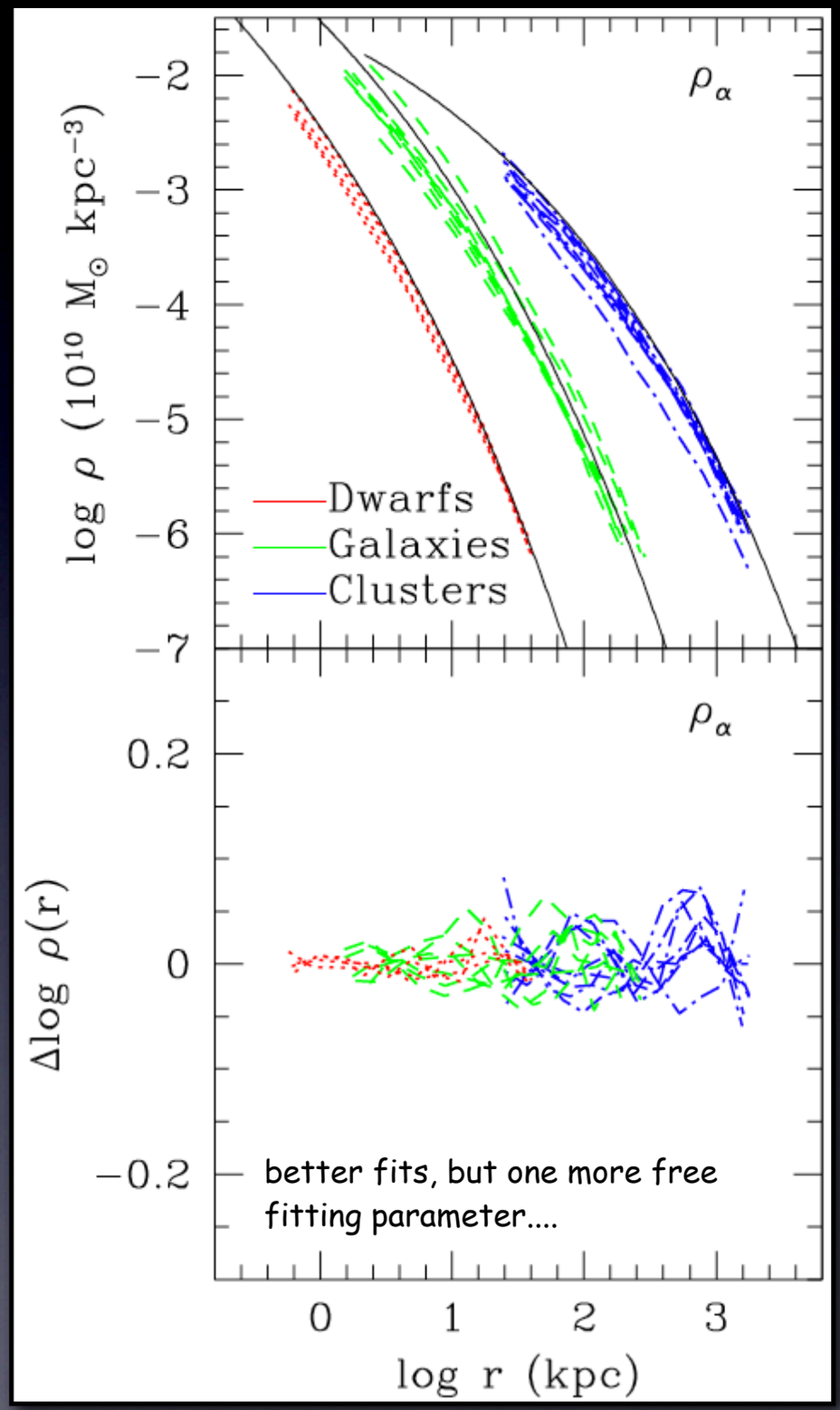

Navarro et al. (2004) showed that dark matter haloes in simulations are better fit by an Einasto profile:

$$\rho(r) = \rho_{-2} \exp\left[\frac{-2}{\alpha}\left\{\left(\frac{r}{r_{-2}}\right)^{\alpha} - 1\right\}\right]$$

The slope of the Einasto profile is a power-law function of radius:

$$\frac{\mathrm{d}\ln\rho}{\mathrm{d}\ln r} = -2\left(\frac{r}{r_{-2}}\right)^{\alpha}$$

The best-fit value of α typically spans the range $0.12 < \alpha < 0.25$

(Gao et al., 2008, MNRAS, 387, 536)

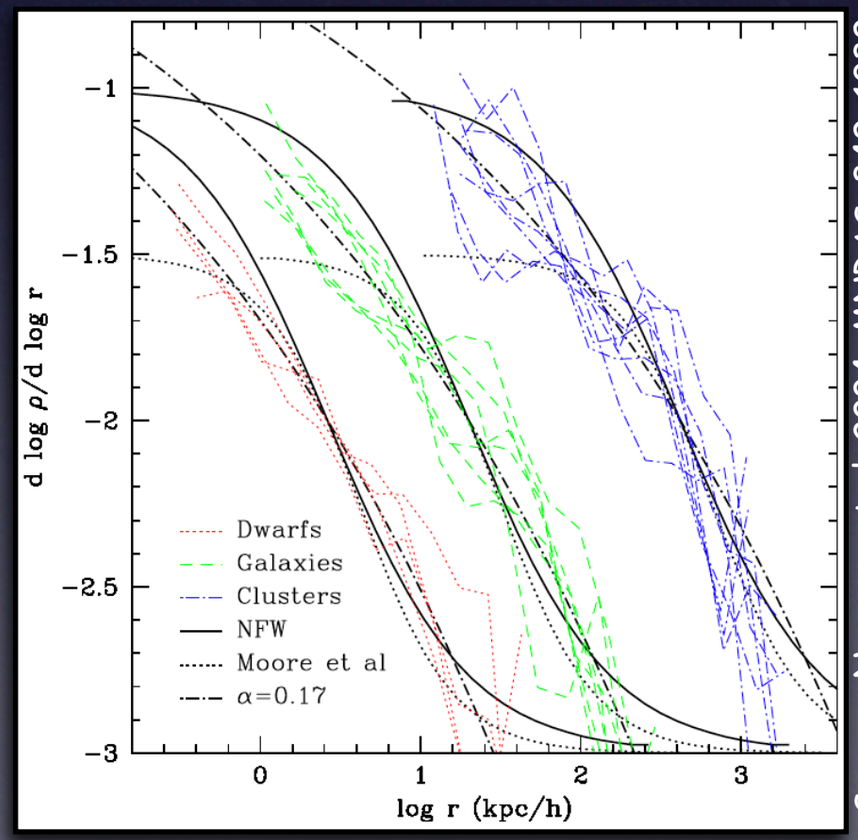

Source: Navarro et al. 2004, MNRAS, 349, 1039

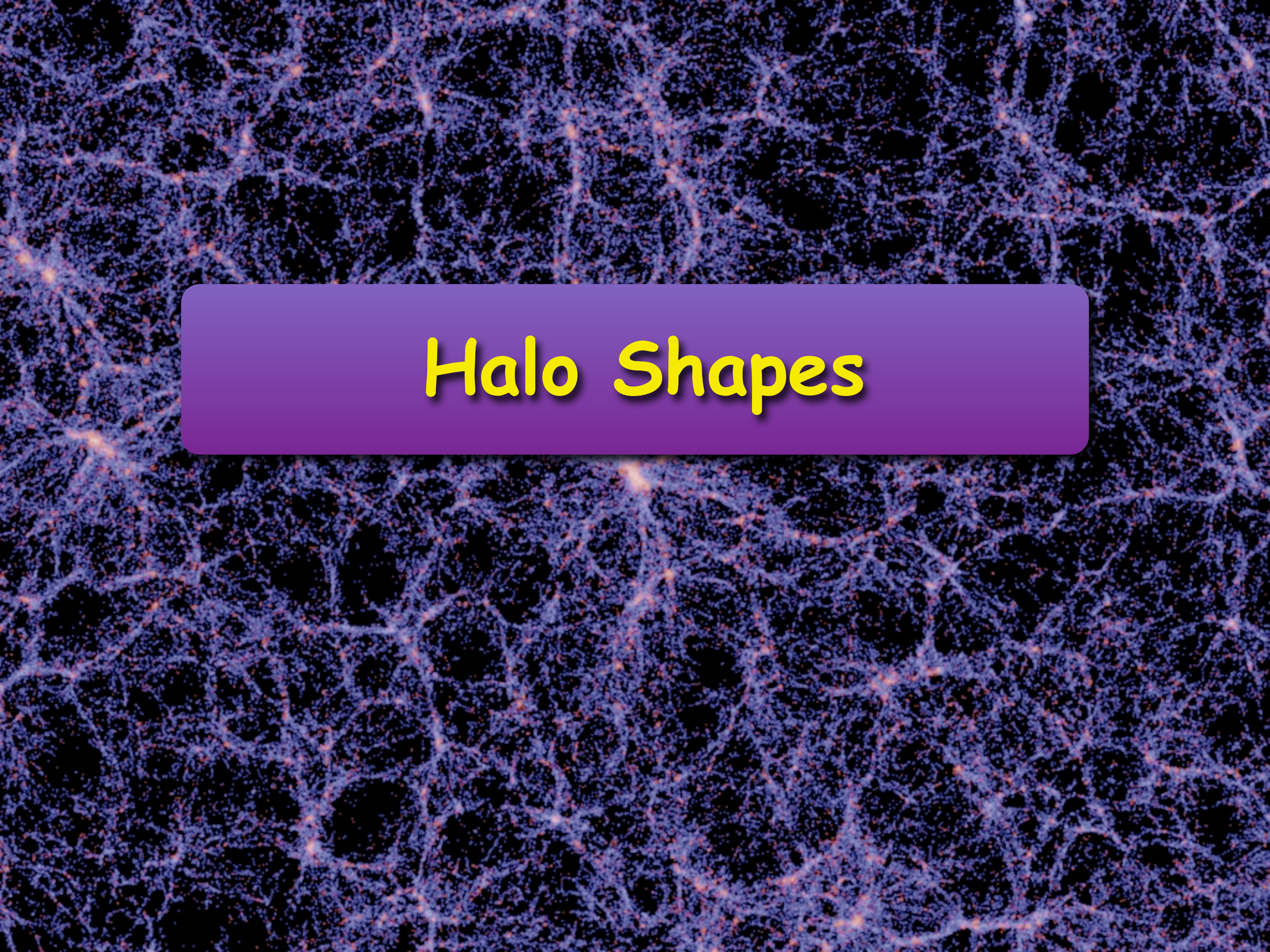

Halo Shapes

Halo Shapes

As we have seen in our discussion of the Zeldovich approximation, because of the tidal tensor $\partial^2\Phi/\partial x_i \partial x_j$ perturbations are not expected to be spherical. Since gravity accentuates non-sphericity, collapsed objects are also not expected to be spherical.

Numerous authors have fitted dark matter haloes in N-body simulations with ellipsoids, characterized by the lengths of the axes $a \geq b \geq c$

These axes can be used to specify the dimensionless shape parameters

$$s = \frac{c}{a} \qquad q = \frac{b}{a} \qquad p = \frac{c}{b}$$

and/or the triaxiality parameter

$$T = \frac{a^2 - b^2}{a^2 - c^3} = \frac{1 - q^2}{1 - s^2}$$

Oblate: T = 0

Prolate: T = 1

CDM haloes in simulations typically have $0.5 < T < 0.85$

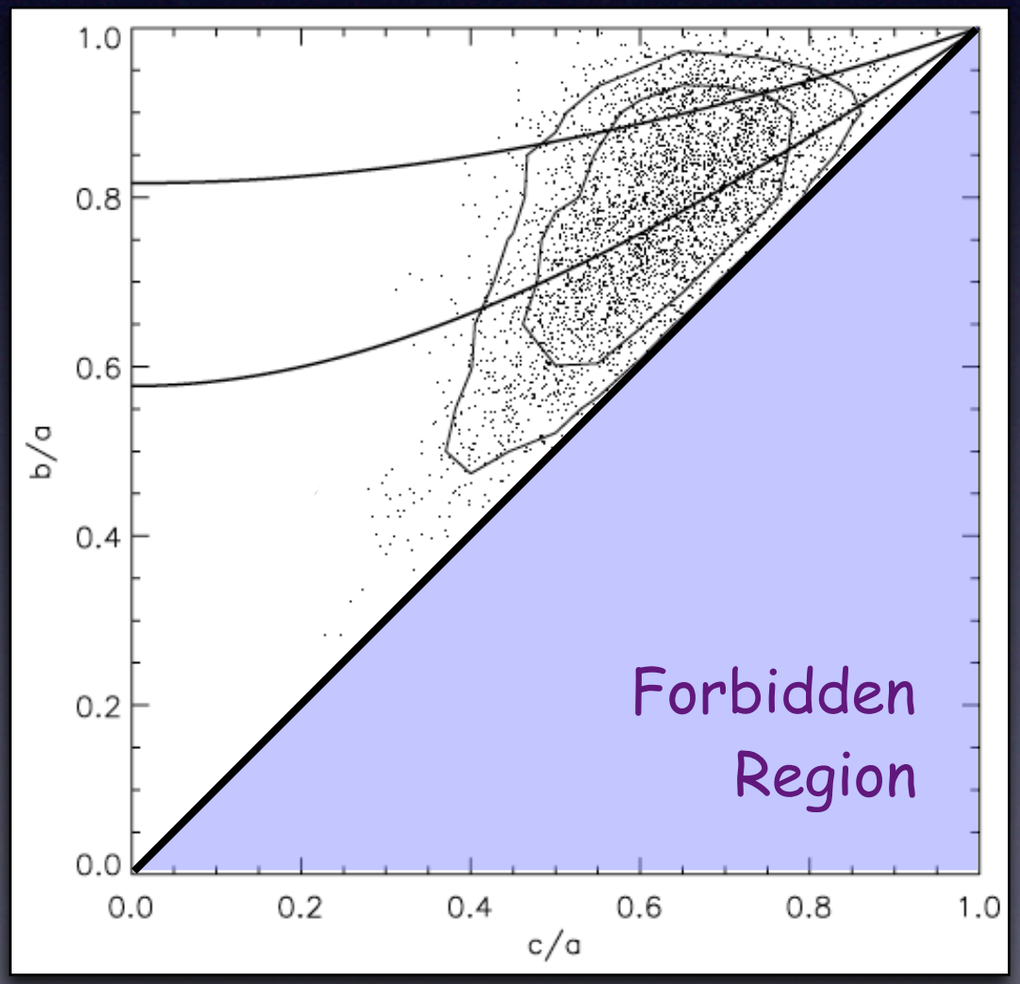

Source: Bailin & Steinmetz, 2005, ApJ, 627,647

Halo Shapes

Simulations show that more massive haloes are more aspherical (more flattened).

Allgood et al. (2006) found that the mass and redshift dependence is well characterized by

$$\langle s \rangle(M,z) = (0.54 \pm 0.03) \left[\frac{M}{M^*(z)}\right]^{-0.050\pm0.003}$$

where $M^*(z)$ is the characteristic halo mass at redshift z.

Simulations suggest that the shape of a halo is tightly correlated with its merger history:

Haloes that assembled earlier are more spherical

Haloes that experienced a recent major merger are typically close to prolate, with major axis reflecting direction along which merger occurred

Currently there are only few observational constraints on halo shapes....

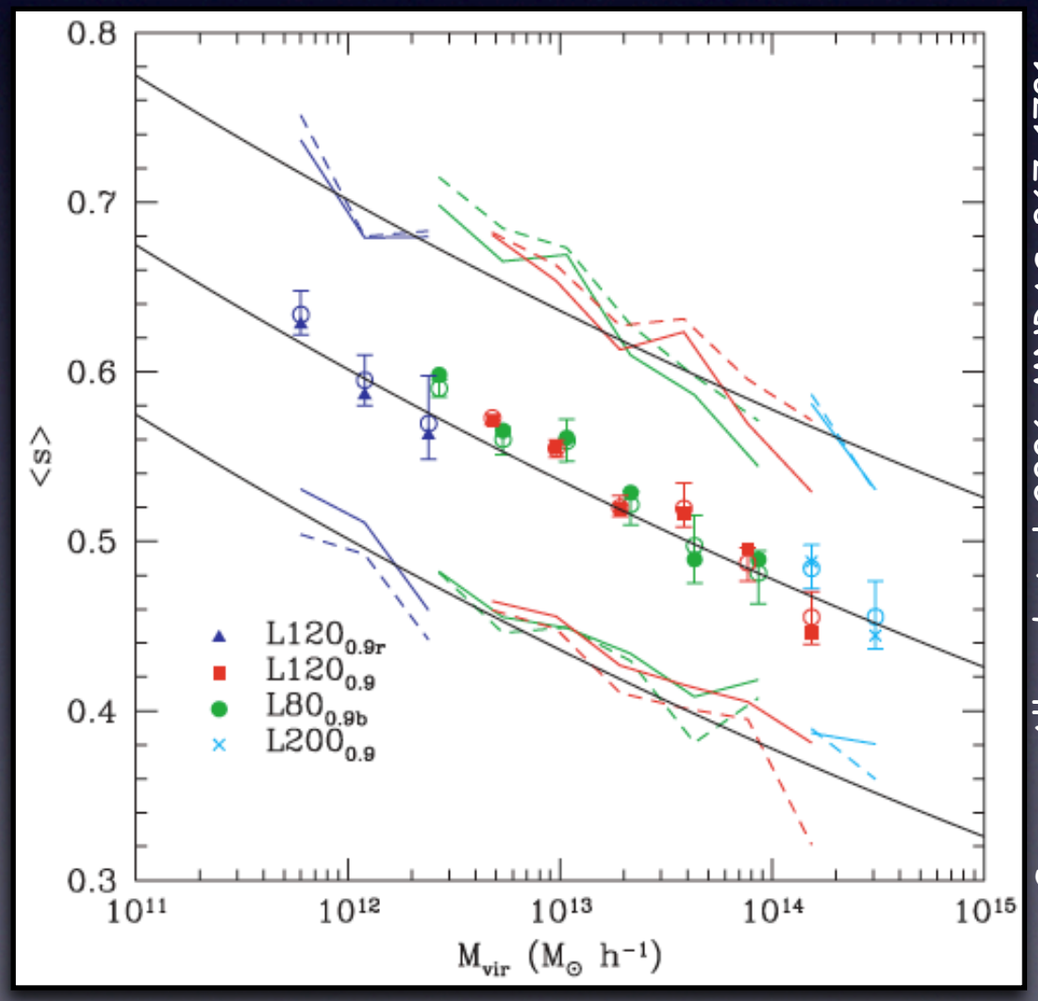

Source: Allgood et al. 2006, MNRAS, 367, 1781

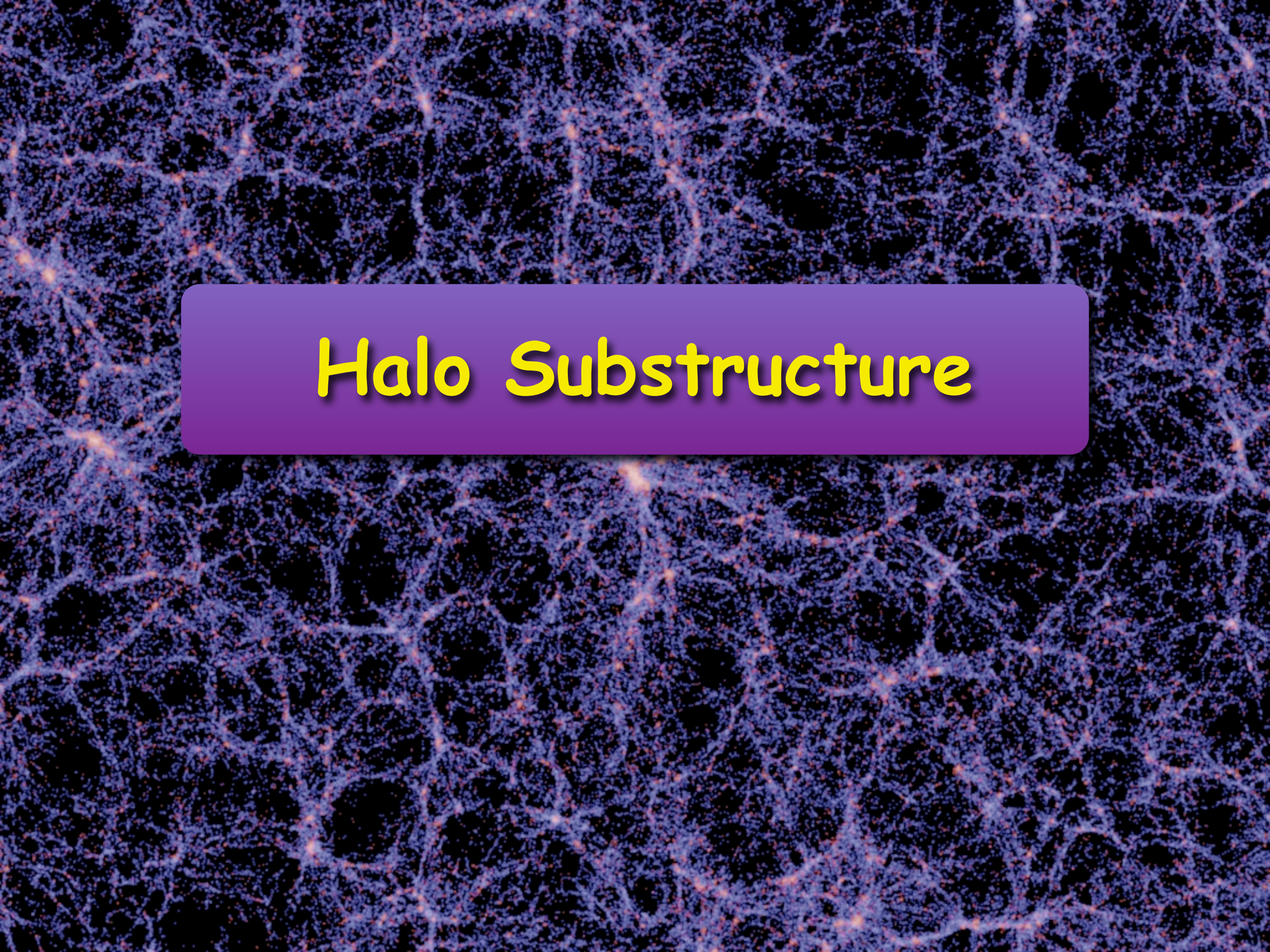

Halo Substructure

Halo Substructure

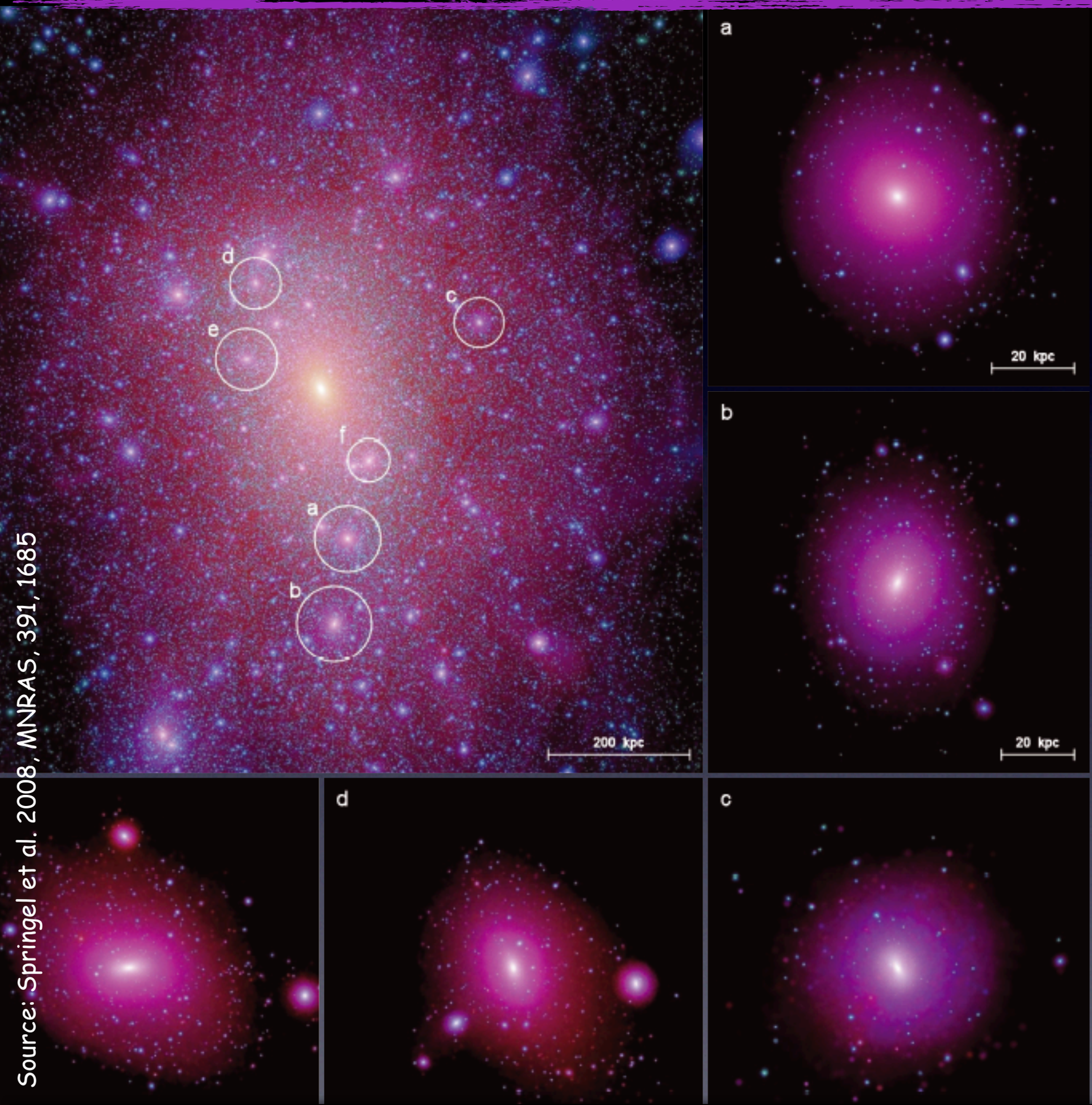

Source: Springel et al. 2008, MNRAS, 391, 1685

Up until the end of the 1990s numerical simulations revealed little if any substructure in dark matter haloes.

Nowadays, faster computers allow much higher mass- and force-resolution, and simulations routinely reveal a wealth of substructure...

Dark matter subhaloes are the remnants of host haloes that survived accretion/merging into a bigger host halo.

While orbiting their hosts, they are subjected to forces that try to dissolve them: dynamical friction, impulsive encounters, and tidal forces....

The Subhalo Mass Function

The subhalo mass function, which describes the number of subhaloes of a given mass per host halo, is well fit by a Schechter function

$$\frac{\mathrm{d}n}{\mathrm{d}\ln(m/M)} = \frac{f_0}{\beta\,\Gamma(1-\gamma)}\left(\frac{m}{\beta M}\right)^{-\gamma}\exp\left[-\left(\frac{m}{\beta M}\right)\right]$$

Here m and M are the masses of subhalo and host halo. Simulations indicate that $\gamma \sim 0.9 \pm 0.1$ and $0.1 < \beta < 0.5$. The large uncertainties relate to uncertainties in defining (sub)haloes in numerical simulations...

The parameter f_0 is the mean subhalo mass fraction:

$$f_0 = \frac{1}{M}\int m\frac{\mathrm{d}n}{\mathrm{d}m}\,\mathrm{d}m = \int \frac{\mathrm{d}n}{\mathrm{d}\ln(m/M)}\,\mathrm{d}\left(\frac{m}{M}\right)$$

and is difficult to measure reliably in simulations; typically one can only measure it down to the mass resolution of the simulation...

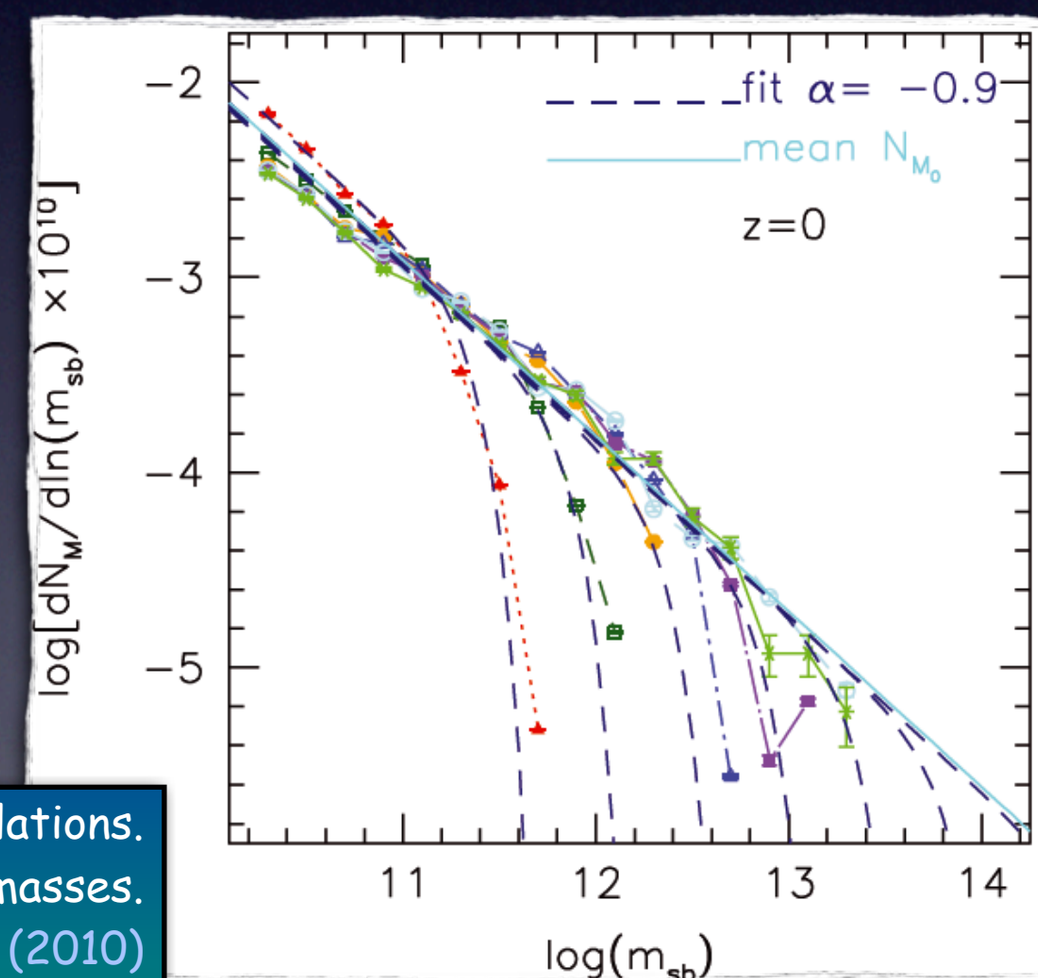

Subhalo mass functions in a series of N-body simulations. Different colors correspond to different host halo masses. Source: Giocoli, Tormen, Sheth & van den Bosch (2010)

Mass Stripping

In addition to the ("evolved") subhalo mass function, which reflects the abundance of subhaloes as a function of their present-day mass, one can also define the un-evolved subhalo mass function, which measures the abundance as function of their mass at infall...

Difference between evolved & un-evolved mass functions reflects mass stripping: Depending on their mass and orbit, subhaloes can loose large fractions of their mass, and even be tidally disrupted....

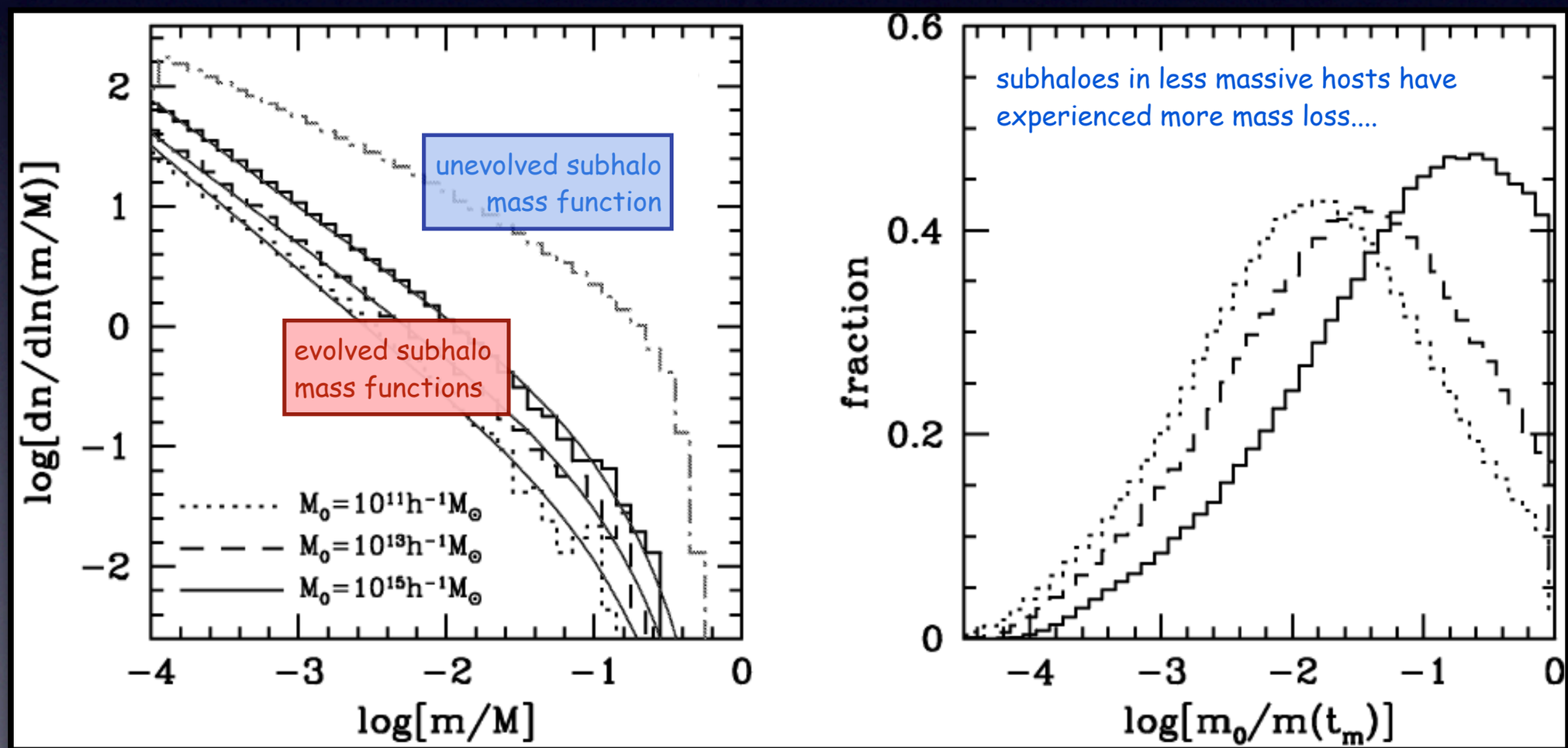

Source: van den Bosch et al. 2005, MNRAS, 359, 1029

Subhalo Mass Functions

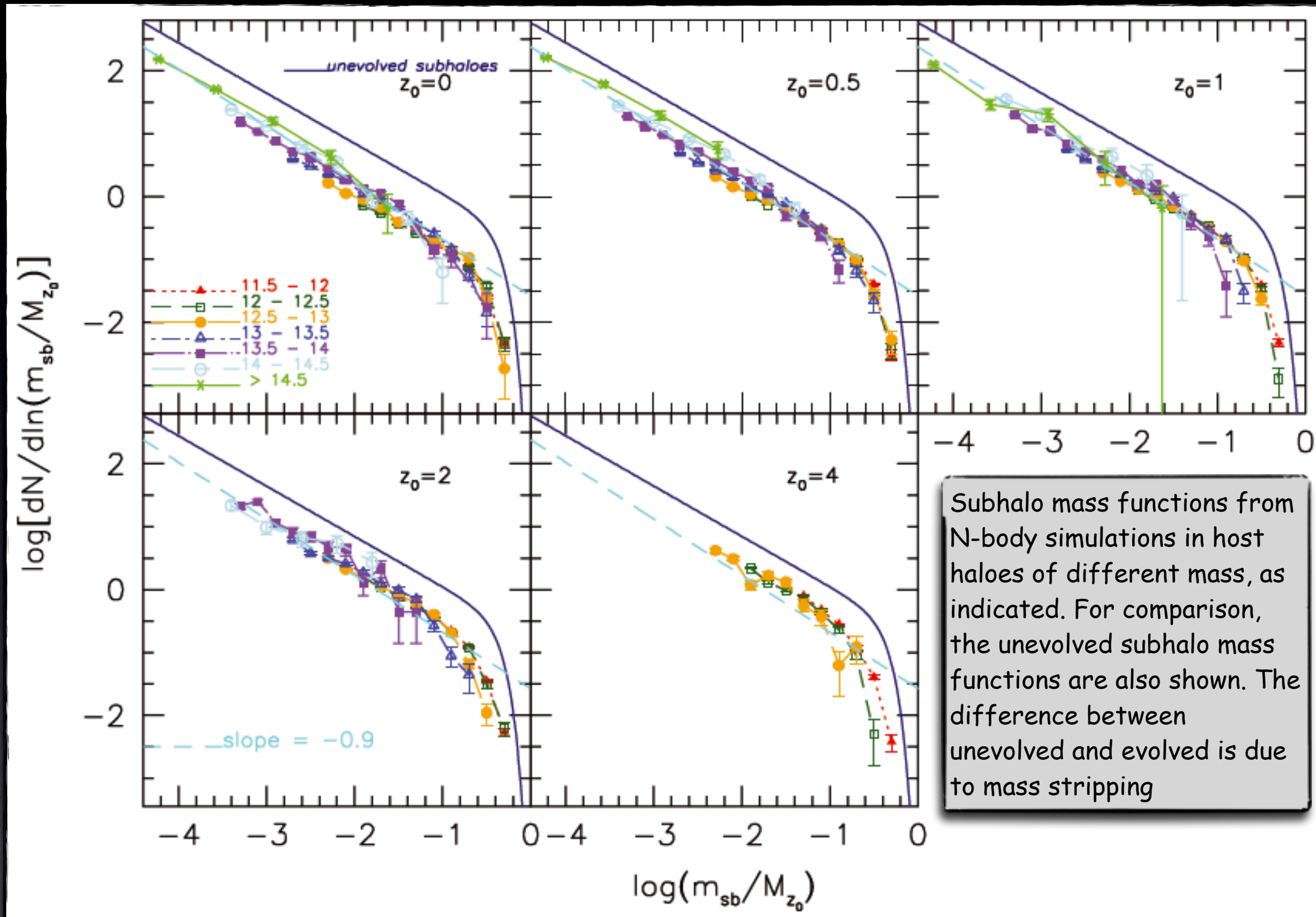

Subhalo mass functions from N-body simulations in host haloes of different mass, as indicated. For comparison, the unevolved subhalo mass functions are also shown. The difference between unevolved and evolved is due to mass stripping

Source: Giocoli et al, 2010, MNRAS, 404, 502

Subhalo Mass Fractions

Simulations show that halos that assemble earlier have, at present day, less substructure. Since more massive haloes assemble later, they, on average, have more substructure.

As shown in van den Bosch (2005), this is a consequence of the fact that the unevolved subhalo mass function is virtually independent of halo mass: all haloes accrete the same subhalo population (in units of m/M). Those that accrete them earlier (=assemble earlier), stripped more mass from them, resulting in lower subhalo mass fraction...

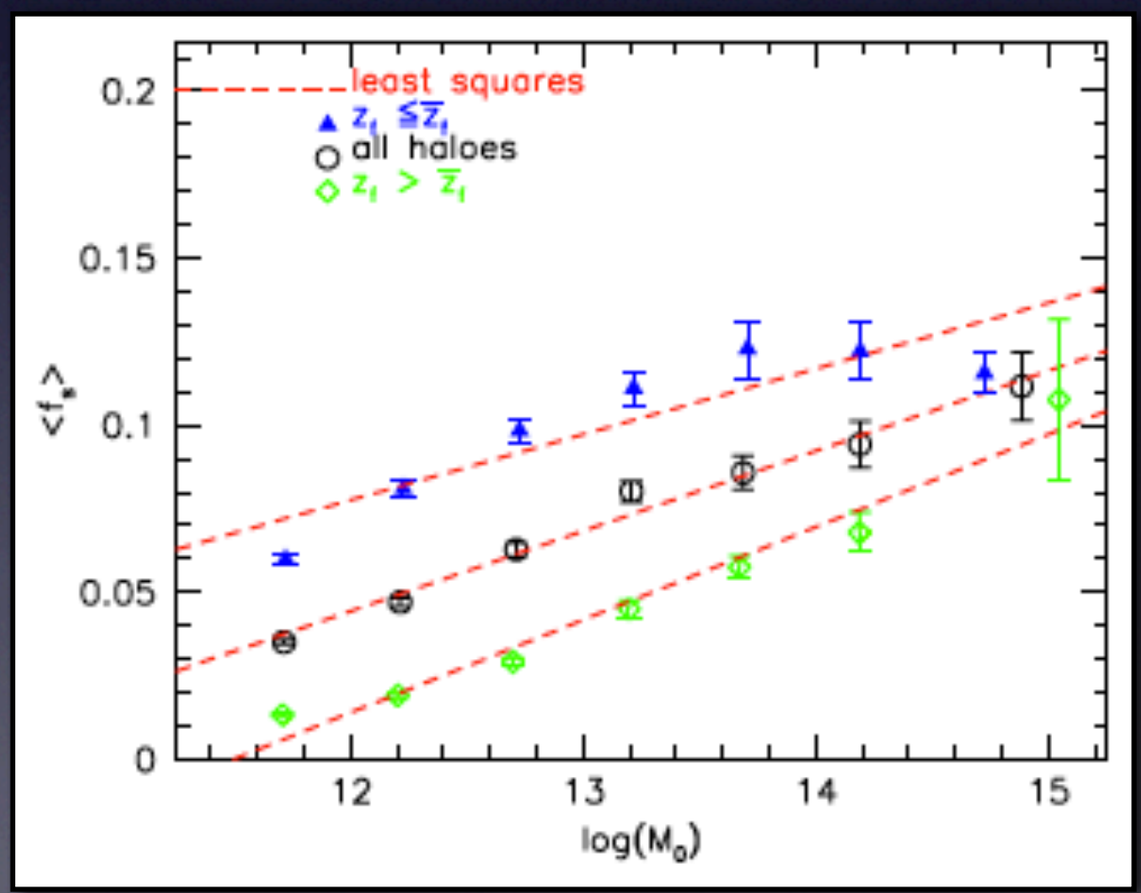

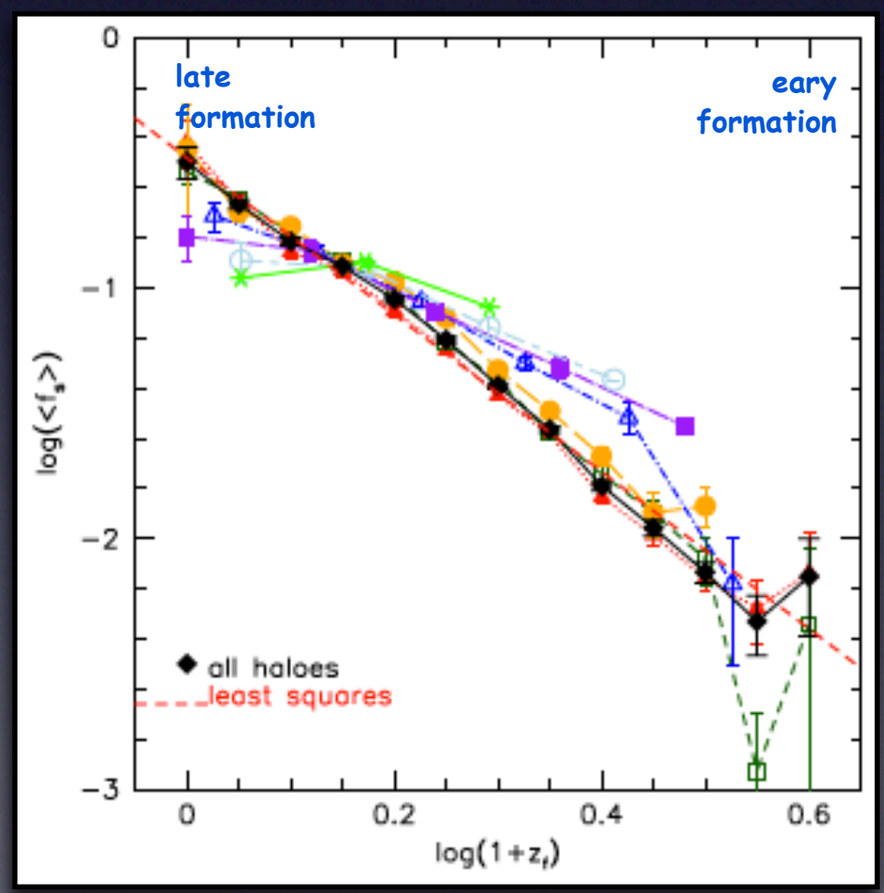

Source: Giocoli et al, 2010, MNRAS, 404, 502

The Spatial Distribution of Subhaloes

Simulations show that dark matter subhaloes are less centrally concentrated than the dark matter, and that the radial distribution is independent of subhalo mass (i.e., there is no indication of mass segregation)

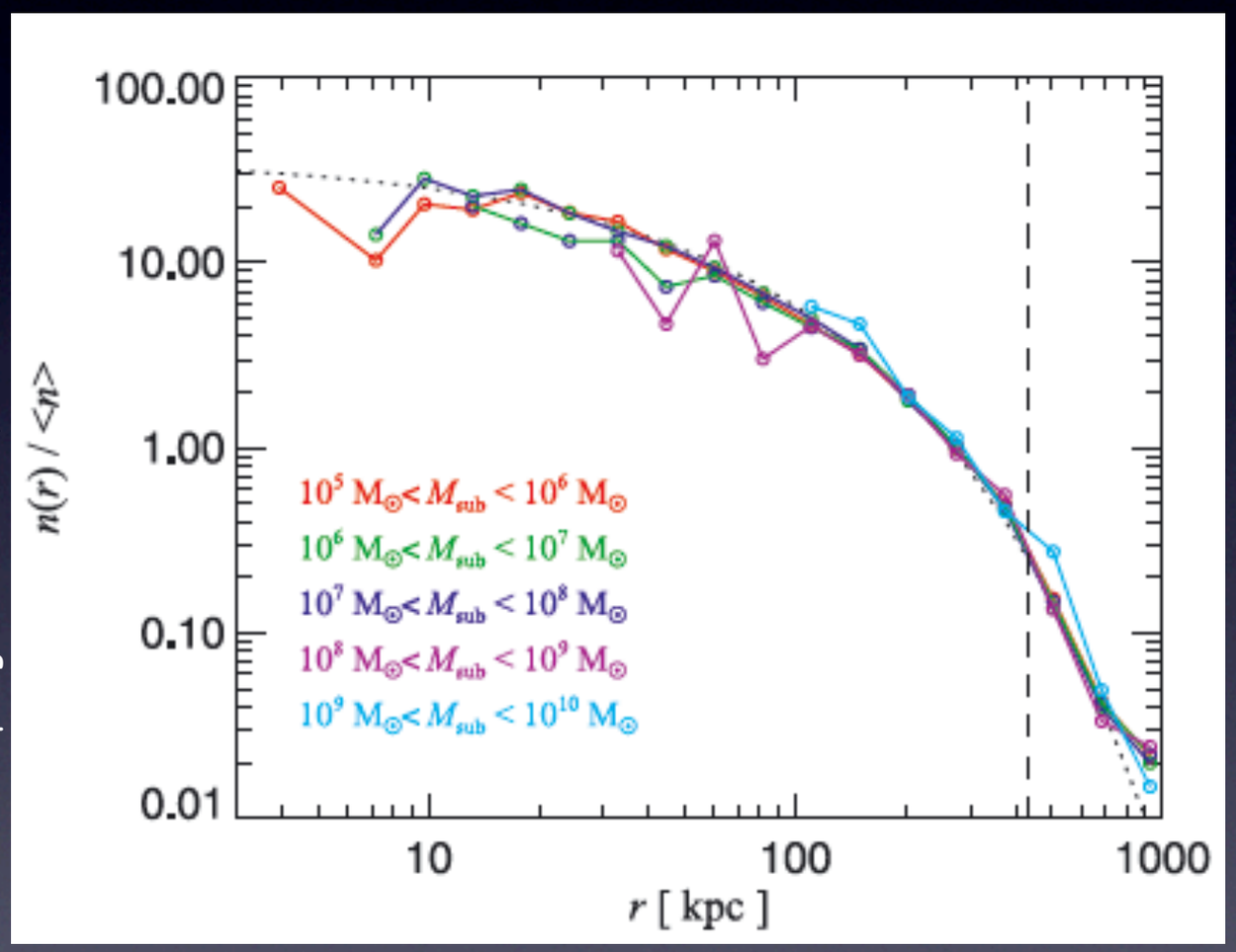

Source: Springel et al. 2008, MNRAS, 391, 1685

normalized radial number density profiles of dark matter subhaloes for five different mass bins. Note that there appears to be no dependence on subhalo mass.

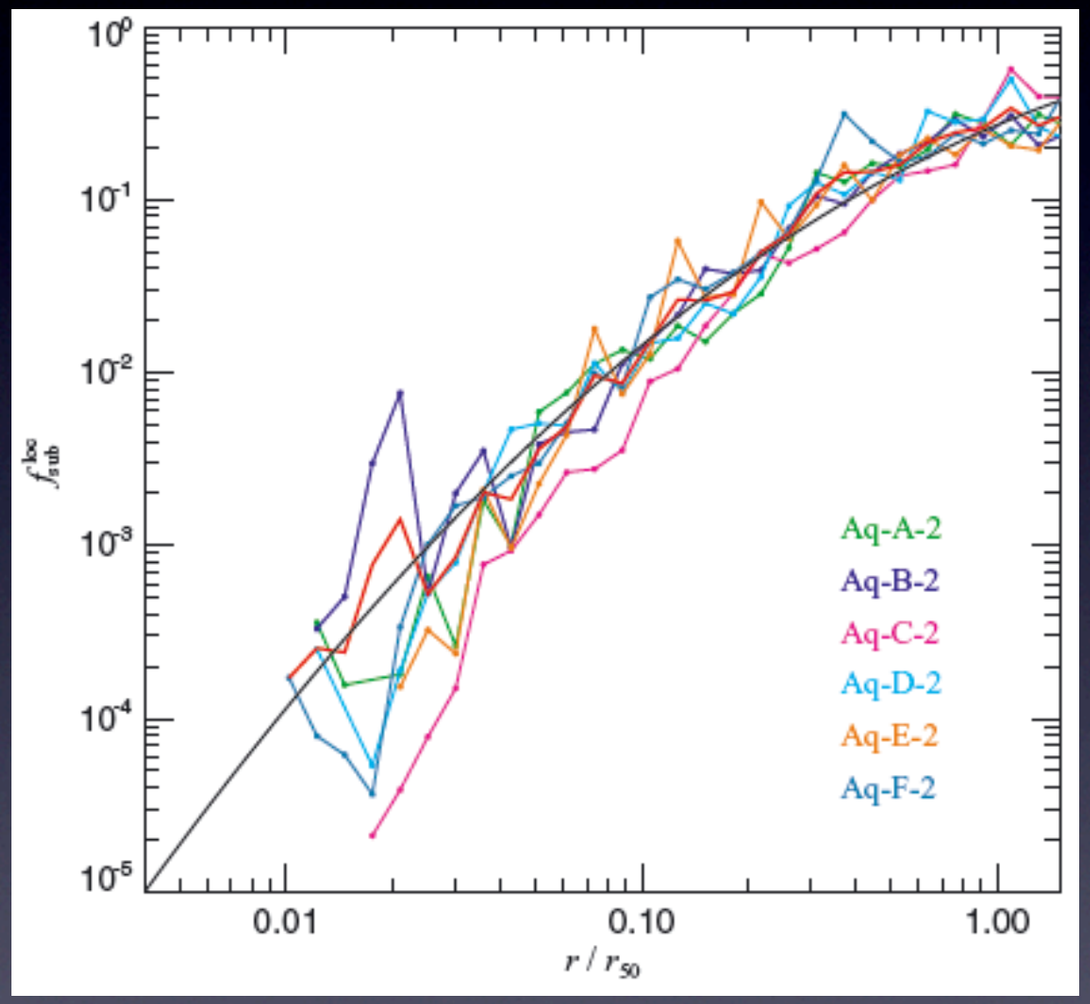

Source: Springel et al. 2008, MNRAS, 391, 1685

local mass fractions in subhaloes as a function of halo-centric radius. Results are shown for 6 MW-sized haloes from the Aquarius project...

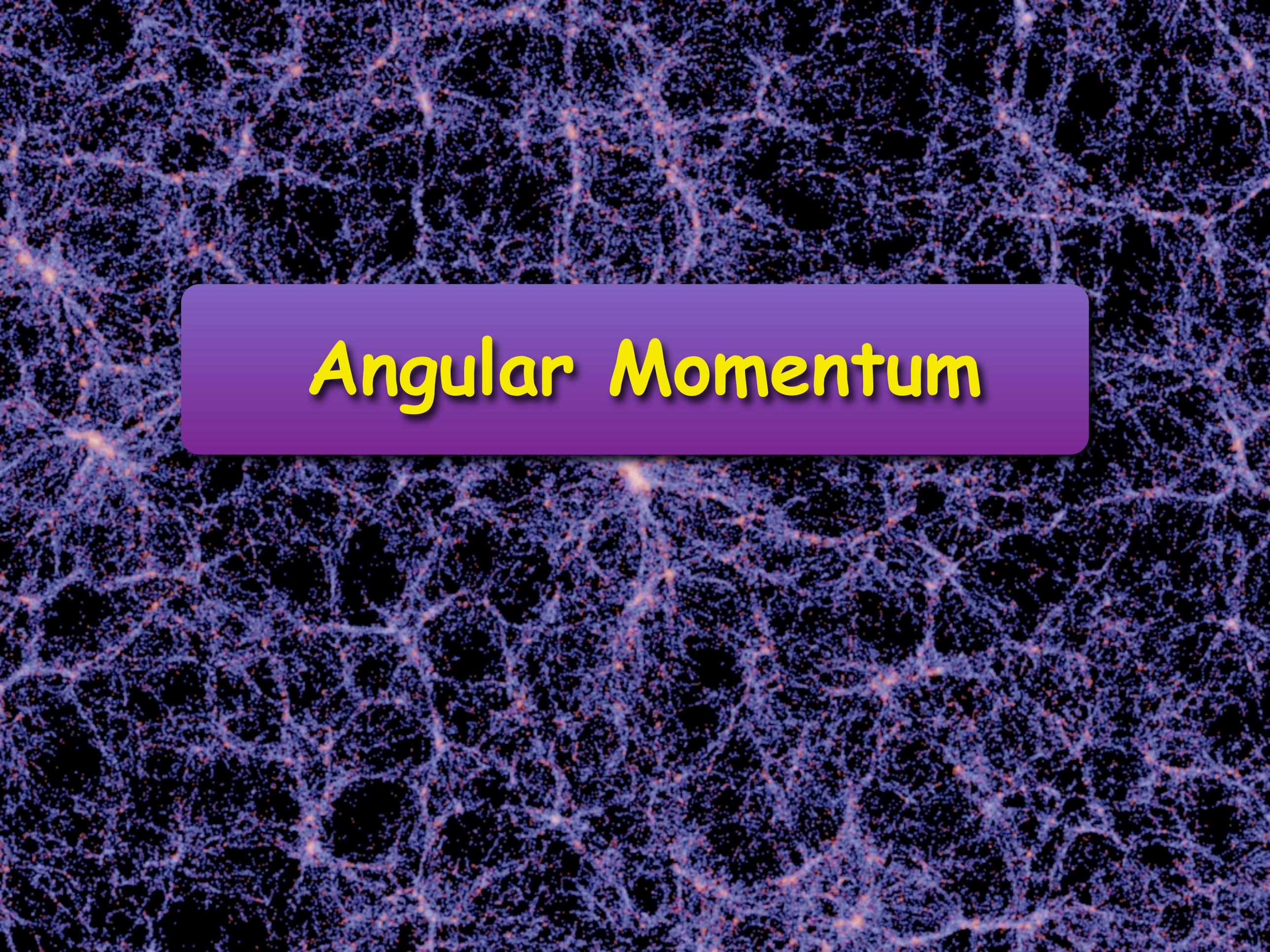

Angular Momentum

Linear Tidal Torque Theory

See MBW §7.5.4 for more details

Dark matter haloes acquire angular momentum in the linear regime due to tidal torques from neighboring overdensities...

Consider the material that ends up as part of a virialized halo. Let V_L be the Lagrangian region that it occupies in the early Universe. The angular momentum of this material can be written as

$$\vec{J} = \int_{V_{\rm L}} {\rm d}^3\vec{x}_{\rm i}\, \bar{\rho}_{\rm m} a^3 \left(a\vec{x} - a\vec{x}_{\rm com}\right) \times \vec{v}$$

where $\vec{x}_{\rm com}$ is the center of mass (the barycenter) of the volume.

Using the Zel'dovich approximation for the velocities $\vec{v}$ inside the volume, and second-order Taylor series expansion of the potential, one finds that

$$J_i(t) = a^2(t)\, \dot{D}(t)\, \epsilon_{ijk} T_{jl}\, I_{lk}$$

Einstein summation convention

Here $\dot{D}(t)$ is the time-derivative of the linear-growth rate, T_{ij} is the tidal tensor at the barycenter at the initial time, I_{ij} is the inertial tensor at the initial time, and ϵ_{ijk} is the 3D Levi-Civita tensor.

This derivation for the growth of the angular momentum of `proto-haloes' , due to White (1984), is known as linear tidal torque theory (TTT)

Linear Tidal Torque Theory

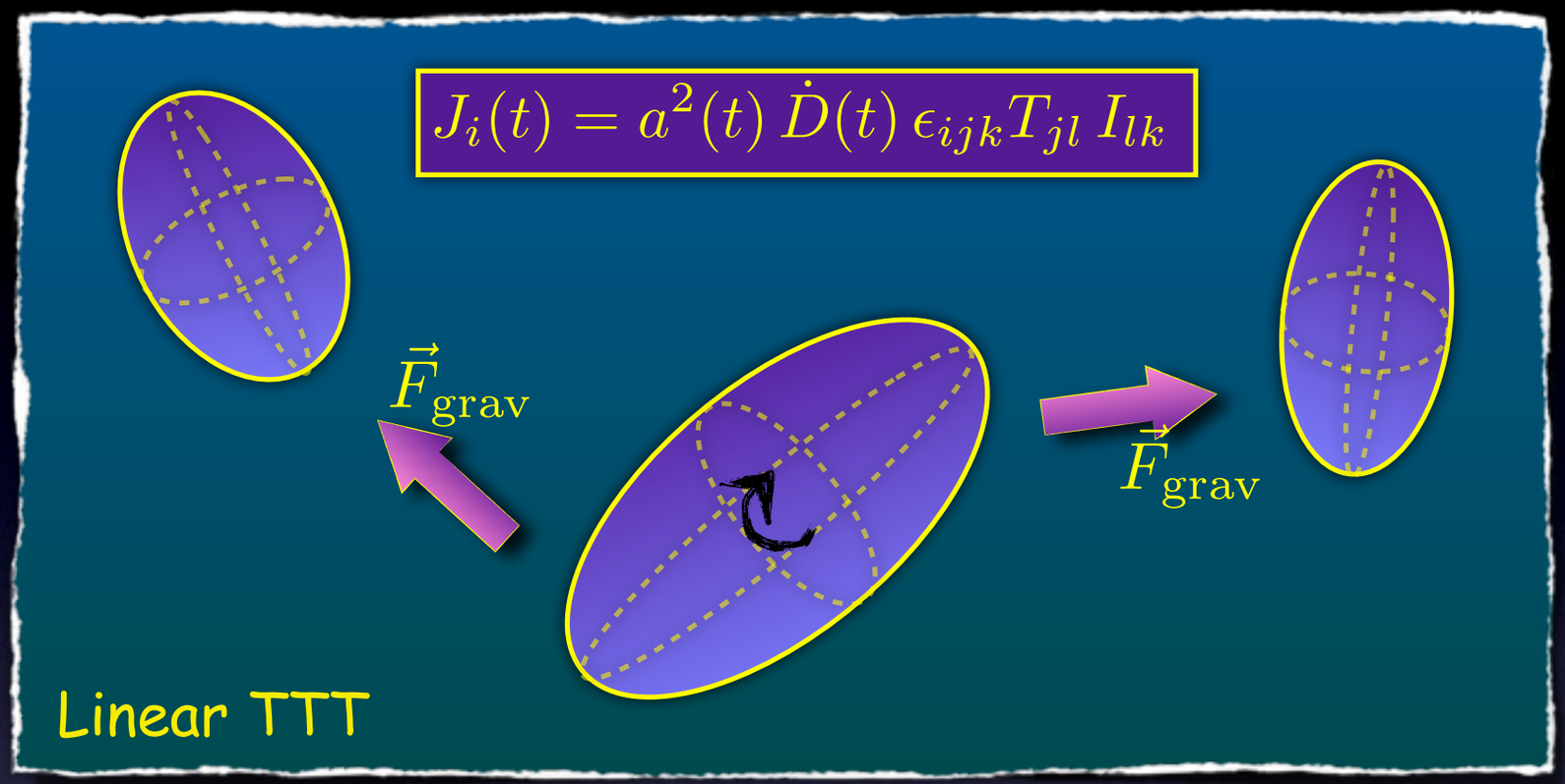

Since principal axes of the tidal and inertia tensors are, in general, not aligned for a non-spherical volume, this linear angular momentum should be non-zero.

According to linear TTT, $J \propto a^2\,\dot{D}$, which for an EdS cosmology implies that $J \propto t$

According to linear TTT, the acquisition of angular momentum stops once a proto-halo turns around and starts to collapse: after turn-around, the moment of inertia starts to decline rapidly...Hence, according to linear TTT the final angular momentum of a virialized dark matter halo should (roughly) be equal to

$$J_{\rm vir} = \int_0^{t_{\rm ta}} J(t)\,{\rm d}t = \epsilon_{ijk}\,T_{jl}\,I_{lk} \int_0^{t_{\rm ta}} a^2(t)\,\dot{D}(t)\,{\rm d}t$$

Testing Linear Tidal Torque Theory

Linear TTT can be tested using numerical simulations. These show that although the overall behavior of angular momentum growth of proto-haloes is consistent with TTT, it typically overpredicts the total angular momentum of a virialized halo by a factor ~3.

Two effects contribute to this `failure' :

- there is substantial angular momentum growth between turn-around and collapse, not anticipated by linear TTT
- angular momenta of haloes continue to evolve due to accretion of/ merging with other haloes (Maller et al. 2002; Vitvitska et al. 2002)

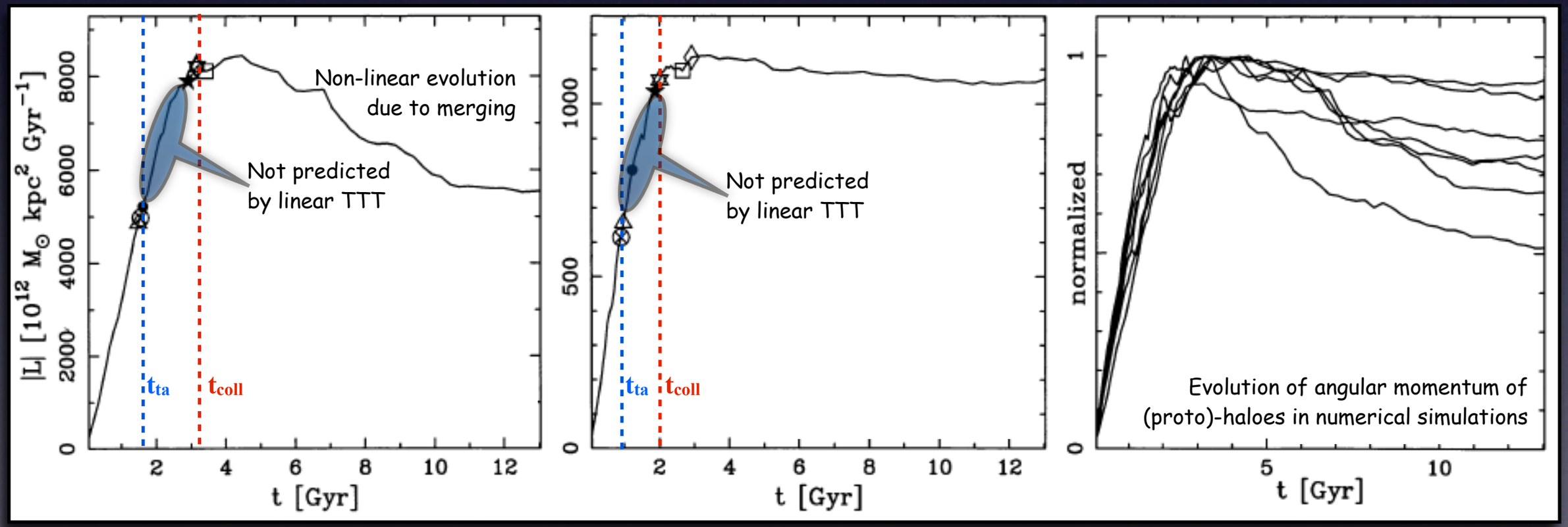

Source: Sugerman, Summers & Kamionkowski, 2000, MNRAS, 311, 762

The Halo Spin Parameter

The angular momentum of a dark matter halo is traditionally parameterized through the dimensionless spin parameter:

$$\lambda = \frac{J\,|E|^{1/2}}{G\,M^{5/2}}$$

where J, E and M are the angular momentum, energy and mass of the halo.

An alternative definition for the spin parameter, which avoids having to calculate the halo energy is:

$$\lambda' = \frac{J}{\sqrt{2}M\,V\,R}$$

where V and R are the virial velocity and viral radius, respectively. Definitions are equal if halo is singular isothermal sphere; otherwise they differ by factor of order unity....

Simulations show that PDF for spin parameter of haloes is a log-normal

$$\mathcal{P}(\lambda)\,\mathrm{d}\lambda = \frac{1}{\sqrt{2\pi}\,\sigma_{\ln\lambda}}\exp\left(-\frac{\ln^2(\lambda/\bar{\lambda})}{2\sigma^2_{\ln\lambda}}\right)\frac{\mathrm{d}\lambda}{\lambda}$$

with $\bar{\lambda} \simeq 0.03$ and $\sigma_{\ln\lambda} \simeq 0.5$, with virtually no dependence on halo mass or cosmology...

The Halo Spin Parameter

NOTE: the fact that the (median) spin parameter is so small indicates that dark matter haloes are not supported by rotation; flattening is due to velocity anisotropy, not rotation...

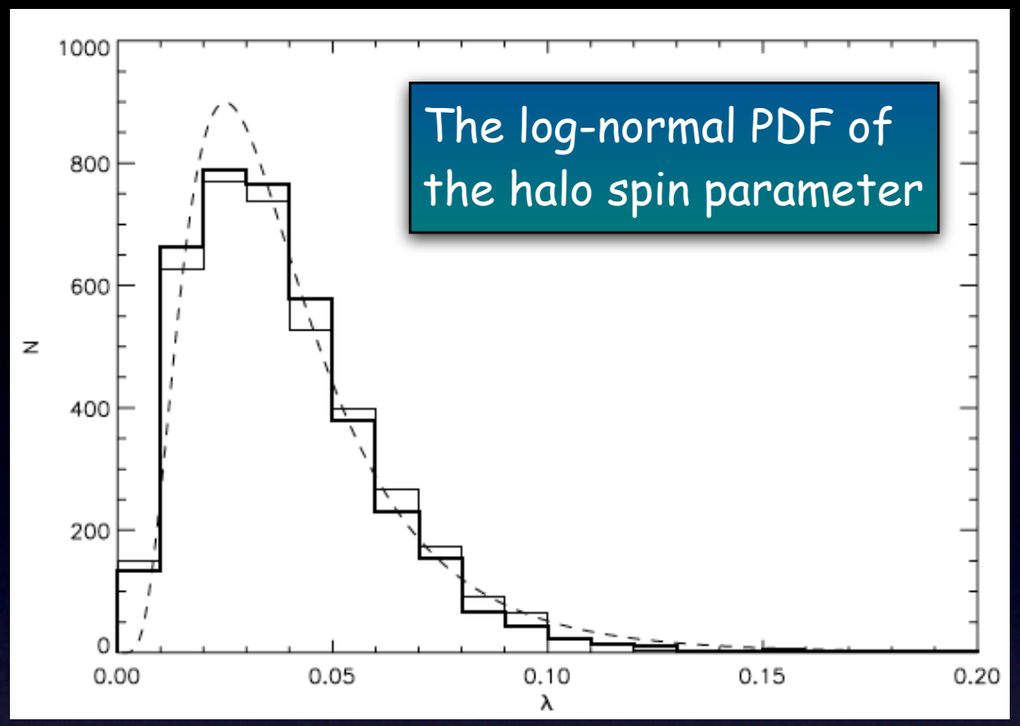

Source: Bailin & Steinmetz, 2005, ApJ, 627, 647

for comparison, the spin parameter of a typical disk galaxy is ~0.4, roughly an order of magnitude larger than that of a dark matter halo....

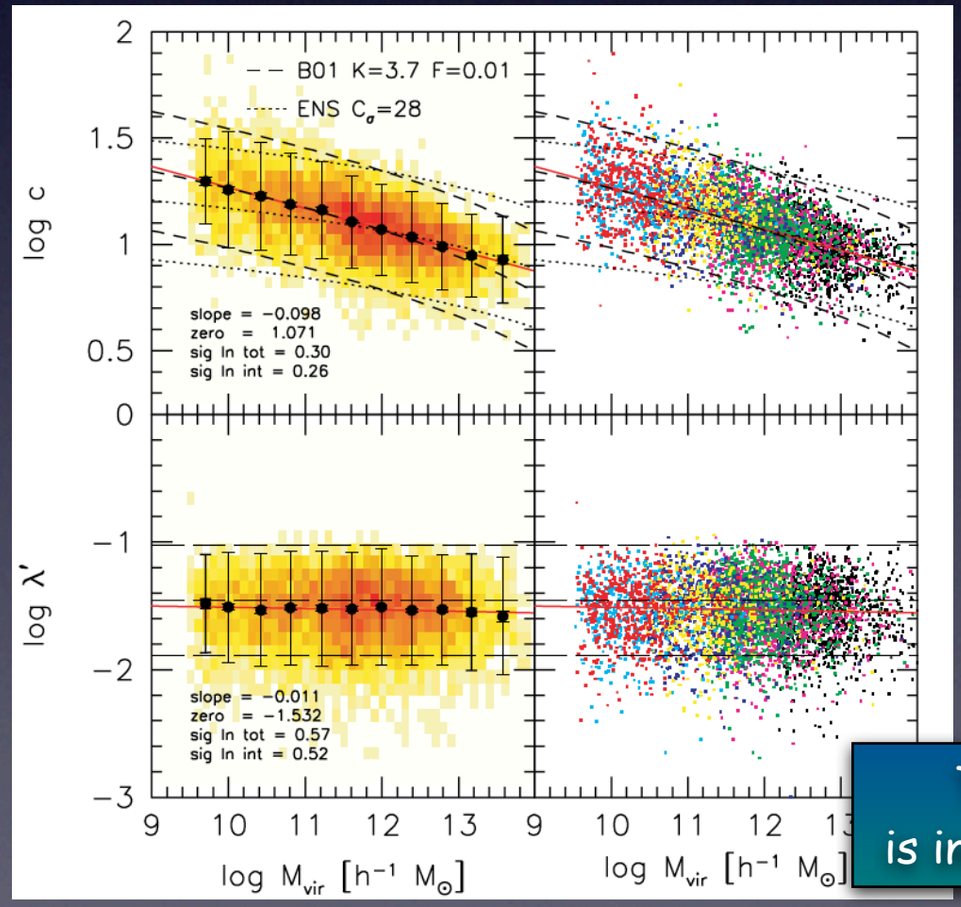

Source: Maccio et al. 2007, MNRAS, 378, 55

The halo spin parameter is independent of halo mass

Haloes that experienced a recent major merger have higher spin parameters than average . This reflects the large orbital angular momentum supplied by the merger

(e.g., Vitvitska et al 2001; Hetznecker & Burkert 2006)

However, this spin-merger correlation only persists for short time; virialization & accretion of new matter quickly brings spin parameter of halo back to average, non-conspicuous value

(e.g., D'Onghia & Navarro 2007)

The (specific) Angular Momentum Distribution

Using N-body simulations, Bullock et al. (2001) showed that dark matter haloes have a universal angular momentum profile with characteristic value j_0 and shape parameter μ :

$$\mathcal{P}(j) = \frac{\mu j_0}{(j + j_0)^2} \quad \Rightarrow \quad M(<j) = M_{\rm vir}\,\frac{\mu j}{(j + j_0)}$$

This distribution has a maximum specific angular momentum, $j_{\rm max} = j_0/(\mu - 1)$, which is related to the halo's total specific angular momentum according to

$$j_{\rm tot} = \sqrt{2}\,\lambda'\,r_{\rm vir}\,V_{\rm vir} = j_{\rm max}\left[1 - \mu\left\{1 - (\mu - 1)\ln\left(\frac{\mu}{\mu - 1}\right)\right\}\right]$$

- The pair $(\lambda\,,\mu)$ completely specifies the angular momentum content of a dark matter halo.
- The shape parameter is characterized by a log-normal distribution with $\bar{\mu} \simeq 1.25$ and $\sigma_{\ln\mu} \simeq 0.4$.
- An alternative characterization of the angular momentum distribution within dark matter haloes is:

$$j(r) \propto r^{\alpha} \qquad \text{with} \qquad \alpha \simeq 1.1 \pm 0.3$$

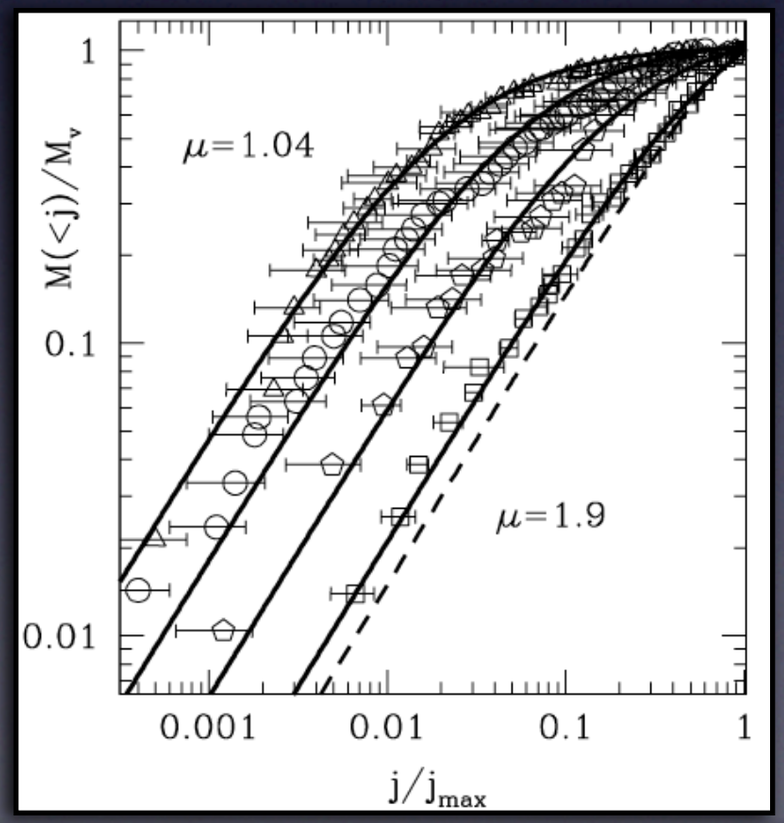

Source: Bullock et al. 2001, ApJ, 555, 240

The (specific) Angular Momentum Distribution

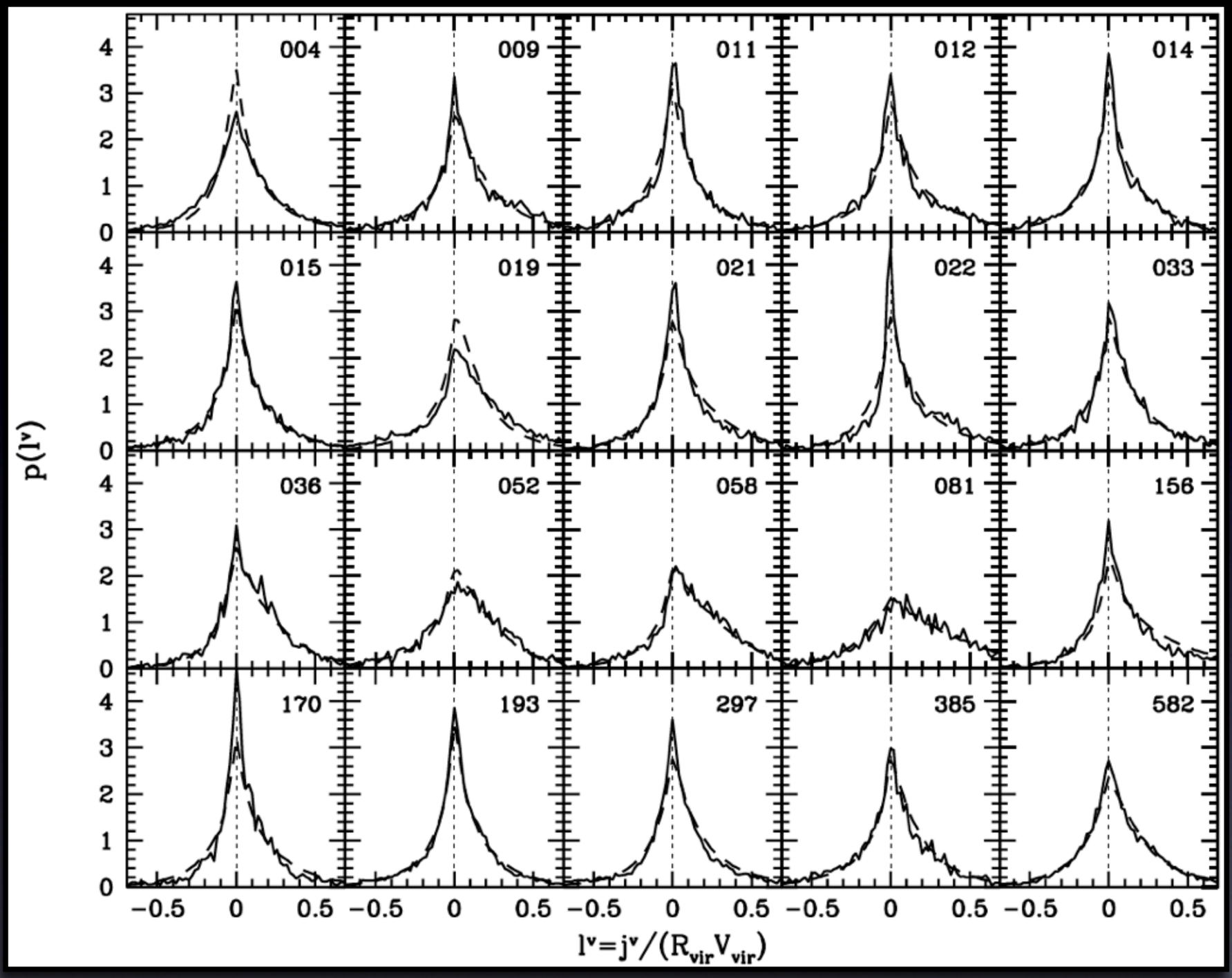

Source: van den Bosch et al. 2002, ApJ, 576, 21

Angular momentum distributions of dark matter (solid) and gas (dashed) in numerical simulations. Here j^v is the component of the specific angular momentum in the direction of the halo's total angular momentum vector. Note that there is only a slight excess of positive over negative j^v...

The Halo Model

The Halo Model

The Halo model is an analytical model that describes dark matter density distribution in terms of its halo building blocks, under ansatz that all dark matter is partitioned over haloes.

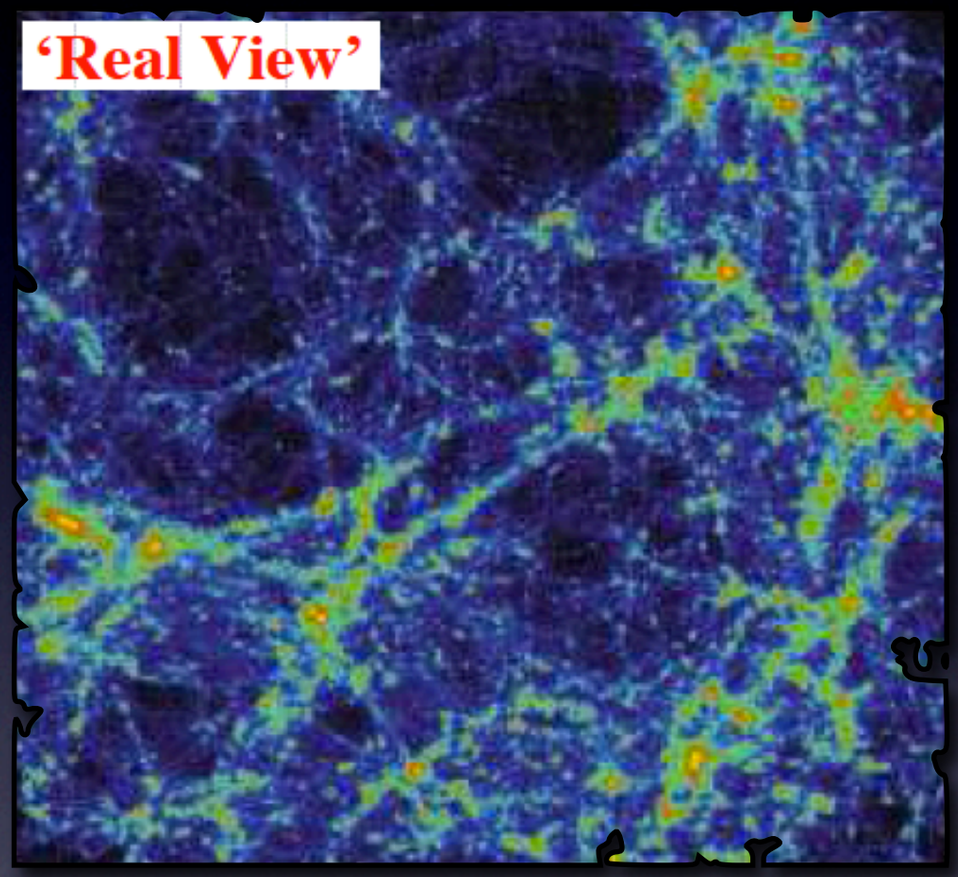

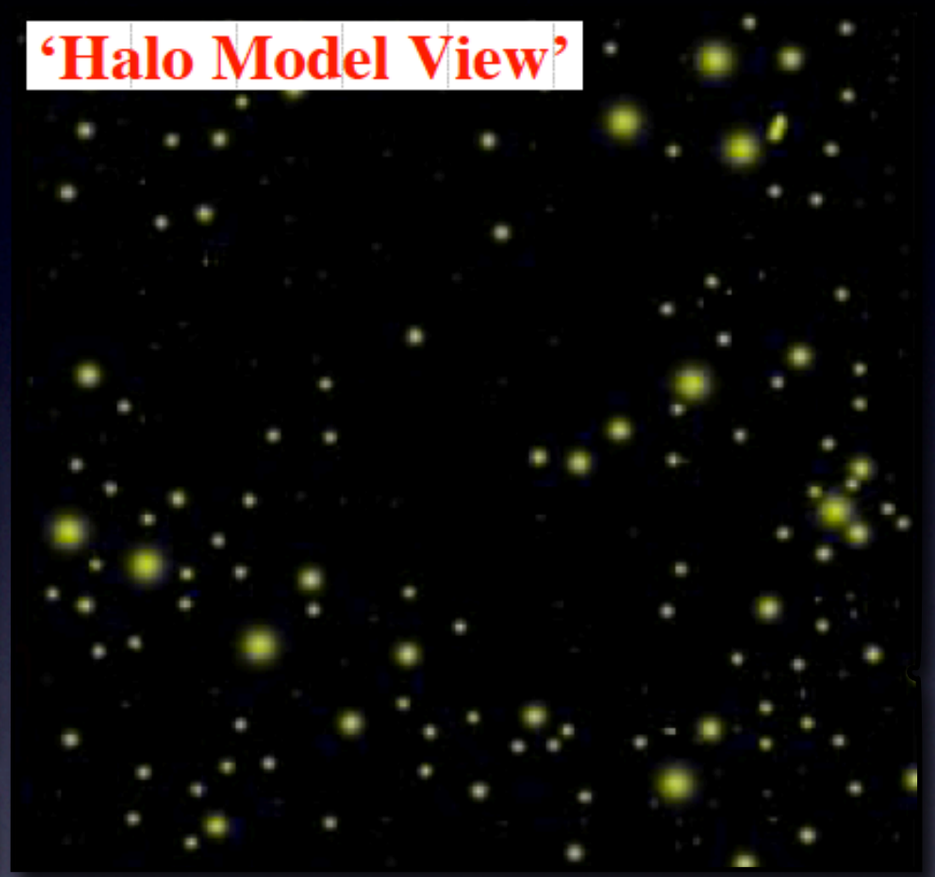

Throughout we assume that all dark matter haloes are spherical, and have a density distribution that only depends on halo mass:

$$\rho(r|M) = M\,u(r|M)$$

Here $u(r|M)$ is the normalized density profile:

$$\int \mathrm{d}^3\vec{x}\,u(\vec{x}|M) = 1$$

The Halo Model

Imagine space divided into many small volumes, ΔV_i ,which are so small that none of them contain more than one halo center.

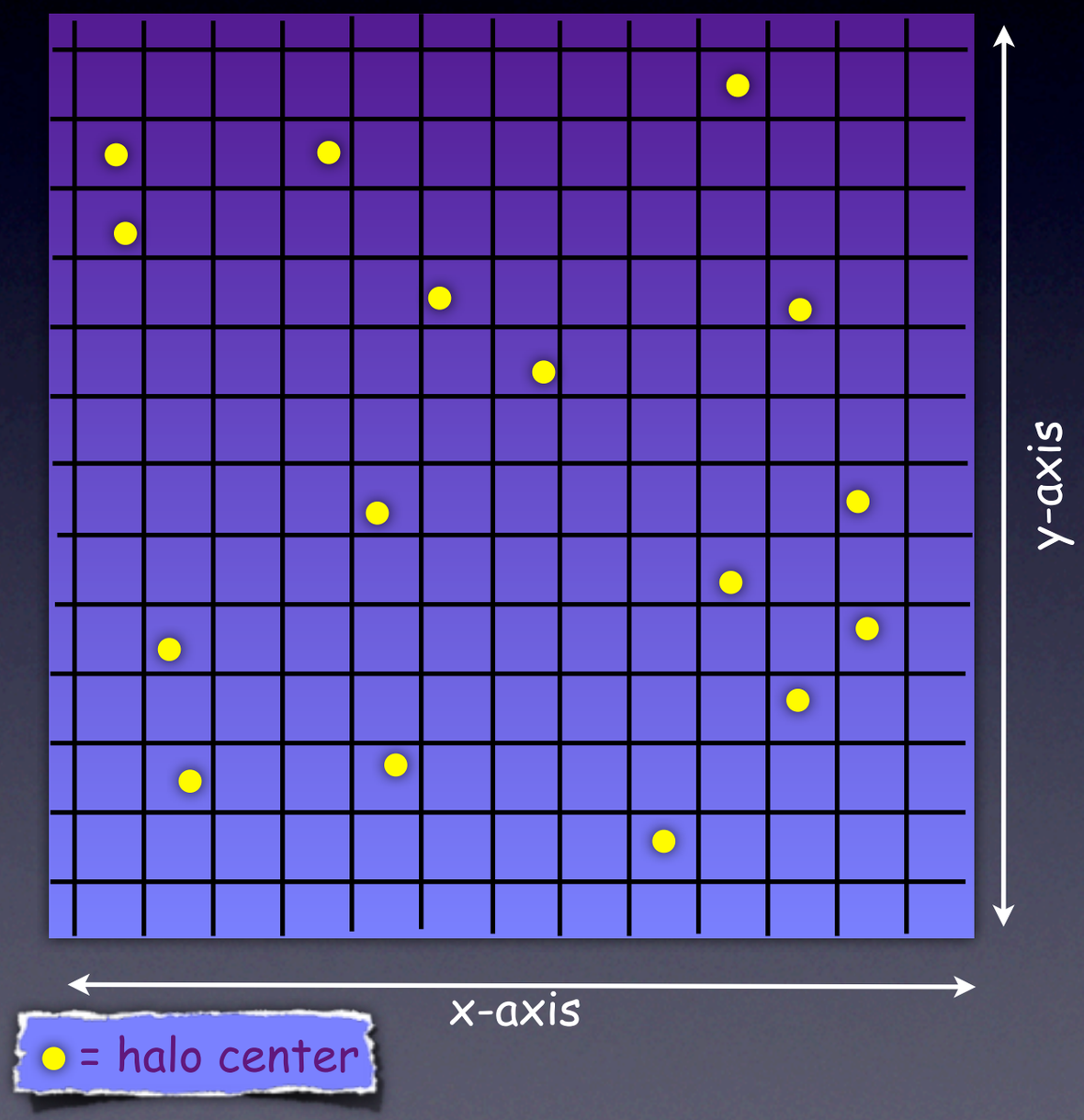

Let $\mathcal{N}_i$ be the occupation number of dark matter haloes in cell i

Then we have that $\mathcal{N}_i = 0, 1$ and therefore $\mathcal{N}_i = \mathcal{N}_i^2 = \mathcal{N}_i^3 =$

This allows us to write the matter density field as a summation:

$$\rho(\vec{x}) = \sum_i \mathcal{N}_i \, M_i \, u(\vec{x} - \vec{x}_i | M_i)$$

The Halo Model

$$\rho(\vec{x}) = \sum_i \mathcal{N}_i\, M_i\, u(\vec{x} - \vec{x}_i | M_i)$$

We can also use this to compute the two-point correlation function of matter:

$$\xi_{\rm mm}(r) \equiv \langle \delta(\vec{x})\, \delta(\vec{x} + \vec{r}) \rangle = \frac{1}{\bar{\rho}^2} \langle \rho(\vec{x})\, \rho(\vec{x} + \vec{r}) \rangle - 1$$

$$\langle \rho(\vec{x})\, \rho(\vec{x} + \vec{r}) \rangle = \left\langle \sum_i \mathcal{N}_i\, M_i\, u(\vec{x}_1 - \vec{x}_i | M_i) \cdot \sum_j \mathcal{N}_j\, M_j\, u(\vec{x}_2 - \vec{x}_j | M_j) \right\rangle$$

$$\vec{x}_2 = \vec{x}_1 + \vec{r}$$

$$= \sum_i \sum_j \langle \mathcal{N}_i\, \mathcal{N}_j\, M_i M_j\, u(\vec{x}_1 - \vec{x}_i | M_i) u(\vec{x}_2 - \vec{x}_j | M_j) \rangle$$

We split this in two parts: the 1-halo term $(i = j)$, and the 2-halo term $(i \neq j)$

For the 1-halo term we obtain:

$$\mathcal{N}_i^2 = \mathcal{N}_i$$

$$\langle \rho(\vec{x})\, \rho(\vec{x} + \vec{r}) \rangle_{\rm 1h} = \sum_i \langle \mathcal{N}_i\, M_i^2\, u(\vec{x}_1 - \vec{x}_i | M_i) u(\vec{x}_2 - \vec{x}_i | M_i) \rangle$$

$$= \sum_i \int {\rm d}M\, M^2\, n(M)\, \Delta V_i\, u(\vec{x}_1 - \vec{x}_i | M) u(\vec{x}_2 - \vec{x}_i | M)$$

$$= \int {\rm d}M\, M^2\, n(M) \int {\rm d}^3\vec{y}\, u(\vec{x}_1 - \vec{y} | M) u(\vec{x}_2 - \vec{y} | M)$$

convolution integral

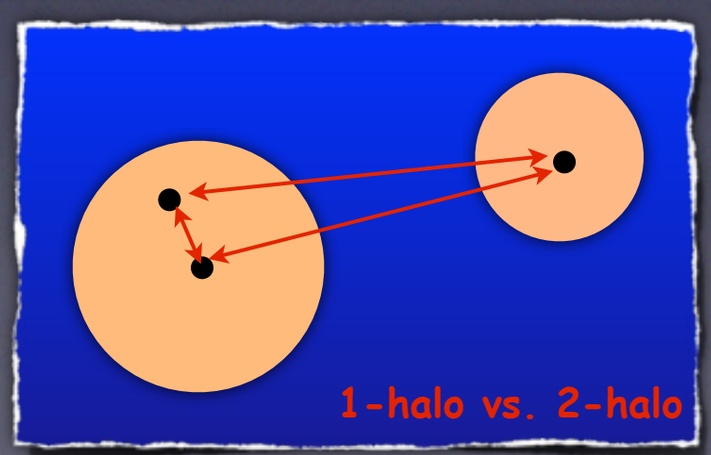

The Halo Model

$$\rho(\vec{x}) = \sum_i \mathcal{N}_i \, M_i \, u(\vec{x} - \vec{x}_i | M_i)$$

For the 2-halo term we obtain:

$$\langle \rho(\vec{x}) \, \rho(\vec{x} + \vec{r}) \rangle_{\rm 2h} = \sum_i \sum_{j \neq i} \langle \mathcal{N}_i \, \mathcal{N}_j \, M_i \, M_j \, u(\vec{x}_1 - \vec{x}_i | M_i) \, u(\vec{x}_2 - \vec{x}_j | M_j) \rangle$$

$$\stackrel{?}{\neq} \sum_i \sum_{j \neq i} \int {\rm d}M_1 \, M_1 \, n(M_1) \int {\rm d}M_2 \, M_2 \, n(M_2) \, \Delta V_i \, \Delta V_j \; \times$$

$$\text{[redacted]} \; u(\vec{x}_1 - \vec{x}_i | M_1) \, u(\vec{x}_2 - \vec{x}_j | M_2) \; = \bar{\rho}^2$$

NO: dark matter haloes themselves are clustered, i.e., have a non-zero two point correlation function. This needs to be taken into account.

Clustering of dark matter haloes is characterized by halo-halo correlation function:

$$\xi_{\rm hh}(r | M_1, M_2) = b(M_1) \, b(M_2) \, \xi^{\rm lin}_{\rm mm}(r)$$

Here $b(M)$ is the halo bias function. Note: the above description of the halo-halo correlation function is only valid on large (linear) scales! On small scales non-linearities and halo exclusion become important....[not covered here]...

The Halo Model

$$\rho(\vec{x}) = \sum_i \mathcal{N}_i \, M_i \, u(\vec{x} - \vec{x}_i | M_i)$$

For the 2-halo term we obtain:

$$\langle \rho(\vec{x}) \, \rho(\vec{x} + \vec{r}) \rangle_{\rm 2h} = \sum_i \sum_{j \neq i} \langle \mathcal{N}_i \, \mathcal{N}_j \, M_i \, M_j \, u(\vec{x}_1 - \vec{x}_i | M_i) \, u(\vec{x}_2 - \vec{x}_j | M_j) \rangle$$

$$= \sum_i \sum_{j \neq i} \int {\rm d}M_1 \, M_1 \, n(M_1) \int {\rm d}M_2 \, M_2 \, n(M_2) \, \Delta V_i \, \Delta V_j \, \times$$

$$[1 + \xi_{\rm hh}(\vec{x}_i - \vec{x}_j | M_1, M_2)] \, u(\vec{x}_1 - \vec{x}_i | M_1) \, u(\vec{x}_2 - \vec{x}_j | M_2)$$

$$= \bar{\rho}^2 + \int {\rm d}M_1 \, M_1 \, n(M_1) \int {\rm d}M_2 \, M_2 \, n(M_2) \, \times$$

$$\int {\rm d}^3\vec{y}_1 \int {\rm d}^3\vec{y}_2 \, u(\vec{x}_1 - \vec{y}_1 | M_1) \, u(\vec{x}_2 - \vec{y}_2 | M_2) \, \xi_{\rm hh}(\vec{y}_1 - \vec{y}_2 | M_1, M_2)$$

$$= \bar{\rho}^2 + \int {\rm d}M_1 \, M_1 \, b(M_1) \, n(M_1) \int {\rm d}M_2 \, M_2 \, b(M_2) \, n(M_2) \, \times$$

$$\int {\rm d}^3\vec{y}_1 \int {\rm d}^3\vec{y}_2 u(\vec{x}_1 - \vec{y}_1 | M_1) \, u(\vec{x}_2 - \vec{y}_2 | M_2) \, \xi^{\rm lin}_{\rm mm}(\vec{y}_1 - \vec{y}_2)$$

convolution integral

The Halo Model: Summary (part I)

$$\xi(r) = \xi^{1\rm h}(r) + \xi^{2h}(r)$$

$$\xi^{1\rm h}(r) = \frac{1}{\bar{\rho}^2}\int {\rm d}M\, M^2\, n(M) \int {\rm d}^3\vec{y}\, u(\vec{x}-\vec{y}|M) u(\vec{x}+\vec{r}-\vec{y}|M)$$

$$\xi^{2\rm h}(r) = \frac{1}{\bar{\rho}^2}\int {\rm d}M_1\, M_1\, b(M_1)\, n(M_1) \int {\rm d}M_2\, M_2\, b(M_2)\, n(M_2) \times$$
$$\int {\rm d}^3\vec{y}_1 \int {\rm d}^3\vec{y}_2 u(\vec{x}-\vec{y}_1|M_1)\, u(\vec{x}+\vec{r}-\vec{y}_2|M_2)\, \xi^{\rm lin}_{\rm mm}(\vec{y}_1-\vec{y}_2)$$

Halo Model Ingredients:

- the halo density profiles $\rho(r|M) = M u(r|M)$
- the halo mass function $n(M)$
- the halo bias function $b(M)$
- the linear correlation function of matter $\xi^{\rm lin}_{\rm mm}(r)$

All of these are (reasonably) well calibrated against numerical simulations.

The Halo Model in Fourier Space

$$
\begin{aligned}
P(k) &= P^{\rm 1h}(k) + P^{\rm 2h}(k) \\
P^{\rm 1h}(k) &= \frac{1}{\overline{\rho}^2} \int {\rm d}M\, M^2\, n(M)\, |\tilde{u}(k|M)|^2 \\
P^{\rm 2h}(k) &= P^{\rm lin}(k) \left[\frac{1}{\overline{\rho}} \int {\rm d}M\, M\, b(M)\, n(M)\, \tilde{u}(k|M) \right]^2
\end{aligned}
$$

$$
P^{\rm lin}(k) = \int \xi^{\rm lin}_{\rm mm}(\vec{x}) e^{-i\vec{k}\cdot\vec{x}} {\rm d}^3\vec{x} = 4\pi \int_0^\infty \xi^{\rm lin}_{\rm mm}(r) \frac{\sin kr}{kr}\, r^2\, {\rm d}r
$$

$$
\tilde{u}(\vec{k}|M) = \int u(\vec{x}|M) e^{-i\vec{k}\cdot\vec{x}}\, {\rm d}^3\vec{x} = 4\pi \int_0^\infty u(r|M) \frac{\sin kr}{kr}\, r^2\, {\rm d}r
$$

Since convolutions in real-space become multiplications in Fourier space, the halo model expression for the power spectrum is much easier. Therefore, in practice, one computes $P(k)$ and then uses Fourier transformation to obtain two-point correlation function $\xi(r)$

The Halo Model in Fourier Space

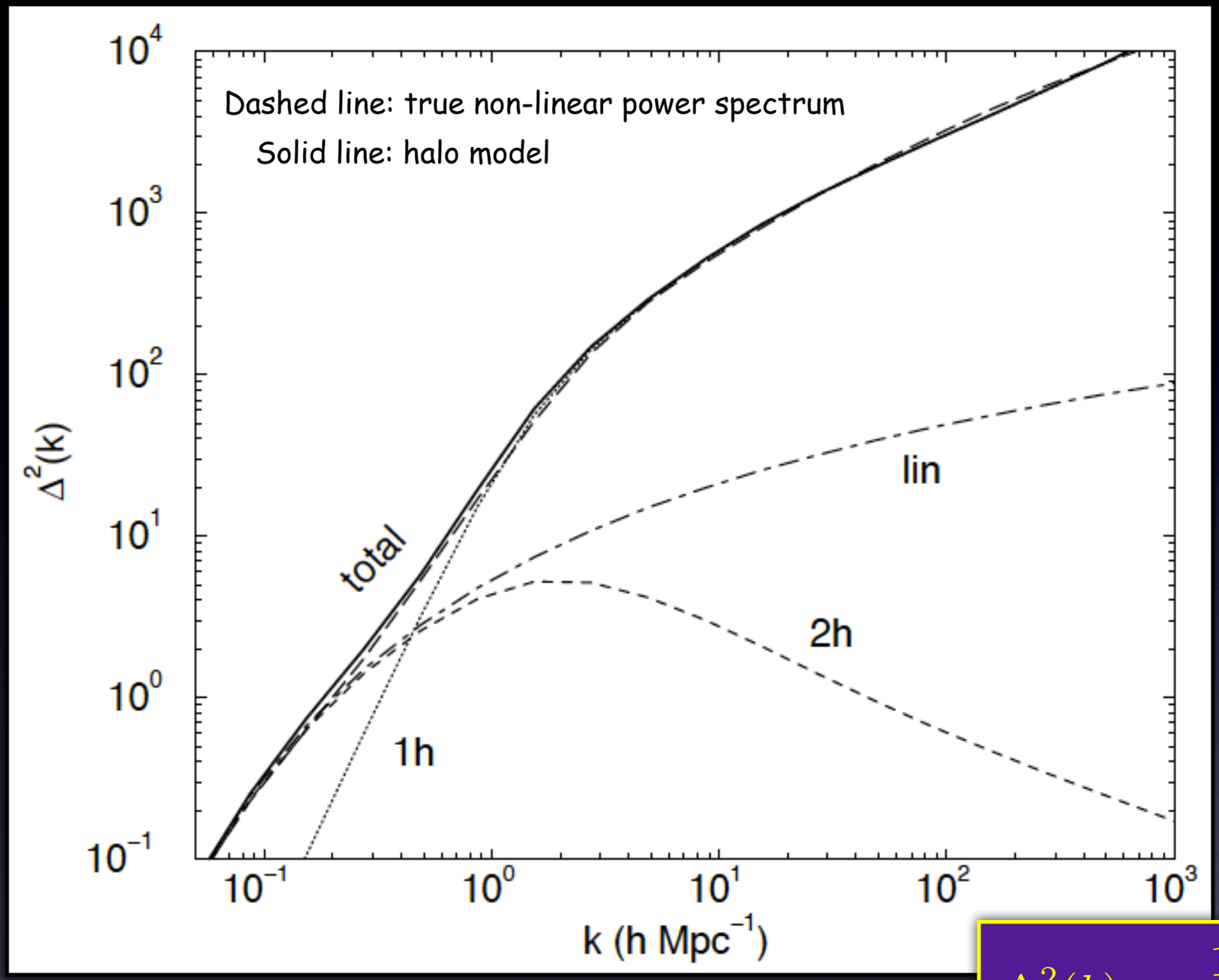

Source: Cooray & Sheth (2002)

$$\Delta^2(k) = \frac{1}{2\pi^2} k^3 P(k)$$

Dimensionless power spectrum

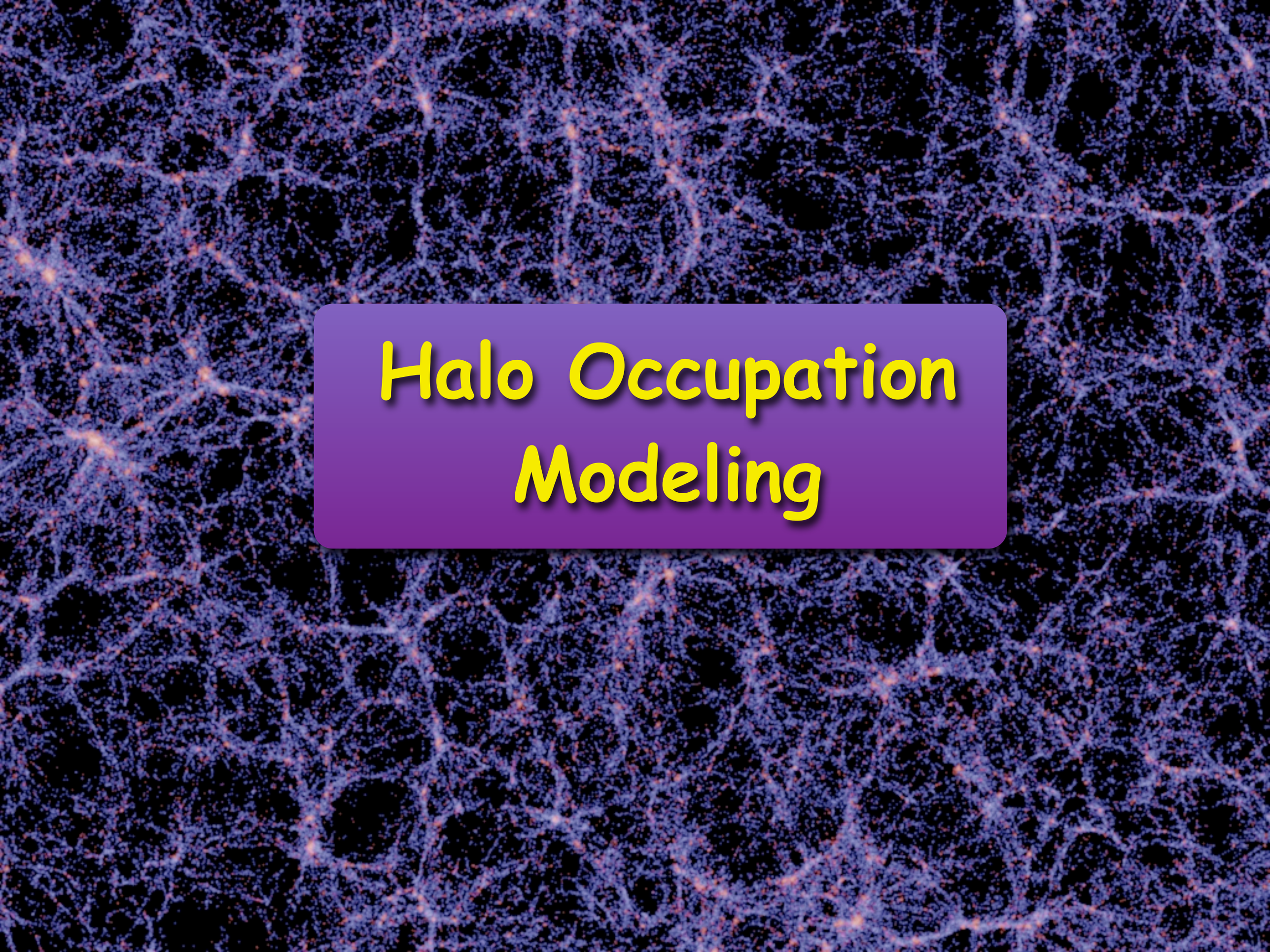

Halo Occupation Modeling

The Galaxy Power Spectrum

$$P^{\rm 1h}(k) = \frac{1}{\bar{\rho}^2}\int {\rm d}M\, M^2\, n(M)\, |\tilde{u}(k|M)|^2$$

$$P^{\rm 2h}(k) = P^{\rm lin}(k)\left[\frac{1}{\bar{\rho}}\int {\rm d}M\, M\, b(M)\, n(M)\, \tilde{u}(k|M)\right]^2$$

The above equations describe the halo model predictions for the matter power spectrum

The same formalism can also be used to compute the galaxy power spectrum:

simply replace:

$$\frac{M}{\bar{\rho}} \Rightarrow \frac{\langle N\rangle_M}{\bar{n}_{\rm g}}$$

$$\frac{M^2}{\bar{\rho}^2} \Rightarrow \frac{\langle N(N-1)\rangle_M}{\bar{n}_{\rm g}^2}$$

$$\tilde{u}(k|M) \Rightarrow \tilde{u}_{\rm g}(k|M)$$

Here $\langle N\rangle_M$ describes average number of galaxies (with certain properties) that reside in a halo of mass M, $\bar{n}_{\rm g}$ is the average number density of those galaxies, and $u_{\rm g}(r|M)$ is the normalized, radial number density distribution of galaxies in haloes of mass M.

Halo Occupation Statistics

When describing halo occupation statistics, it is important to treat central and satellite galaxies separately.

Central Galaxies: those galaxies that reside at the center of their dark matter (host) halo

Satellite Galaxies: those galaxies that reside at the center of a dark matter sub-halo, and are orbitting inside a larger host halo.

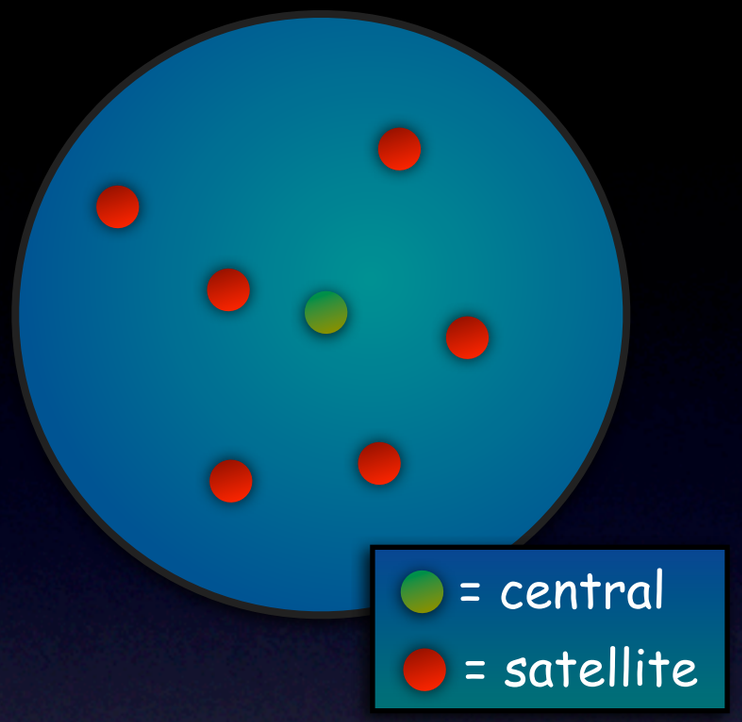

Central Galaxies

$$\langle N_{\rm c}\rangle_M = \sum_{N_{\rm c}=0}^{1} N_{\rm c}\, P(N_{\rm c}|M) = P(N_{\rm c}=1|M)$$

$$\langle N_{\rm c}^2\rangle_M = \sum_{N_{\rm c}=0}^{1} N_{\rm c}^2\, P(N_{\rm c}|M) = P(N_{\rm c}=1|M) = \langle N_{\rm c}\rangle_M$$

$$u_{\rm c}(r|M) = \delta^{\rm D}(r)$$

Satellite Galaxies

$$\langle N_{\rm s}\rangle_M = \sum_{N_{\rm s}=0}^{\infty} N_{\rm s}\, P(N_{\rm s}|M)$$

$$\langle N_{\rm s}^2\rangle_M = \sum_{N_{\rm s}=0}^{\infty} N_{\rm s}^2\, P(N_{\rm s}|M)$$

$$u_{\rm s}(r|M) = {\rm TBD}$$

Halo Occupation Statistics

Central Galaxies

$$\langle N_{\rm c}\rangle_M = \sum_{N_{\rm c}=0}^{1} N_{\rm c}\, P(N_{\rm c}|M) = P(N_{\rm c}=1|M)$$

$$\langle N_{\rm c}^2\rangle_M = \sum_{N_{\rm c}=0}^{1} N_{\rm c}^2\, P(N_{\rm c}|M) = P(N_{\rm c}=1|M) = \langle N_{\rm c}\rangle_M$$

$$u_{\rm c}(r|M) = \delta^{\rm D}(r)$$

Satellite Galaxies

$$\langle N_{\rm s}\rangle_M = \sum_{N_{\rm s}=0}^{\infty} N_{\rm s}\, P(N_{\rm s}|M)$$

$$\langle N_{\rm s}^2\rangle_M = \sum_{N_{\rm s}=0}^{\infty} N_{\rm s}^2\, P(N_{\rm s}|M)$$

$$u_{\rm s}(r|M) = {\rm TBD}$$

Calculating galaxy-galaxy correlation functions requires following halo occupation statistic ingredients:

Halo occupation distribution for centrals	$P(N_{\rm c}\|M)$
Halo occupation distribution for satellites	$P(N_{\rm s}\|M)$
Radial number density profile of satellites	$u_{\rm s}(r\|M)$

In principle, as we will see, one also requires the probability function $P(N_{\rm c}, N_{\rm s}|M)$, but it is common practice to assume that the occupation statistics of centrals and satellites are independent, i.e., that $P(N_{\rm c}, N_{\rm s}|M) = P(N_{\rm c}|M) \times P(N_{\rm s}|M)$

Halo Occupation Statistics: the first moment

Consider a luminosity threshold sample; all galaxies brighter than some threshold luminosity. The halo occupation statistics for such a sample are typically parameterized as follows:

$$\langle N_{\rm c}\rangle_M = \frac{1}{2}\left[1+{\rm erf}\left(\frac{\log M - \log M_{\rm min}}{\sigma_{\log M}}\right)\right]$$

$$\langle N_{\rm s}\rangle_M = \begin{cases} \left(\frac{M}{M_1}\right)^{\alpha} & \text{if } M > M_{\rm cut} \\ 0 & \text{if } M < M_{\rm cut} \end{cases}$$

$M_{\rm min}$ = characteristic minimum mass of haloes that host centrals above luminosity threshold

$\sigma_{\log M}$ = characteristic transition width due to scatter in L-M relation of centrals

$M_{\rm cut}$ = cut-off mass below which you have zero satellites above luminosity threshold

M_1 = normalization of satellite occupation numbers

α = slope of satellite occupation numbers

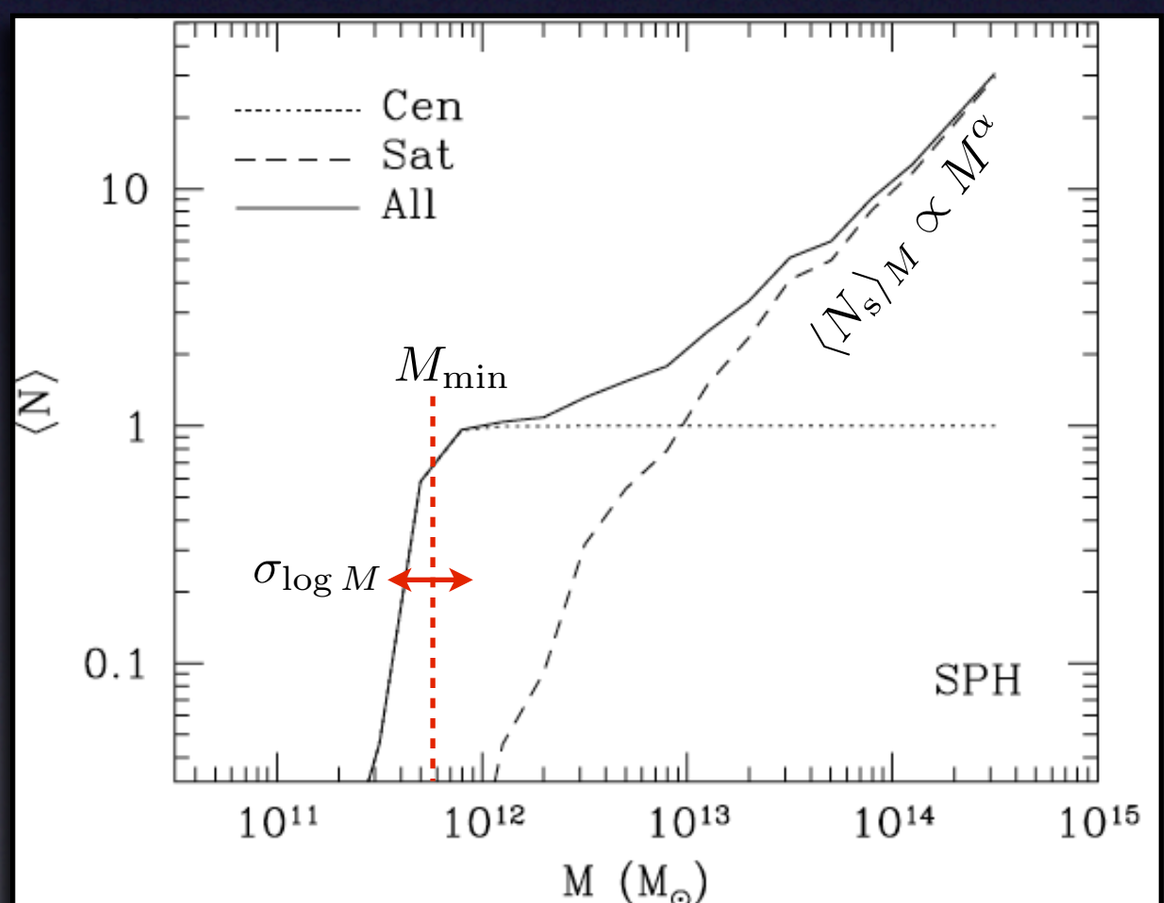

Source: Zheng et al., 2005, ApJ, 633, 791

This particular HOD model, which is fairly popular in the literature, requires 5 parameters $(M_{\rm min}, M_1, M_{\rm cut}, \sigma_{\log M}, \alpha)$ to characterize the occupation statistics of a given luminosity threshold sample, and is (partially) motivated by the occupation statistics in hydro simulations of galaxy formation...

Halo Occupation Statistics: the first moment

Increasing the slope $\alpha = \mathrm{d}\log\langle N_\mathrm{s}\rangle/\mathrm{d}\log M$ boosts the 1-halo term of the correlation function. It also boosts the 2-halo term, but to a lesser extent.

The latter arises because a larger value of α implies that satellites, on average, reside in more massive haloes, which are more strongly biased.

The 1-halo term scales with satellite occupation numbers as $\langle N_\mathrm{s}\rangle_M^2$ while the 2-halo term scales as $\langle N_\mathrm{s}\rangle_M$. This means that the relative clustering strengths in the 1-halo and 2-halo regimes constrains the satellite fractions.

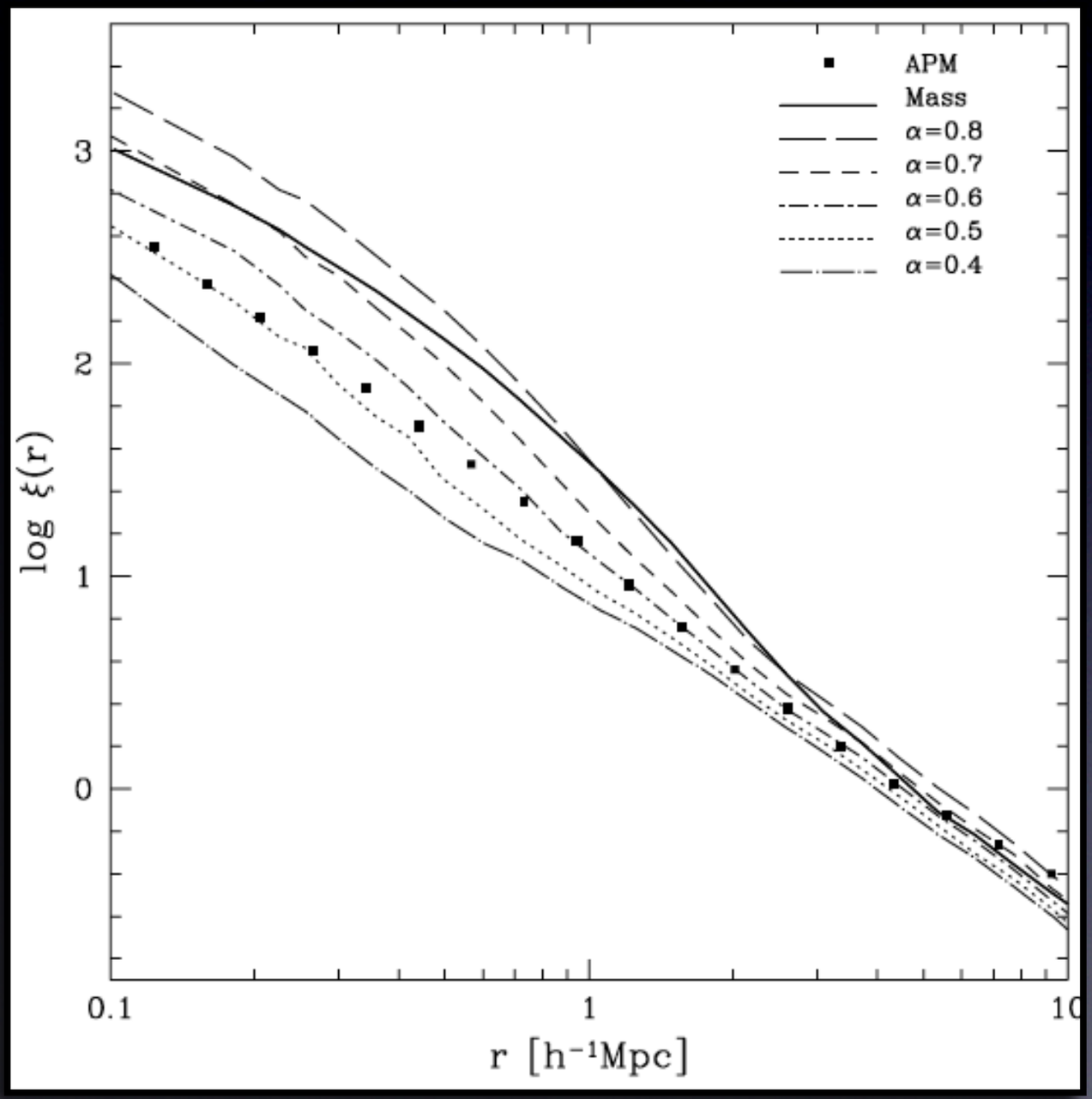

Source: Berlind & Weinberg, 2002, ApJ, 575, 587

Halo Occupation Statistics: the first moment

An alternative parameterization, which has the advantage that it describes the occupation statistics for any luminosity sample (not only threshold samples), is the conditional luminosity function.

$$\Phi(L|M) = \Phi_{\rm c}(L|M) + \Phi_{\rm s}(L|M)$$

The CLF describes the average number of galaxies of luminosity L that reside in a dark matter halo of mass M.

$$\Phi(L) = \int_0^\infty \Phi(L|M)\, n(M)\, {\rm d}M$$

CLF is the direct link between the halo mass function and the galaxy luminosity function.

$$\langle L \rangle_M = \int_0^\infty \Phi(L|M)\, L\, {\rm d}L$$

CLF describes link between luminosity and mass

$$\langle N_{\rm x} \rangle_M = \int_{L_1}^{L_2} \Phi_{\rm x}(L|M)\, {\rm d}L$$

CLF describes first moments of halo occupation statistics of any luminosity sample

The Conditional Luminosity Function

The CLF can be obtained from galaxy group catalogues. Yang, Mo & van den Bosch (2008) have shown that the CLF is well parameterized using the following functional form:

$$\Phi_{\rm c}(L|M){\rm d}L = \frac{1}{\sqrt{2\pi}\sigma_{\rm c}} \exp\left[-\left(\frac{\ln(L/L_{\rm c})}{\sqrt{2}\sigma_{\rm c}}\right)^2\right]\frac{{\rm d}L}{L}$$

$$\Phi_{\rm s}(L|M){\rm d}L = \frac{\phi_{\rm s}}{L_{\rm s}}\left(\frac{L}{L_{\rm s}}\right)^{\alpha_{\rm s}} \exp\left[-(L/L_{\rm s})^2\right]{\rm d}L$$

Note: $\{L_{\rm c}, L_{\rm s}, \sigma_{\rm c}, \phi_{\rm s}, \alpha_{\rm s}\}$ all depend on halo mass. These dependencies are typically parameterized using ~10 free parameters.

Free parameters are constrained by the data, which can be galaxy group catalogs, galaxy clustering, galaxy-galaxy lensing, satellite kinematics, etc...

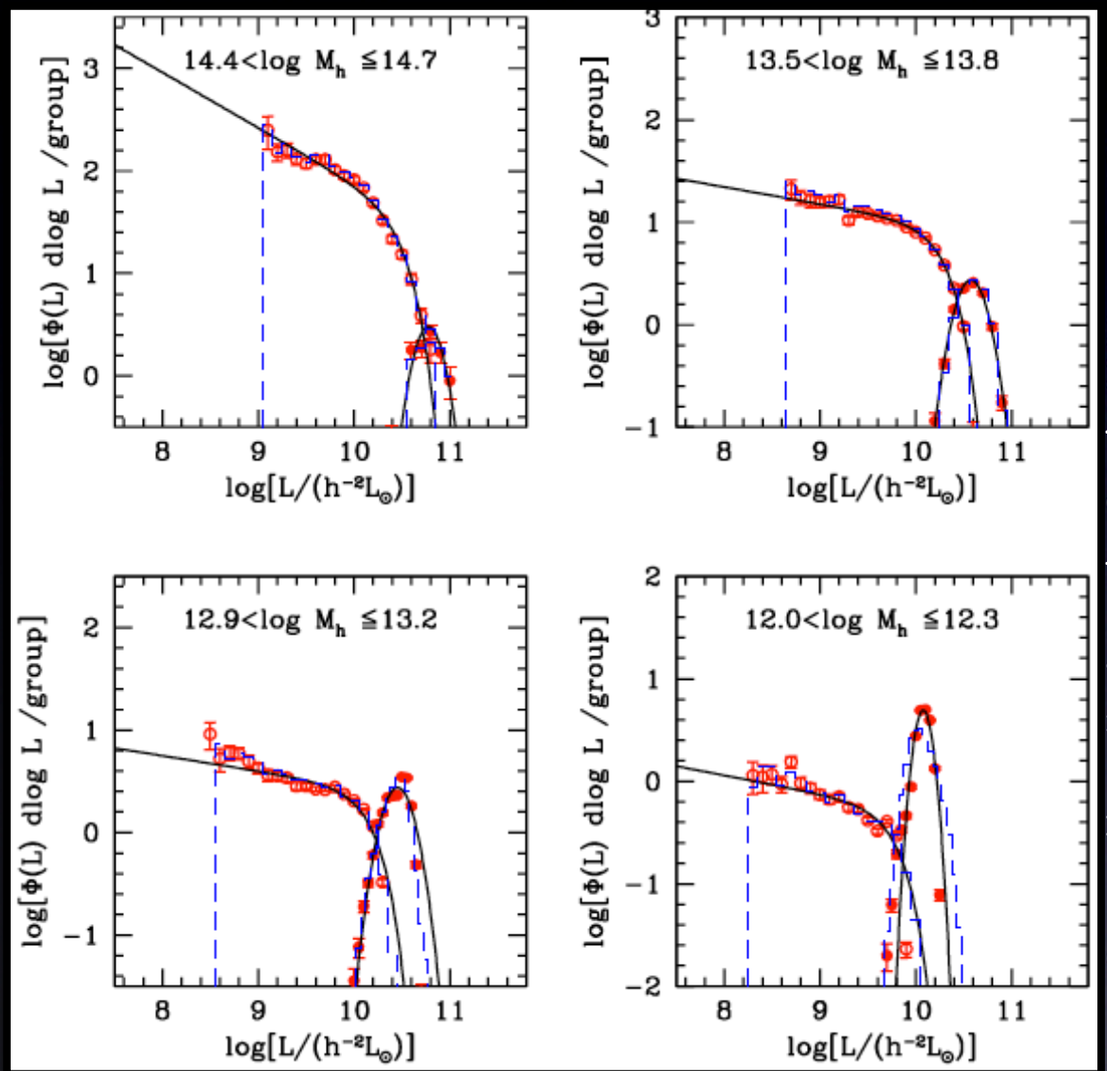

Source: Yang, Mo & van den Bosch, 2008, ApJ, 676, 248

The CLFs inferred from a SDSS galaxy group catalog. Symbols are data, while the solid, black line is best-fit using the CLF parameterization indicated above...

Halo Occupation Statistics: the second moment

The 1-halo term of the galaxy-galaxy correlation function requires the second moment

$$\langle N(N-1)\rangle_M = \langle N_{\rm c}^2\rangle_M + 2\langle N_{\rm c}N_{\rm s}\rangle_M + \langle N_{\rm s}^2\rangle_M - \langle N_{\rm c}\rangle_M - \langle N_{\rm s}\rangle_M$$
$$= \langle N_{\rm s}(N_{\rm s}-1)\rangle_M - 2\langle N_{\rm c}\rangle_M \langle N_{\rm s}\rangle_M$$

where we assumed that occupation statistics of centrals and satellites are independent

Thus, we need to specify the second moment of the satellite occupation distribution:

$$\langle N_{\rm s}(N_{\rm s}-1)\rangle_M = \sum_{N_{\rm s}=0}^{\infty} N_{\rm s}(N_{\rm s}-1)\, P(N_{\rm s}|M) \equiv \beta(M)\,\langle N_{\rm s}\rangle^2$$

where we have introduced the function $\beta(M)$

If the occupation statistics of satellite galaxies follow Poisson statistics, i.e.,

$$P(N_{\rm s}|M) = \frac{\lambda^{N_{\rm s}}\, e^{-\lambda}}{N_{\rm s}!} \qquad \textbf{with} \qquad \lambda = \langle N_{\rm s}\rangle_M$$

then $\beta(M) = 1$. Distributions with $\beta > 1$ ($\beta < 1$) are broader (narrower) than Poisson.

The second moment of the halo occupation statistics is completely described by $\beta(M)$

Occupation Statistics from Galaxy Group Catalog

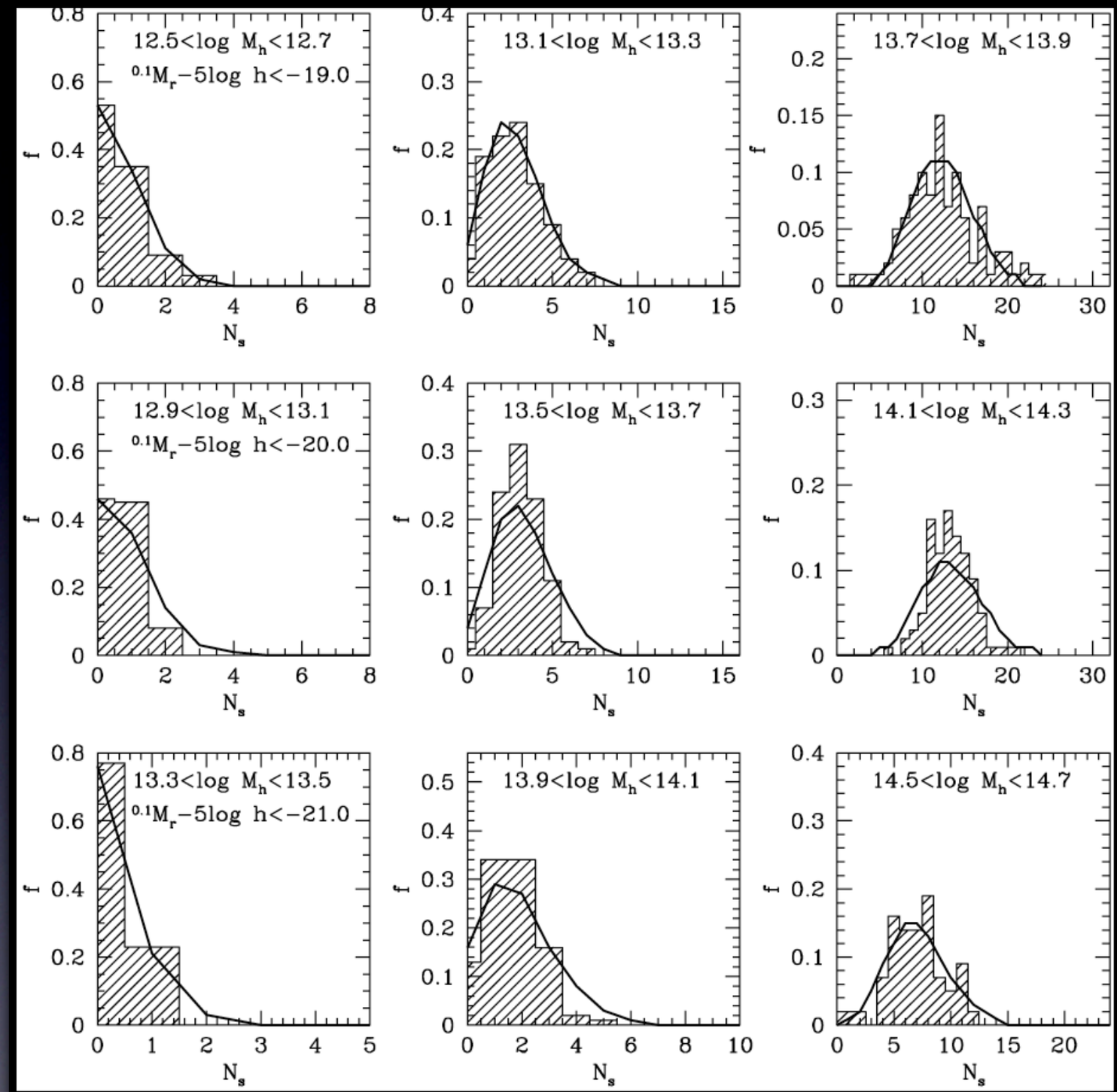

Source: Yang, Mo & van den Bosch, 2008, ApJ, 676, 248

Galaxy group catalogs show that occupation statistics of satellites are (close to) Poissonian.

The Radial Number Density Profile of Satellites

The radial number density profile of satellite galaxies is typically modelled as a `generalized NFW profile':

$$u_{\rm s}(r|M) \propto \left(\frac{r}{\mathcal{R}\, r_{\rm s}}\right)^{-\gamma} \left[1+\frac{r}{\mathcal{R}\, r_{\rm s}}\right]^{\gamma-3}$$

Here γ is a parameter that controls the central cusp slope, and $\mathcal{R} = c_{\rm sat}/c_{\rm dm}$ sets the ratio between the concentration parameter of the satellites and that of the dark matter. For $\gamma = \mathcal{R} = 1$ satellites are an unbiased tracer of the mass distribution (within individual haloes)

The radial number density profile of satellites controls the clustering on small scales (only has significant effect on 1-halo term).

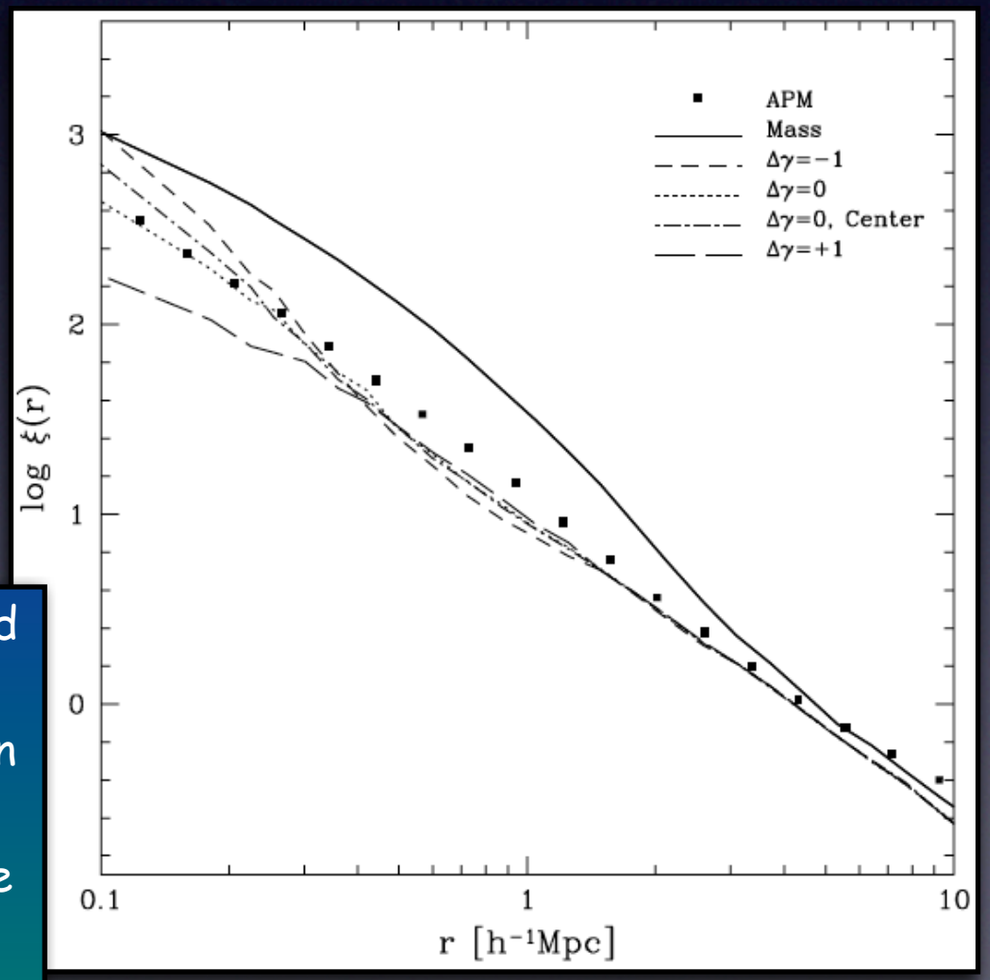

Source: Berlind & Weinberg, 2002, ApJ, 575, 587

The two-point correlation function of galaxies, calculated using the halo model. Solid dots are data from the APM catalogue. The solid line is the model's matter correlation function, and the other lines are galaxy correlation functions in which the number density profile of satellite galaxies is varied.

The Radial Number Density Profile of Satellites

The radial number density profile of satellite galaxies can be constrained using the clustering data itself, or by directly measuring the (projected) profiles of satellite galaxies in groups/clusters, or around isolated centrals...

Source: Lin, Mohr & Stanford, 2004, ApJ, 610, 745

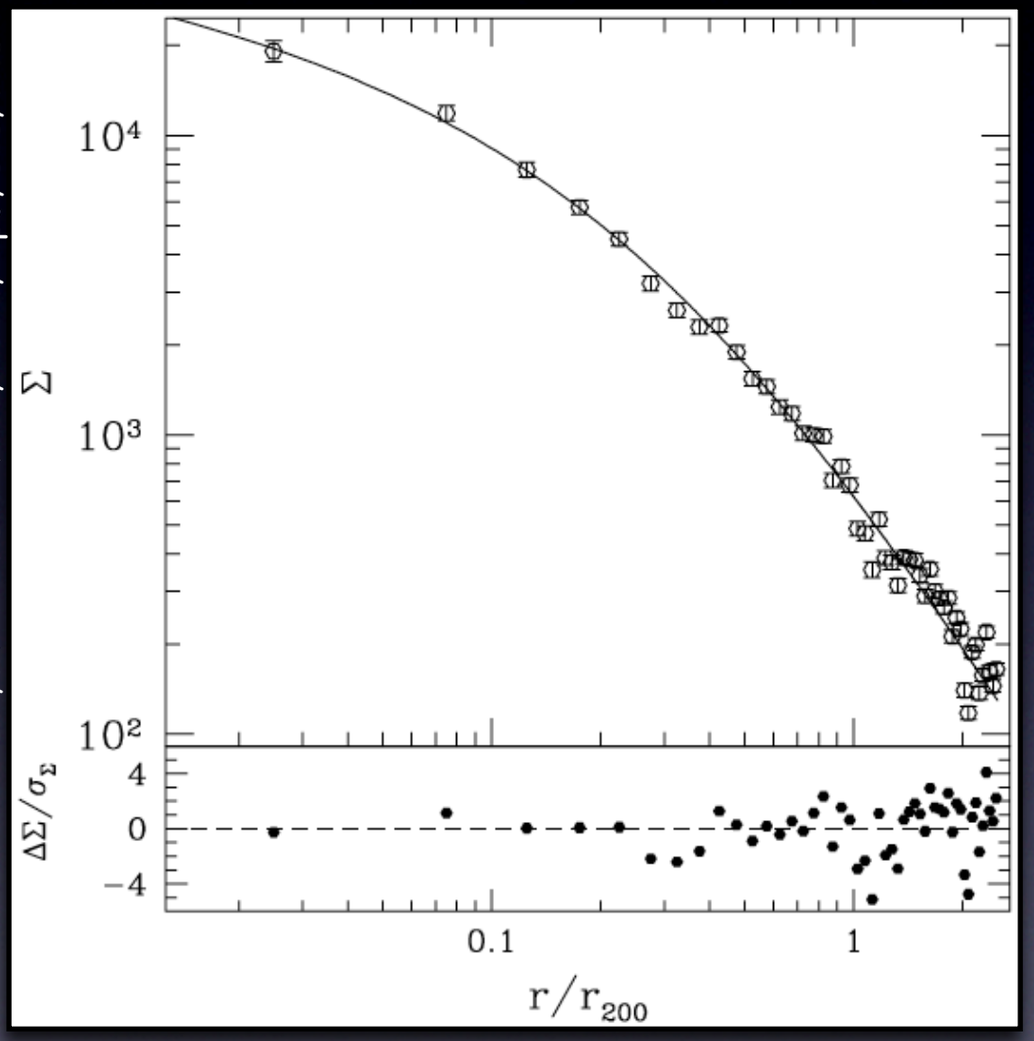

The surface density profile of satellite galaxies in clusters. Solid line is the best-fit NFW profile.

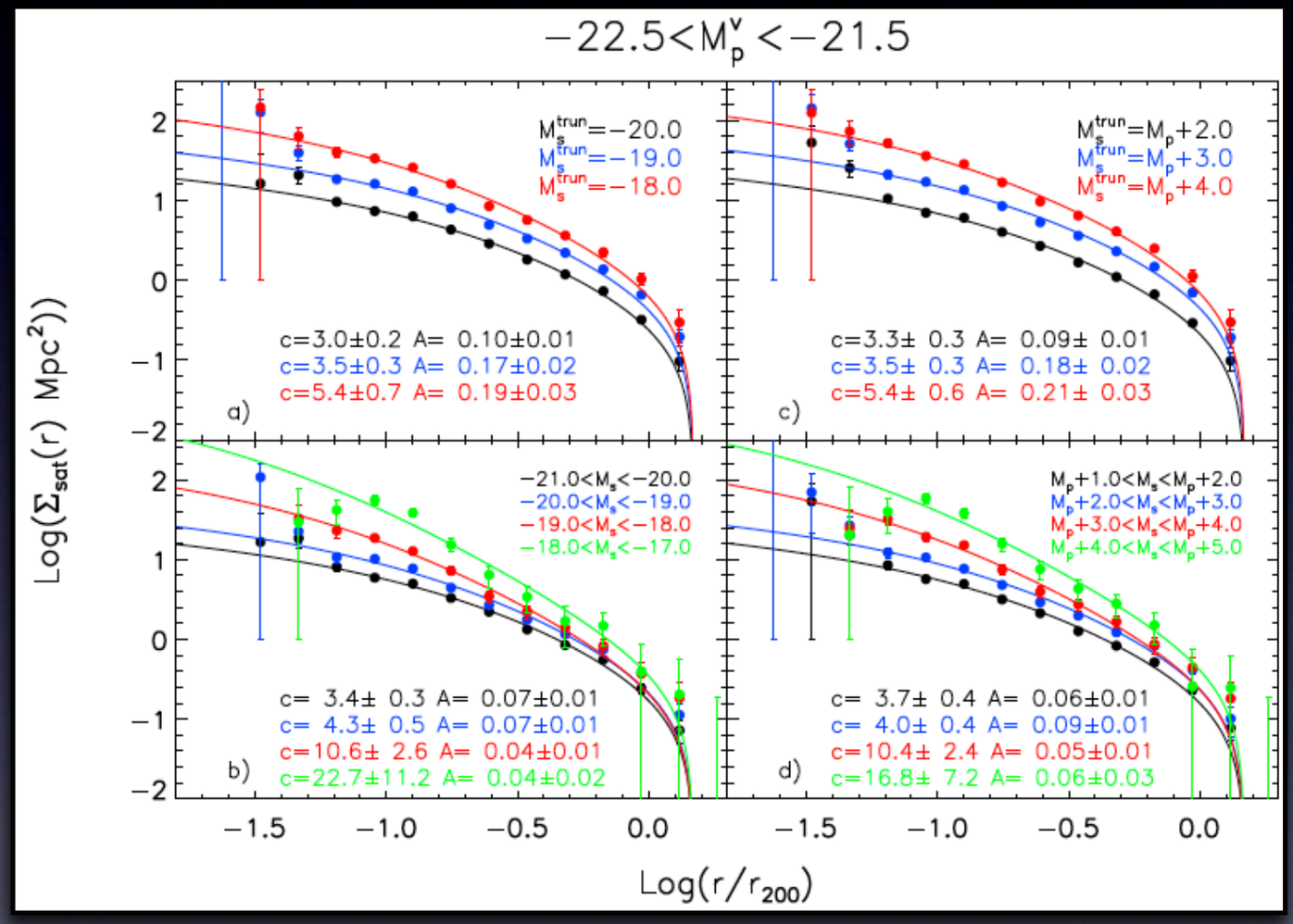

Source: Guo et al. 2012, arXiv: 1201.1296

The surface density profiles of satellite galaxies around isolated centrals in the SDSS. Satellites are identified in photometric catalogue using statistical background subtraction. Lines are best-fit NFW profiles.

The Radial Number Density Profile of Satellites

Although several studies have suggested that satellite galaxies follow a radial number density profile that is well fitted by NFW profile, others find that $u_{\rm s}(r|M)$ has a core and is less centrally concentrated than the dark matter.
This is consistent with distribution of subhaloes in dark-matter-only simulations....

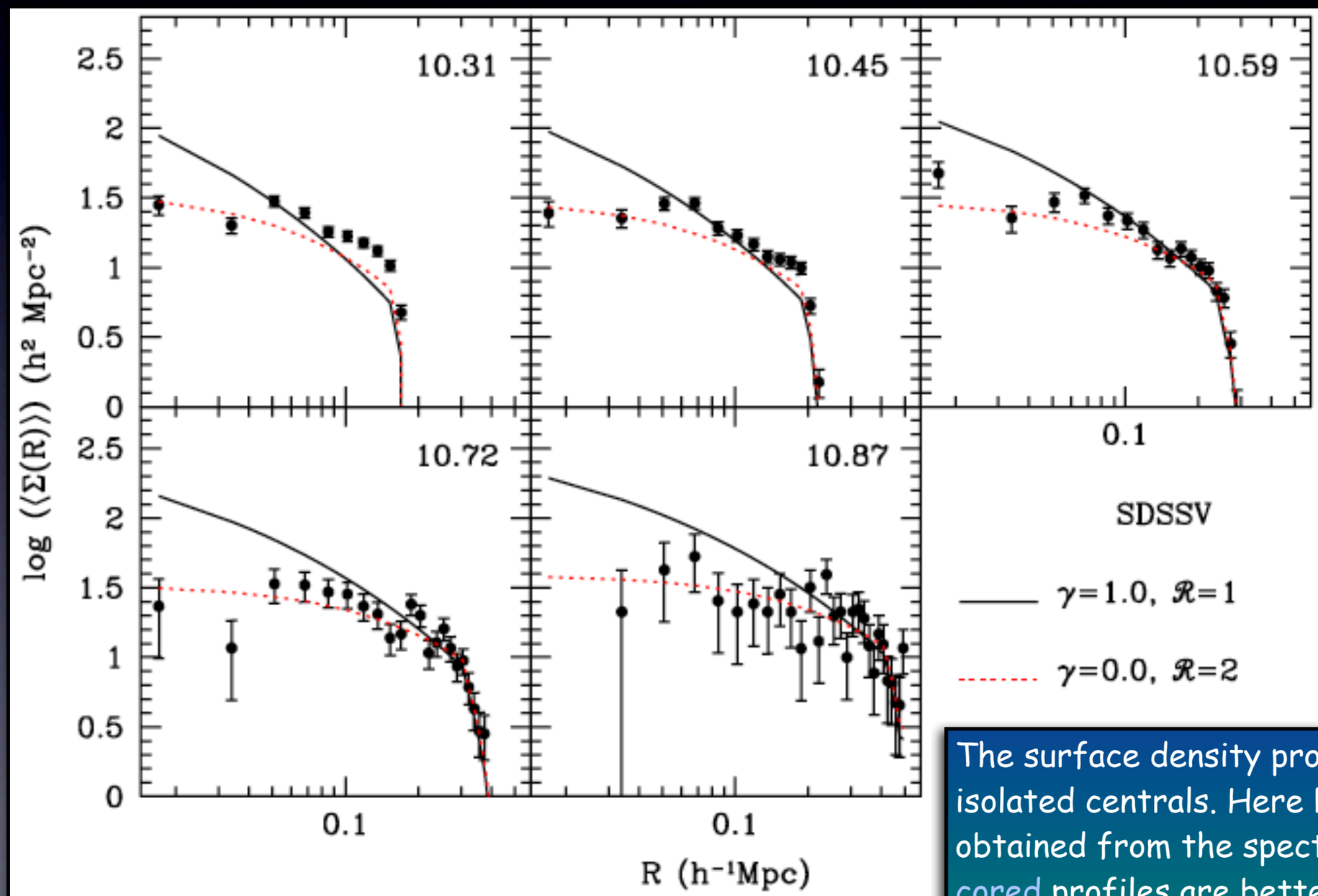

Source: More, vdB, et al. 2009, MNRAS, 392, 801

The surface density profile of satellite galaxies found isolated centrals. Here both centrals & satellites are obtained from the spectroscopic SDSS. Note that cored profiles are better fit than NFW profile.

Testing with Galaxy Mock Catalogs

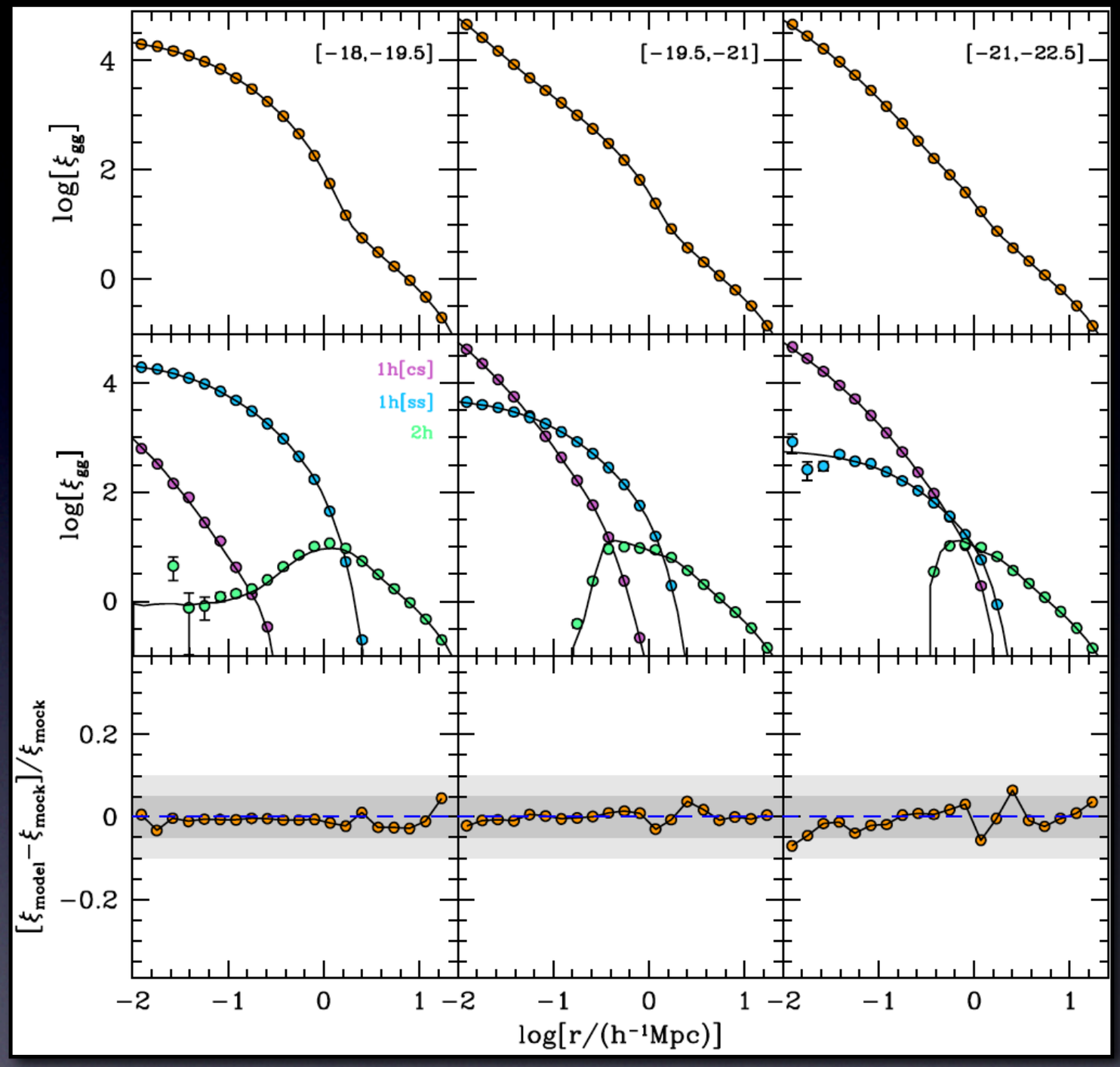

Source: van den Bosch, et al. 2012, arXiv: 1206.6890

One can test accuracy of halo model using mock redshift surveys. These can be constructed by populating haloes in numerical simulations with mock galaxies. Dots show mock data from simulation box, while solid lines show the model predictions from CLF+halo model.

Constraints on Halo Occupation Statistics

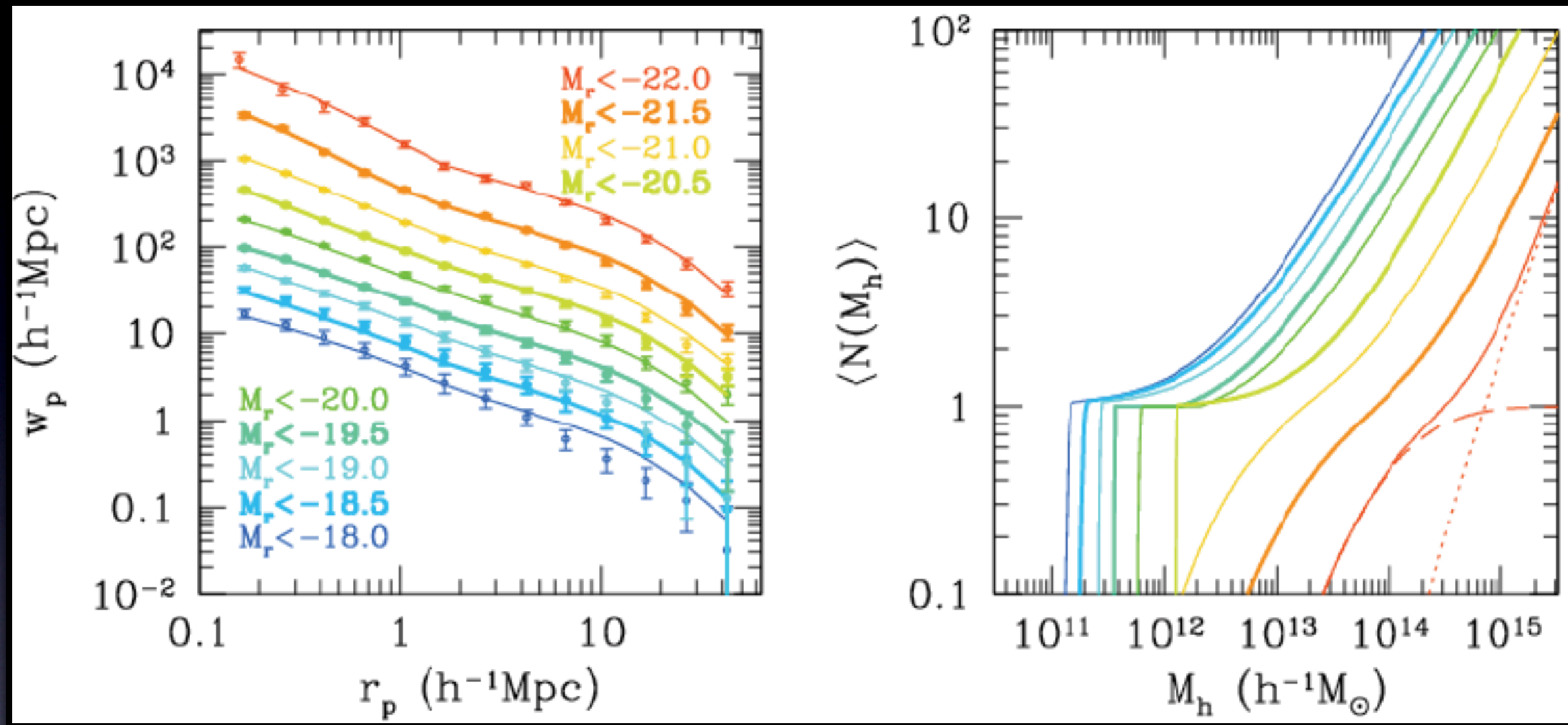

Source: Zehavi et al. 2011, ApJ, 736, 59

Zehavi et al. 2011 used halo occupation models to fit the projected correlation functions obtained from the SDSS for 9 different luminosity threshold samples.

- The left-hand panel shows data+fits (offset vertically for clarity).
- The right-hand panel shows first moments of best-fit halo occupation distributions.

The Galaxy - Dark Matter Connection

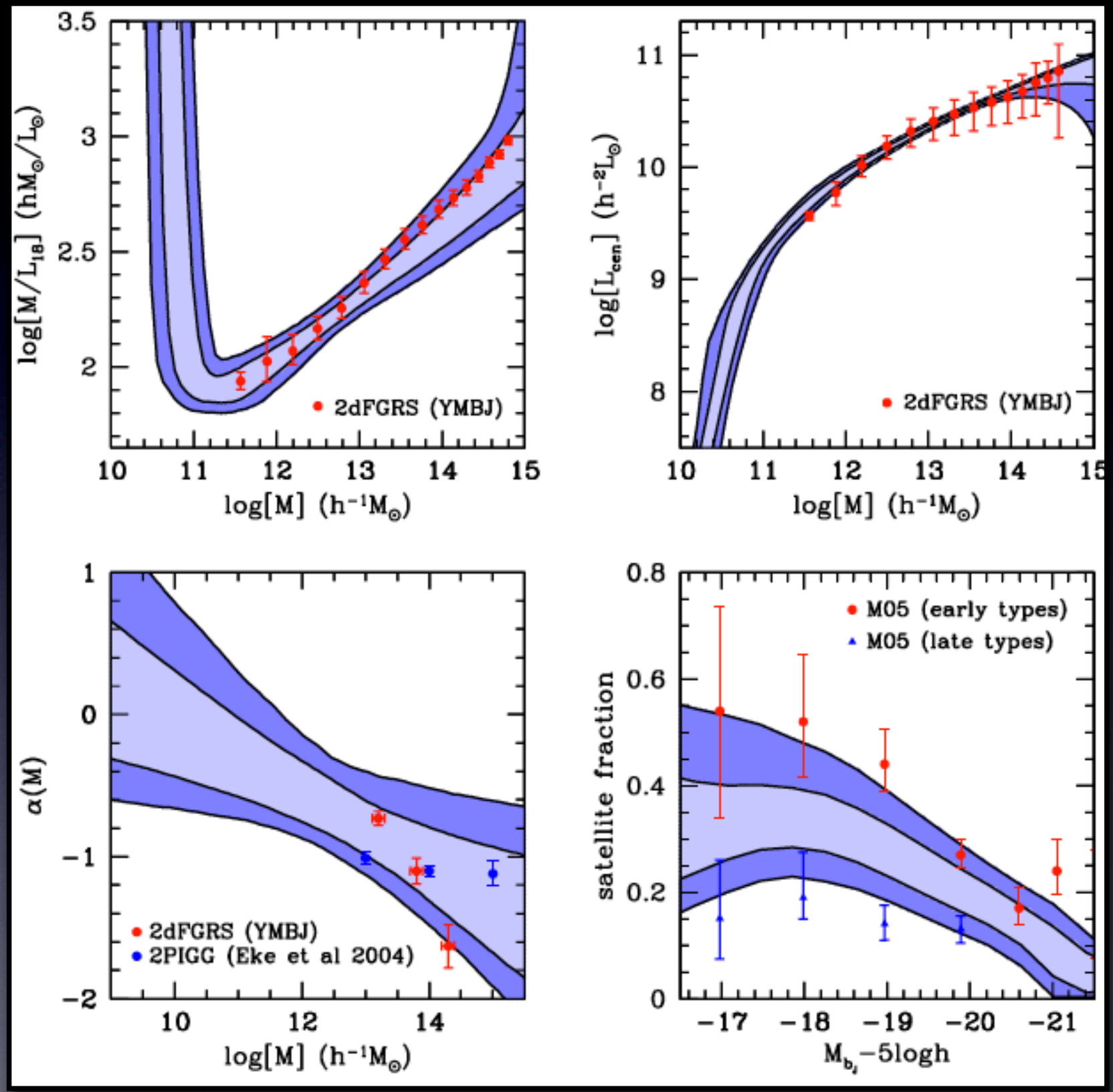

Source: van den Bosch et al. 2007, MNRAS, 376, 841

Summary

- Dark matter haloes have universal density profiles, universal subhalo mass functions, and universal angular momentum profiles.
- More massive haloes are less concentrated, less spherical, and have more substructure. All these trends are a direct consequence of the fact that more massive haloes assemble later.
- At fixed halo mass, haloes that assemble earlier are more concentrated, more spherical, and have less substructure.
- Halo spin parameter is independent of halo mass; adiabatic gas has same specific angular momentum distribution as dark matter.
- Halo model allows one to analytically compute correlation function of matter in the non-linear regime to accuracy of ~10%.
- When combined with halo occupation models, halo model can also be used to compute correlation functions of galaxies.
- Clustering data can be used to constrain halo occupation statistics.